U.S. ARMY MISSILE RESEARCH AND DEVELOPMENT COMMAND

Redstone Arsenal, Alabama 35809

TECHNICAL REPORT TK–77–5

X–RAY FLUORESCENCE ANALYSIS OF COMPOSITE PROPELLANTS FOR ARMY MISSILE SYSTEMS

Propulsion Directorate
Technology Laboratory

3 June 1977

Approved for public release; distribution unlimited.

DISPOSITION INSTRUCTIONS

DESTROY THIS REPORT WHEN IT IS NO LONGER NEEDED. DO NOT RETURN IT TO THE ORIGINATOR.

DISCLAIMER

THE FINDINGS IN THIS REPORT ARE NOT TO BE CONSTRUED AS AN OFFICIAL DEPARTMENT OF THE ARMY POSITION UNLESS SO DESIGNATED BY OTHER AUTHORIZED DOCUMENTS.

TRADE NAMES

USE OF TRADE NAMES OR MANUFACTURERS IN THIS REPORT DOES NOT CONSTITUTE AN OFFICIAL INDORSEMENT OR APPROVAL OF THE USE OF SUCH COMMERCIAL HARDWARE OR SOFTWARE.

UNCLASSIFIED

SECURITY CLASSIFICATION OF THIS PAGE (When Data Entered)

REPORT DOCUMENTATION PAGE

READ INSTRUCTIONS BEFORE COMPLETING FORM

1. REPORT NUMBER: TK-77-5

2. GOVT ACCESSION NO.

3. RECIPIENT'S CATALOG NUMBER

4. TITLE (and Subtitle): X-RAY FLUORESCENCE ANALYSIS OF COMPOSITE PROPELLANTS FOR ARMY MISSILE SYSTEMS.

5. TYPE OF REPORT & PERIOD COVERED: Technical Report,

6. PERFORMING ORG. REPORT NUMBER: TK-77-5

7. AUTHOR(s): Bernard J. Alley

8. CONTRACT OR GRANT NUMBER(s)

9. PERFORMING ORGANIZATION NAME AND ADDRESS
Commander
US Army Missile Research and Development Command
ATTN: DRDMI-TK
Redstone Arsenal, Alabama 35809

10. PROGRAM ELEMENT, PROJECT, TASK AREA & WORK UNIT NUMBERS
AMCMS Code 53970M6350
A1-6-P6350-01-AW-D1

11. CONTROLLING OFFICE NAME AND ADDRESS
Commander
US Army Missile Research and Development Command
ATTN: DRDMI-TI
Redstone Arsenal, Alabama 35809

12. REPORT DATE: 3 June 1977

13. NUMBER OF PAGES: 164

14. MONITORING AGENCY NAME & ADDRESS (if different from Controlling Office): DRDMI-TK-77-5

15. SECURITY CLASS. (of this report): Unclassified

15a. DECLASSIFICATION/DOWNGRADING SCHEDULE

16. DISTRIBUTION STATEMENT (of this Report)

Approved for public release; distribution unlimited.

164p.

17. DISTRIBUTION STATEMENT (of the abstract entered in Block 20, if different from Report)

18. SUPPLEMENTARY NOTES: This project has been accomplished as part of the US Army Materials Testing Technology Program, which has for its objective the timely establishment of testing techniques, procedures or prototype equipment (in mechanical, chemical, or nondestructive testing) to insure efficient inspection methods for materiel/material procured or maintained by DARCOM.

19. KEY WORDS (Continue on reverse side if necessary and identify by block number)

X-ray fluorescence analysis	Ballistic modifier
Composite propellants	Mulitple linear calibration methods
Ammonium perchlorate	Stable reference standards
Aluminum determinations	Statistical procedures

20. ABSTRACT (Continue on reverse side if necessary and identify by block number)

Wavelength dispersive X-ray fluorescence spectrometric procedures were developed for the determination of ingredient percentages and average particle sizes in uncured and cured solid composite propellants of interest in Army missile systems. Three different types of propellent analyses were investigated as follows:

DD FORM 1 JAN 73 1473 EDITION OF 1 NOV 65 IS OBSOLETE

UNCLASSIFIED

SECURITY CLASSIFICATION OF THIS PAGE (When Data Entered)

AB

410 311

Block 20. Abstract (concluded)

1) The determination of ingredient percentages with solids particle-sizes held constant.

2) The in-situ determination of ammonium perchlorate and aluminum particle sizes with ingredient percentages held constant.

3) The simultaneous determination of ingredient percentages and solids particle sizes.

The methodology was developed and demonstrated for low-burning-rate polybutadiene acrylic acid type propellants and high-burning-rate hydroxyl-terminated polybutadiene propellants containing ultrafine ammonium perchlorate. Quantitative procedures were developed for determining ferric oxide, polybutadiene acrylic acid polymer, ammonium perchlorate, and aluminum in polybutadiene acrylic acid propellants, and ammonium perchlorate, aluminum, and a ballistic modifier in high rate hydroxyl-terminated polybutadiene propellants. The procedures are generally applicable to all types of composite propellants. Emphasis was placed on the eatabliahment of procedures directly applicable to a propellant manufacturing process.

Propellant aamples were analyzed nondeatructively in most caaes with an estimated relative atandard deviation and a relative error for ingredient determinations of 1% to 2%. Ultrafine ammonium perchlorate agglomeration in high-rate propellants reduced the precision of aluminum determinations. The estimated relative standard deviation in this case was 4% to 5%. The total analysis time for four replicates of a propellant batch was 15 to 30 min with the manual instrumentation uaed. Multiple linear calibration methods were uaed to correct for matrix effects. Stable reference standards were used to compensate for inatrumental fluctuationa; correctiona were made for variable emission line absorption by the Mylar filma used on the sample holders. Statiatical procedures were developed for placing joint confidence intervals on the actual ingredient percentages of a production propellant batch.

CONTENTS

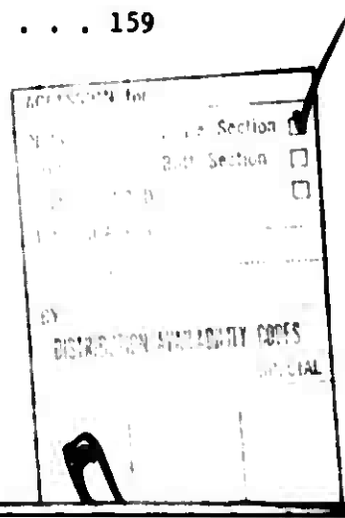

ACKNOWLEDGMENT

The author expresses appreciation to Raymond H. Myers of Virginia Polytechnic Institute and State University for advice and assistance with statistical procedures and for the development of statistical methodology in Appendices A and B.

I. INTRODUCTION

Solid composite propellants are used in the propulsion systems of many types of Army rockets and missiles. These composite propellants, depending on the particular application, are composed of various combinations of a rubber-base binder; an oxidizer such as ammonium perchlorate; a fuel such as aluminum powder; a ballistic modifier such as ferric oxide or ferrocenes; and an aliphatic or aromatic ester type plasticizer. The propellant mechanical properties are controlled primarily by the type of binder system used and by the binder-solids interaction characteristics. The propellant ballistic and rheological properties are strongly affected by the particle sizes of the solids and the types and percentages of the ballistic modifier and plasticizer. The propellant burning rate at fixed pressure is a particularly significant ballistic parameter and the particle size of the ammonium perchlorate plays a significant role in rate adjustment and control.

Clearly, both the propellant ingredient percentages and the solid particle sizes must be carefully controlled during propellant manufacture to insure that the finished propellant will have acceptable performance and reproducible ballistic, mechanical, and rheological properties. Although uncured composite propellants can be analyzed by a combination of existing wet-chemical and instrumental methods, these methods lack the speed and selectivity required for routine quality control applications in propellant manufacturing. Moreover, existing instrumental methods are not suitable for controlling the particle sizes of propellant solids after they are incorporated in the propellant. Cured propellants are very difficult to analyze by wet-chemical methods because of the intractable nature of the cured binder.

X-ray fluorescence spectrometry has been used by the Army Propulsion Directorate of the US Army Missile Research and Development Command [1] for many years in propellant research applications. Early applications of X-ray fluorescence spectrometry to composite propellant analysis were also reported by the Thiokol Corporation [2]. The in-house research conducted prior to initiation of this project demonstrated that the X-ray fluorescence method can be advantageously used as a tool to monitor, control, and improve the quality of production propellants. X-ray fluorescence spectrometry [3] is especially attractive for propellant analysis because of its speed, high degree of precision, and the fact that samples can be analyzed nondestructively without prior chemical treatment. Furthermore, X-ray fluorescence spectrometry is the only known technique that is capable of in-situ propellant-solids particle size measurements [1]. Because of these unique features, X-ray fluorescence analysis of uncured production propellants prior to motor casting enables a decision to accept or reject the batch to be made thereby preventing subsequent costly motor rejections. If unexplained propellant problems arise later, the cured propellant can be analyzed by a similar nondestructive procedure.

This project was conducted as part of the US Army Materials Testing Technology Program. The objective was to develop a rapid, precise, and accurate X-ray fluorescence method of analysis for general application to all types of composite propellants used in Army missile systems. Emphasis was placed on the development of techniques directly applicable to propellant manufacture. The method was specifically applied to polybutadiene acrylic acid (PBAA), low burning rate propellants, and hydroxyl-terminated polybutadiene (HTPB) high burning rate propellants because these types afforded the best combinations of variables needed to develop the required analytical procedures. The developed procedures can be readily applied with little or no modification to other types of composite propellants. Three experimental cases were considered as follows:

a) The determination of propellant ingredient percentages with solids particle sizes held constant.

b) The determination of ammonium perchlorate and aluminum particle sizes with ingredient percentages held constant.

c) The simultaneous determination of ingredient percentages and particle sizes.

Appropriate calibration procedures were developed to handle each of these experimental cases. Both cured and uncured propellants were analyzed.

II. EXPERIMENTAL METHODS

A. Instrumentation

A wavelength-dispersive universal vacuum X-ray spectrometer marketed by Philips Electronic Instruments was used. The flat-crystal X-ray optical system of the spectrometer is shown in Figure 1. The spectrometer has four sample compartments each of which can be individually rotated above the primary X-ray beam. With the inverted optical system the bottom surface of the sample is irradiated. Either a Philips PW 1404/00 (1600 W) chromium target X-ray tube, or a Philips PW 1404/01 (1900 W) tungsten target X-ray tube was used depending on the analysis requirements. Both X-ray tubes were powered by a 3-kVA water-cooled generator. The voltage to the generator was stabilized with a 5-kVA line voltage stabilizer.

Other spectrometer components consisted of a 10.2 cm × 0.51 mm parallel plate entrance collimator, sodium chloride (200), pentaerythritol (002), and ethylenediamine D-tartrate (020) analyzing crystals, a coarse exit collimator, and a gas-flow proportional detector. The associated electronic circuit panel (Type 12206/0) has a decade scaler and a single channel pulse height analyzer. The X-ray optical path

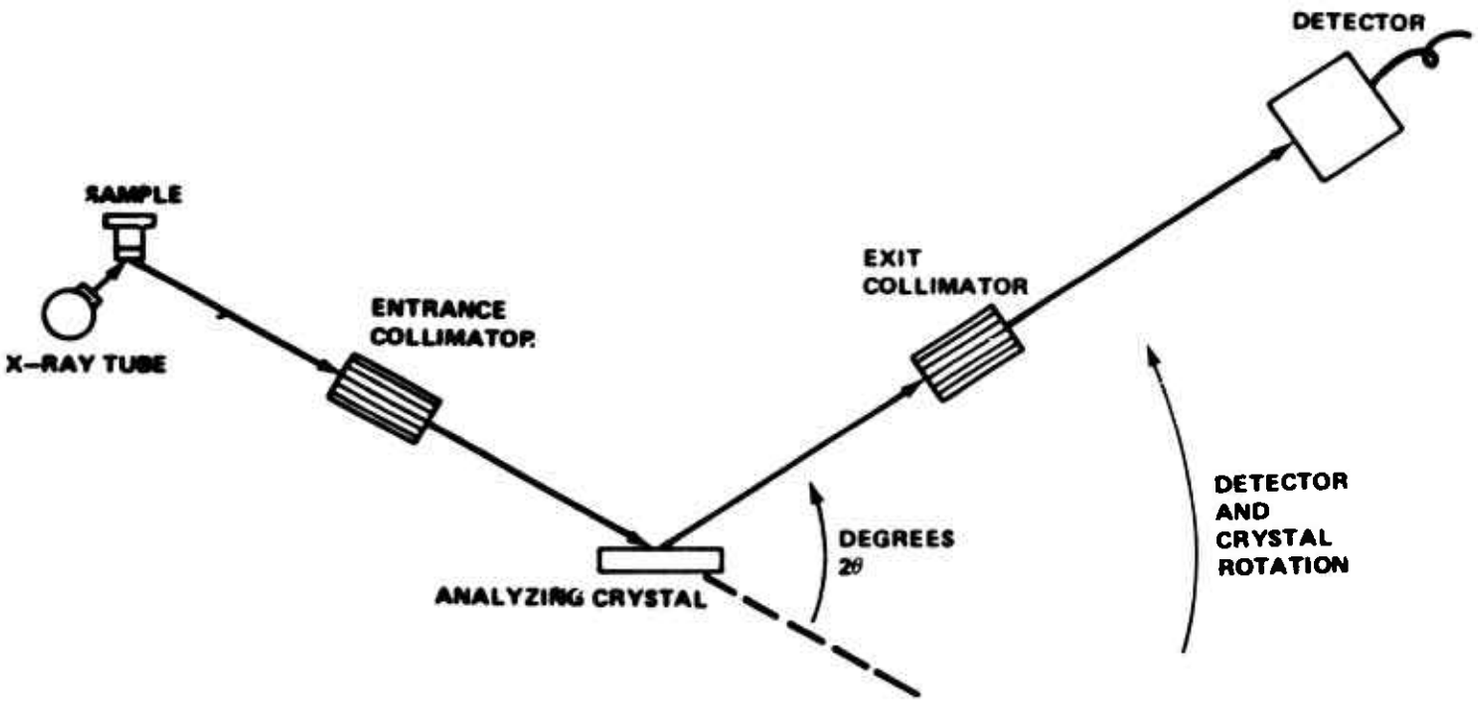

Figure 1. Inverted flat-crystal X-ray optics.

was flushed with helium for uncured propellant analysis and evacuated (< 0.1 torr) for cured propellant analysis. More specific instrumental operating conditions are given along with each experiment described later.

The choice of X-ray tube depends on the elements to be analyzed. A comparison of emission line intensities for propellant elements of interest in this investigation using tungsten and chromium target X-ray tubes is given in Table 1. The chromium target tube is a better choice for the analysis of sulfur, chlorine, and aluminum; therefore, it is a more generally useful tube for light-element propellant analyses.

TABLE 1. COMPARISON OF EMISSION LINE INTENSITIES FOR PROPELLANT ELEMENTS USING TUNGSTEN AND CHROMIUM TARGET X-RAY TUBES

Emission Line	Intensity (counts/sec)		Ratio (Cr/W)
	Chromium Tube	Tungsten Tube	
FeK_α	3418	25,090	0.14
ClK_α	55,990	25,390	2.21
SK_α	1823	766	2.38
AlK_α	7435	2926	2.54

Sample: Uncured propellant reference standard.
Chromium tube: 50 kV, 28 mA constant potential.
Tungsten tube: 50 kV, 50 mA constant potential.

The sodium chloride crystal was selected primarily for the determination of the low percentage of sulfur in the PBAA polymer. Either the ethylenediamine D-tartrate (EDDT) or the pentaerythritol (PET) crystal must be used for the aluminum determination. The relative reflectivities of these crystals for several light elements K_α emission lines are shown in Table 2. The PET crystal is a better choice when maximum emission line intensity is required. The interplanar d-spacing of the PET crystal varies with temperature, however, so that the emission line angle must be adjusted to detect the emission line peak as the crystal temperature varies.

Pulse height analysis was used to reduce background and increase the peak-to-background ratios for aluminum and sulfur determinations. Pulse height discrimination was less effective for sulfur K_α measurements, however, because the chlorine K_α fluorescence from the sodium

TABLE 2. COMPARISON OF THE REFLECTIVITIES OF EDDT AND PET CRYSTALS FOR THE K_α EMISSION LINES OF SEVERAL LIGHT ELEMENTS

Emission Line	Element or Compound	Intensity (counts/sec)		Ratio PET/EDDT	Tube* Setting
		EDDT	PET		
AlK_α	Al	9035	16,975	1.88	40 kV, 30 mA
SiK_α	Si	3986	7197	1.81	40 kV, 30 mA
PK_α	$NaH_2PO_4 \cdot H_2O$	1024	1673	1.63	40 kV, 30 mA
SK_α	S	13,537	20,109	1.49	35 kV, 30 mA

*Cr target tube operated at constant potential.

chloride crystal was also passed by the pulse height analyzer. In both cases the pulse height analyzer primarily eliminated scattered short wavelength radiation from the X-ray tube continuum. There was no problem with spectral line interference. A typical pulse height distribution curve for aluminum K_α radiation measured with the gas-flow proportional detector is shown in Figure 2. The effect of increasing the gas-flow detector gain (voltage) on intensities of the analytical emission lines is shown in Figure 3. The detector voltage was operated in the plateau region for each element.

Only peak X-ray intensity measurements were made; that is, no correction was made for background radiation. The use of X-ray intensity measurements only at the peaks of the analytical emission lines is justified because of the calibration method used and the fact that experimental conditions were chosen to give large peak-to-background ratios. Typical peak-to-background ratios for the analysis of light elements in PBAA propellants are given in Table 3. The peak intensities were generally kept below 25,000 counts/sec because at higher intensities the response was nonlinear due to the dead time of the linear amplifier of the electronic circuit panel.

B. Propellant Preparation

All propellants were made in 500-g batches (0.47-liter size) in a vertical double-sigma blade Baker-Perkins type mixer. The mixer bowl was heated to a temperature of 55° to 60°C. Then the liquid components, except for the binder curing agent, were added and blended together. The propellant solids were then added incrementally. After the last solids addition, the propellant was mixed for 2 hr. Then the curing agent was added and mixing was continued for 20 min under vacuum.

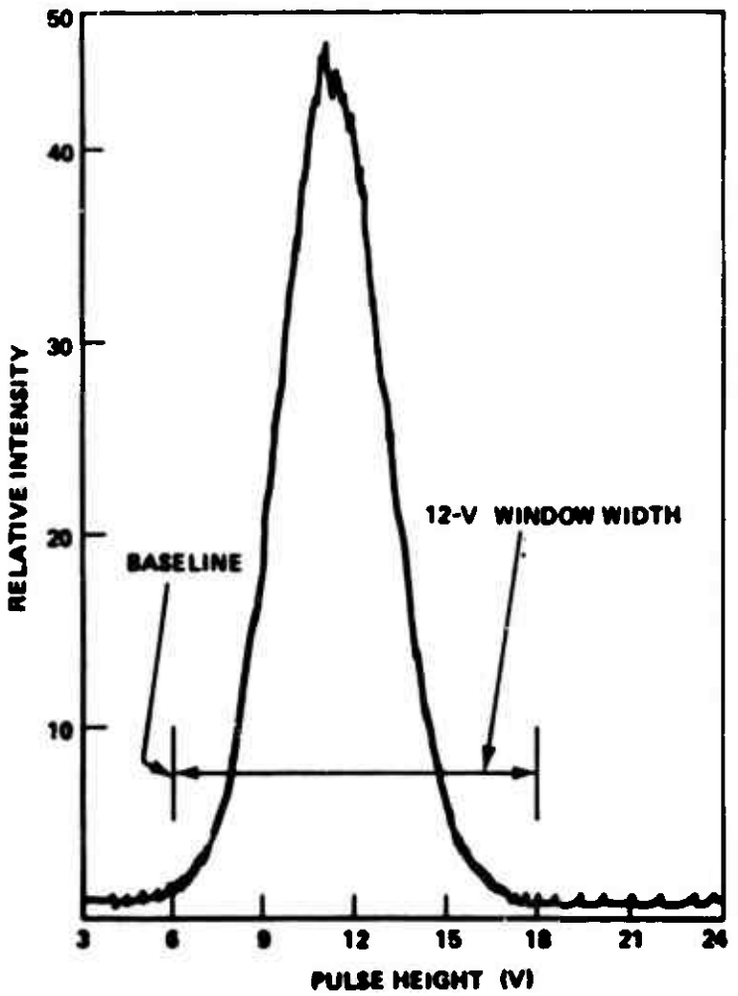

Figure 2. Pulse height distribution curve (differential) for aluminum K_α radiation and a gas-flow detector set at 1600 Vdc.

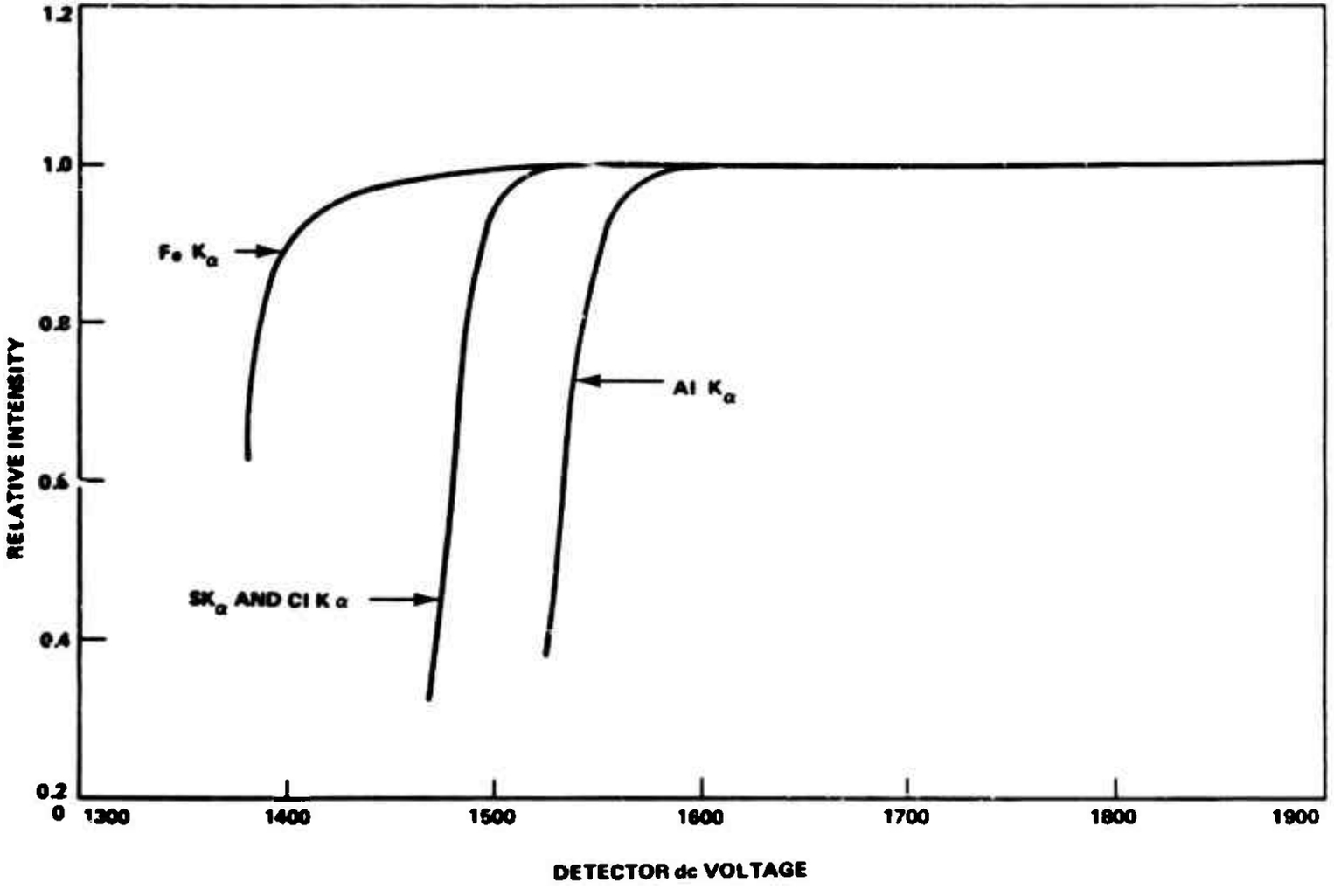

Figure 3. Gas-flc ector plateaus for propellant elements.

TABLE 3. PEAK-TO-BACKGROUND RATIOS FOR THE ANALYSIS OF LIGHT ELEMENTS IN PBAA PROPELLANTS

Emission Line	Uncured Propellant		Cured Propellant	
	Without PHA	With PHA	Without PHA	With PHA
AlK_α	6.0	180.1	15.3	275.5
SK_α	5.9	10.3	5.8	9.6
ClK_α	176.5	265.7	290.0	457.4
FeK_α	56.0	85.5	47.2	72.0

The resulting uncured propellant slurry having a viscosity of 1 to 15 kilopoise was taken from the mixer and analyzed directly. Cured propellant samples were prepared by vacuum casting the propellant slurry into an appropriate 2.5- to 5.1-cm diameter container such as a mailing carton or Teflon tube and then curing the propellant at 55° to 60°C for several days. This is a generalized procedure. Some deviations were made to accommodate specific formulations.

Production propellants are made in generally the same manner except that the batch sizes are much larger. Typical production mixer sizes are 1135- to 2271-liter capacities.

C. Mylar Film Corrections

Uncured propellant samples are analyzed in a circular aluminum holder fitted with a thin Mylar film. The propellant is pressed against the film and held in place by gravity. As shown in Figure 1, the primary X-rays from the X-ray tube pass through the Mylar film and excite the elements in the propellant surface to fluoresce. The characteristic X-ray fluorescence emission lines than pass through the Mylar film where they are dispersed by the analyzing crystal and detected by the gas-flow proportional counter. The Mylar film must be strong enough to support the propellant sample, but thin enough to transmit a high percentage of the incident fluorescent radiation. The transmittance for a given film thickness varies significantly with the wavelength of the fluorescent radiation, becoming smaller as the wavelength increases. An experimental determination of the transmittance of several emission lines of interest through two different Mylar film thicknesses is shown in Table 4. Aluminum K_α radiation is strongly absorbed even by the 3.8-μm film; whereas iron K_α radiation is absorbed very little. The 3.8-μm Mylar film was used for most of this work because of its higher transmittance.

TABLE 4. TRANSMISSION OF SOFT X-RAYS BY MYLAR FILMS

Emission Line	Wavelength, A	Transmittance	
		6.4-μm Mylar	3.8-μm Mylar
FeK_α	1.94	0.98	0.99
ClK_α	4.73	0.76	0.85
SK_α	5.37	0.68	0.79
AlK_α	8.34	0.24	0.43

The absorption of the K_α emission lines of chlorine, sulfur, and aluminum by the film would have little effect on uncured propellant analysis if the film thickness remained constant from sample to sample. Unfortunately, the thickness varies sufficiently among Mylar samples to introduce significant intensity measurement errors if a correction for the film thickness variation is not made for chlorine K_α, sulfur K_α, and aluminum K_α intensity measurements. As indicated by the data in Table 4, no correction need be made for the iron K_α intensity measurements.

An empirical procedure to correct for the effects of variable Mylar film thickness on the measured intensities of chlorine K_α, sulfur K_α, and aluminum K_α radiations was previously reported by Ailey and Higgins [4]. The same procedure was used here except that the accuracy of film thickness corrections was improved by using a better model derived from X-ray absorption theory, and by reanalyzing standard samples to get a better fit of the experimental data to the model. In this procedure aluminum K_α correction factors are determined directly by analyzing identical aluminum standards, and the chlorine K_α and sulfur K_α correction factors are calculated using the aluminum K_α data. The equations for calculating the chlorine K_α and sulfur K_α correction factors are as follows:

$$\log C_{Cl} = 0.2078 \log C_{Al} \quad (1)$$

$$\log C_S = 0.3189 \log C_{Al} \quad (2)$$

where C_{Cl}, C_S and C_{Al} are the correction factors for the elements indicated as subscripts. For routine applications where large numbers of samples are analyzed, it is convenient and facilitates the analysis to have the correction factors tabulated as shown in Table 5.

An example of the procedure for determining Mylar film thickness correction factors for aluminum K_α, sulfur K_α, and chlorine K_α radiations is given in Table 6. Application of the factors to propellant data will be illustrated later. In practice, identical high purity aluminum standards are sequentially analyzed in the holder that will be used for the stable reference standard and in each sample holder. In this example a total of four samples of the same propellant batch will be analyzed as a replication of duplicates. The aluminum K_α intensity from each aluminum standard after transmission through the Mylar film on the holder was measured in seconds to collect 500,000 total counts. The aluminum K_α correction factor for each sample holder is obtained by dividing the seconds for the reference standard holder by the seconds for the particular sample holder. The correction factors for sulfur K_α and chlorine K_α emission lines are then calculated using Equations (1) and (2), or they are obtained from the tabulated values in Table 5.

D. Reference Standards

There are several inherent short- and long-term sources of variation in X-ray spectrometry that affect the measured intensities of X-ray fluorescent emission lines. Some of these are as follows:

1) Fluctuations in the X-ray tube output.

2) Mechanical errors of positioning samples and the goniometer.

3) Electronic drift.

To insure the highest possible analytical precision and accuracy, some type of standard must be employed to compensate for the short- and long-term sources of variation. The preferred approach for propellant analysis (the one used in this work) is to analyze a reference standard in conjunction with the propellants. The reference standard must be stable chemically and toward repeated exposure to the primary X-ray beam. It must be affected by the sources of variation in essentially the same manner as the propellant. Another important advantage of using a stable reference standard is that calibration procedures, which are somewhat involved, are valid over long periods of time.

A substantial amount of effort was devoted to the development, preparation, and evaluation of suitable reference standards for use with uncured PBAA and HTPB propellants, and cured PBAA propellants.

TABLE 5. ALUMINUM K_α, SULFUR K_α, AND CHLORINE K_α CORRECTION FACTORS FOR VARIABLE MYLAR THICKNESS

Aluminum K_α	Sulfur K_α	Chlorine K_α
0.900	0.967	0.978
0.905	0.969	0.979
0.910	0.970	0.981
0.915	0.972	0.982
0.920	0.974	0.983
0.925	0.975	0.984
0.930	0.977	0.985
0.935	0.979	0.986
0.940	0.980	0.987
0.945	0.982	0.988
0.950	0.984	0.989
0.955	0.985	0.990
0.960	0.987	0.992
0.965	0.989	0.993
0.970	0.990	0.994
0.975	0.992	0.995
0.980	0.994	0.996
0.985	0.995	0.997
0.990	0.997	0.998
0.995	0.998	0.999
1.000	1.000	1.000
1.005	1.002	1.001
1.010	1.003	1.002
1.015	1.005	1.003
1.020	1.006	1.004
1.025	1.008	1.005
1.030	1.009	1.006
1.035	1.011	1.007
1.040	1.013	1.008
1.045	1.014	1.009
1.050	1.016	1.010
1.055	1.017	1.011
1.060	1.019	1.012
1.065	1.020	1.013
1.070	1.022	1.014
1.075	1.023	1.015
1.080	1.025	1.016
1.085	1.026	1.017
1.090	1.028	1.018
1.095	1.029	1.019
1.100	1.031	1.020

TABLE 6. EXAMPLE OF MYLAR FILM THICKNESS CORRECTION PROCEDURE

Sample Holder	Mylar Aluminum Standard (sec/500,000 counts)	Aluminum Correction Factor	Sulfur Correction Factor	Chlorine Correction Factor
Reference Standard	21.66			
Sample 1	21.95	0.987	0.996	0.997
Sample 2	22.21	0.975	0.992	0.995
Reference Standard	21.72			
Sample 3	21.47	1.012	1.004	1.002
Sample 4	20.89	1.040	1.013	1.008

The compositions of the standards that were developed and used throughout the program are shown in Table 7. It was necessary to develop a standard for each propellant type and physical state so that analytical emission line intensities from the standards reasonably approximated the line intensities of the same elements from the corresponding propellants. In the case of HTPB propellant only the uncured propellant was analyzed during this program.

TABLE 7. REFERENCE STANDARD COMPOSITIONS (WEIGHT %)

Ingredient	PBAA Propellant		Uncured High Rate HTPB Propellant
	Uncured	Cured	
Sodium Chloride	35.0	54.0	55.0
Aluminum Powder (10 to 35 μm)	22.0	14.0	20.0
α-Cellulose	41.0	30.6	20.0
Iron (II) Oxide	0.8	0.7	
Zinc Sulfide	1.2	0.7	5.0

Sodium chloride was used in place of ammonium perchlorate in the reference standard because ammonium perchlorate decomposes when exposed

to the primary X-ray beam for perlods in excess of approximately 30 min. Zinc sulfide was used in place of PBAA polymer to provide the sulfur K_α emission, because it was desirable to prepare a solid standard. α-cellulose is an excellent binding material composed of light elements, and it is stable toward extended X-ray exposure. Each standard was made by blending the mixture for 15 min on a SPEX No. 8000 mixer/mill, and then pressing the hlended mixture into a pellet in a 3.18-cm die at a pressure of 207 MPa. The pellet was then bonded to a plexiglas disc of the same diameter to facilitate handling. When not being used, the standard pellets are stored in a desiccator. The standards have been found to have excellent long term storage stability.

The ability of the reference standards to compensate for variations in the intensity of the X-ray tube primary radiation is demonstrated for the cured PBAA standard in Table 8. This is a very severe test, because the X-ray tube kV and mA settings were purposely varied over a very wide range. In actual practice the variations will be many orders of magnitude smaller. The constancy of the X-ray intensity ratio for each element in Table 8 as the X-ray tube settings were changed shows the excellent compensating ability of the standard. The other standards are equally effective.

The stability of the uncured PBAA propellant standard upon extended X-ray exposure is shown in Table 9. Again, the essentially constant X-ray intensity ratio for each element demonstrates that the constituents of the standard are not degraded by the X-ray exposure.

The use of compounds in the reference standard for stahility reasons that are not present in the propellant causes an undesirable experimental effect as shown in Tahle 10. It ls well known that the exact wavelength and hence reflectlng angle for a given emission line depends somewhat on the electronic environment of the atom. Thus the peak angles for chlorine K_α radiation from the standard and propellant differ by 0.10° 2θ. Therefore, for the most precise work the goniometer should be set to the peak angle of both the standard and propellant during quantitative ammonium perchlorate determinatlons. The difference hetween the peak angles of sulfur K_α radiation from the standard and propellant was found to he insignlflcant.

E. Spectrometer and Propellant Variables Evaluation

Prior to the development and applicatlon of calibratlon procedures for quantitative determinations and the analyses of large numbers of samples, an extenslve evaluation of propellant mixing and spectrometer operatlng varlables was made to establlsh optimum conditlons. The main variables that were evaluated are shown ln Table 11. These are the ones that were considered most llkely to affect the preclsion and accuracy of quantitative determinatlons.

TABLE 8. ABILITY OF CURED PBAA PROPELLANT REFERENCE STANDARD TO COMPENSATE FOR X-RAY TUBE VARIATIONS

X-Ray Tube Setting	Iron K_α (sec)			Chlorine K_α (sec)			Sulfur K_α (sec)			Aluminum K_α (sec)		
	Standard	Propellant	Ratio	Standard	Propellant	Ratio	Standard	Propellant	Ratio	Standard	Propellant	Ratio
50 kV, 35 mA	12.48	12.39	1.007	14.25	15.02	0.949	53.27	58.75	0.888	35.96	32.05	1.122
45 kV, 30 mA	15.99	15.89	1.006	17.83	18.74	0.952	55.44	61.65	0.899	45.90	49.27	1.115
40 kV, 15 mA	22.[illegible]	21.59	1.009	23.58	24.[illegible]	0.953	54.37	58.58	0.890	61.09	55.01	1.111
Fixed Counts	[illegible],000			500,000			20,000			50,000		

TABLE 9. STABILITY OF UNCURED PBAA PROPELLANT REFERENCE STANDARD TOWARD X-RAYS*

Cumulative Time (hr)	Intensity Ratio			
	Iron K_α	Chlorine K_α	Sulfur K_α	Aluminum K_α
0	1.147	1.230	0.858	1.577
1.52	1.149	1.234	0.852	1.578
2.02	1.149	1.234	0.852	1.567
2.55	1.146	1.236	0.856	1.569
3.38	1.149	1.238	0.855	1.579
3.97	1.146	1.239	0.858	1.577
4.57	1.145	1.243	0.861	1.587
5.17	1.146	1.243	0.862	1.581
5.67	1.145	1.243	0.867	1.573
6.17	1.148	1.242	0.861	1.581

*Tungsten target: 50 kV, 45 mA.

TABLE 10. EFFECT OF ELEMENT ELECTRONIC ENVIRONMENT ON MEASURED ANGLES FOR SELECTED EMISSION LINES

Sample	Analyzing Crystal	Emission Line	Goniometer Angle (deg 2θ)	Δ 2θ
Sodium Chloride	NaCl	Chlorine K_α	114.05	0.10
Ammonium Perchlorate			113.95	
Potassium Sulfate	NaCl	Sulfur K_α	144.57	0.18
PBAA Polymer			144.75	
Aluminum Oxide	EDDT	Aluminum K_α	142.68	0.09
Aluminum			142.77	

TABLE 11. SPECTROMETER, SAMPLING, AND PROPELLANT MIXING VARIABLES INVESTIGATED

Propellant (PBAA) Mixing Variables		
Variable	Level 1	Level 2
Mixing Atmosphere (Exp 1)	Nitrogen	Nitrogen + 72% RH
Mixing Atmosphere (Exp 2)	Nitrogen	Air
Mixing Time	2 hr	4 hr
Mixer Blade Speed	36 rpm	78 rpm
Spectrometer and Propellant Sampling Variables		
Variable	Level 1	Level 2
Spectrometer Environment	Helium	Vacuum
Spectrometer Holder Equivalence	—	—
Sample Temperature	60°C	25°C
Sample Analysis Time (Exp 1)	Immediately after preparation	After standing 30 min
Sample Analysis Time (Exp 2)	1 hr after mixing	24 hr after mixing
Sample Rotation	Rotated	Not rotated
Uncured Sample State	Deaerated	Not Deaerated
Analysts	—	—

The significance of the selected variables was determined by statistical analysis of data obtained from factorial experimental designs. Although statistical significance between the levels was found for several of the variables, in most cases the difference was of no practical significance. There was no practical difference, for example, between the levels of the mixing variables. Analysis under vacuum has an adverse effect on uncured propellant results; whereas cured propellant can be satisfactorily analyzed under vacuum. There is a small effect of sample temperature on analysis results; it is preferable to allow the sample to cool to nearly ambient temperature before analysis. The time at which the sample is analyzed after it has been loaded into the sample holder was not found to affect results significantly; however, it is good analytical procedure to analyze the samples as soon as possible after they are prepared. Rotation of the sample in its own plane had little effect on the precision of uncured propellant analyses, but did improve the precision of some cured propellant analyses, particularly if the propellant tended to be inhomogeneous. Whether the propellant had been deaerated before analysis had no effect on results, but the use of deaerated samples is nevertheless a better choice.

F. Analysis Procedure

1. Uncured Propellant

The sampling components used for the majority of the uncured propellant analyses are shown in Figure 4(a). A 3.8-μm Mylar film was placed on the bottom of each circular aluminum holder to support the reference standard and propellant slurry samples. The Mylar film was then supported with a metal disc. The propellant sample was pressed against the Mylar surface using a plexiglas backing disc. Before the samples were loaded, however, the Mylar film thickness correction factors were established as shown in Table 6. One of the aluminum standards, machined from a piece of bar stock, is shown in Figure 4(a). Properly mounted aluminum foil is also suitable for use as a standard for film thickness corrections.

Although the aluminum holders work very well for uncured propellant analysis, they must be cleaned after each analysis. This is time consuming and therefore not very desirable for rapid, routine quality control analysis of production propellants. Consequently, toward the end of the program disposable Chemplex No. 1530 (Chemplex Industries, Inc.) plastic sample cups were purchased and evaluated. These sampling components are shown in Figure 4(b). Mylar film corrections and sample loadings were accomplished in the same manner as for the aluminum holders. The propellant samples in this case were pressed against the 3.8-μm Mylar surface using the large end of a No. 10 cork stopper. The loaded sample cups are supported by the aluminum holders during analysis, and are subsequently discarded. Results using the disposable sample cups are comparable to those using the aluminum holders; therefore, they are

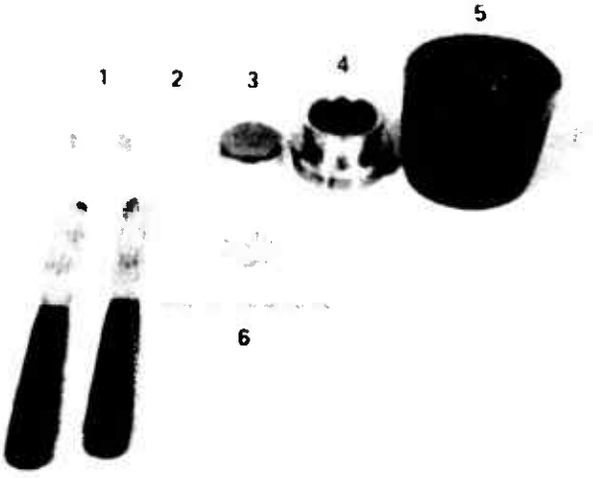

(1) ALUMINUM STANDARD FOR MYLAR CORRECTION
(2) PLEXIGLAS DISC FOR PRESSING PROPELLANT INTO
IJTO SAMPLE HOLDER
(3) REFERENCE STANDARD MOUNTED ON PLEXIGLAS DISC
(4) CIRCULAR ALUMINUM SAMPLE HOLDER
(5) UNCURED PROPELLANT AND CONTAINER
(6) PLATE AND METAL DISC TO SUPPORT MYLAR FILM
ON HOLDER DURING SAMPLE LOADING

Figure 4 (a). Components for uncured propellant analysis by X-ray spectrometry.

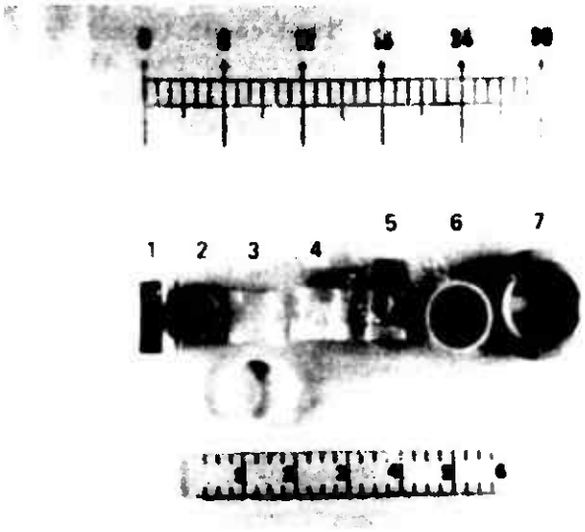

(1) ALUMINUM STANDARD, (2) NO. 10 CORK STOPPER, (3) CHEMPLEX NO. 1530 DISPOSABLE HOLDER AND SNAP–ON RING, (4) ASSEMBLED NO. 1530 HOLDER, (5) NO. 1530 HOLDER LOADED WITH PROPELLANT SAMPLE, (6) PROPELLANT SURFACE IN HOLDER, AND (7) CIRCULAR ALUMINUM SAMPLE HOLDER.

Figure 4 (b). Components for uncured propellant analysis by X-ray spectrometry.

recommended for the analysis of uncured propellant. A certain amount of art, however, is required to install the Mylar film on the cup properly.

Samples were analyzed in a helium environment either in duplicate or triplicate in conjunction with the appropriate reference standards shown in Table 7. Because only peak X-ray intensity measurements were made for each emission line, either a fixed count or fixed time measurement technique was appropriate. The fixed count technique was used for the majority of measurements in this program so that the counting error variance component could be readily separated from the other sources of error. The number of seconds required to collect a preselected fixed count for the reference standard, t_s, and slurry samples, t_c, were measured in rapid succession at the peak analytical goniometer angle for each ingredient. Average X-ray intensity ratios for each propellant batch, in this case for a single replication of duplicate samples, were calculated by

$$R_{ij} = \frac{1}{4} \sum_{q=1}^{4} \left(\frac{t_s}{t_c} \right)_q \qquad (3)$$

where R_{ij} is the X-ray intensity ratio averaged over samples for the ith ingredient in the jth propellant batch. An example of a typical uncured propellant analysis illustrating the calculation procedure and application of the Mylar correction factors is shown in Table 12.

2. Cured Propellant

Cured propellant samples were analyzed in a manner similar to that described for the uncured samples except that Mylar film was not used, and as mentioned earlier, the samples could be analyzed in either helium or vacuum. Neither the cured nor uncured samples can be analyzed in air because it strongly absorbs the long wavelength fluorescent emission lines from the propellant light elements, particularly the aluminum K_α line.

Some of the sample preparation and handling components for cured propellant analysis are shown in Figure 5. The propellant was initially cured in either wax-coated mailing cartons or Teflon tubing. After curing, the container material was removed and the propellant was sliced into 0.65-cm thick discs using a guillotine built especially for this purpose. A microtome blade was used for cutting; it resulted in very smooth propellant surfaces without pulling large ammonium perchlorate particles from the binder. After slicing the propellant, discs of 3.18-cm diameter were punched out to fit the circular holder for analysis. The surfaces of the propellant discs were analyzed as described for the uncured propellant samples.

TABLE 12. EXAMPLE OF UNCURED PROPELLANT (PBAA) ANALYSIS DATA TREATMENT

Sample	Ferric Oxide		Ammonium Perchlorate			PBAA Polymer			Aluminum			
	(sec)	Ratio	(sec)	Mylar Correction	Ratio	(sec)	Mylar Correction	Ratio	Mylar Standard (sec)	Sample (sec)	Mylar Correction	Ratio
Reference Standard	17.43		12.24			17.20			21.66	22.71		
Sample 1	15.31	1.138	15.31	0.997	0.802	22.11	0.996	0.781	21.95	20.44	0.987	1.126
Sample 2	15.58	1.119	15.30	0.995	0.804	22.45	0.992	0.772	22.21	20.65	0.975	1.128
Reference Standard	17.37		12.23			17.21			21.72	22.77		
Sample 3	15.55	1.117	15.20	1.002	0.803	22.54	1.004	0.760	21.47	20.02	1.012	1.124
Sample 4	15.63	1.111	15.11	1.008	0.803	22.55	1.013	0.753	20.89	19.71	1.040	1.113
Mean Ratio	1.121		0.803			0.767				1.122		
Fixed Counts	50,000		500,000			20,000			500,000	100,000		

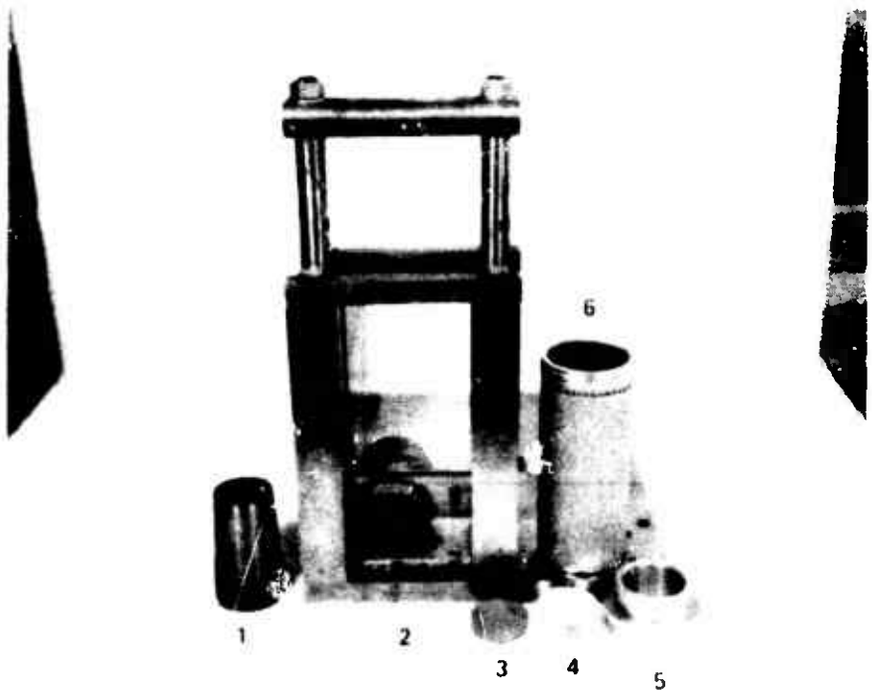

(1) METAL PUNCH FOR CUTTING 3.2-cm PROPELLANT DISC, (2) GUILLOTINE, (3) PROPELLANT SAMPLE, (4) PLEXIGLAS BACKING DISC, (5) CIRCULAR ALUMINUM SAMPLE HOLDER, AND (6) MAILING CARTON IN WHICH PROPELLANT IS CURED.

Figure 5. Components for cured propellant snalysis by X-ray spectrometry.

III. CALIBRATION METHODOLOGY

A. General Considerations

X-ray spectrometry, like many other physical methods, is not absolute. That is, the concentrations and particle sizes of ingredients in unknown propellant samples must be determined with the aid of calibration curves or equations which relate elemental emission line intensities with sizes and concentrations. Although very precise measurements of X-ray emission line intensities can be made by the X-ray fluorescence analysis procedure, accurate elemental determinations are often difficult to achieve because of sample matrix or interelement effects. Thus, simple linear calibration procedures that suffice for a number of other types of spectrometry are generally unsuitable for the X-ray spectrometric analysis of complex mixtures such as propellants. Mitchell [5] has described the qualitative and quantitative aspects of the effects and the associated problems.

Stated simply, a significant sample matrix effect means that the intensity of characteristic radiation from an element in the propellant depends not only on its concentration and particle size but also on the concentrations and particle sizes of all other elements in the sample. The magnitude of these matrix effects can vary markedly depending on the type and relative quantities of elements in the sample. A suitable calibration procedure must accurately compensate for these matrix effects. Three main experimental techniques have been used in X-ray spectrometry to minimize or correct for matrix effects. These are as follows:

1) Addition of one or more internal standards to the sample.

2) Dilution of the sample with an inert component.

3) Restriction of ingredient calibration concentrations and particle sizes to narrow ranges coupled with simple linear calibration.

The first two methods are impractical for the rapid, accurate analysis of production propellants; the last method has limited possibilities.

The most practical calibration approach for propellant analysis is to use mathematical procedures, based on calibration mixtures, to compensate for matrix effects and to estimate unknown ingredient percentages. Many different theoretical and empirical calibration procedures have been developed in the past for application to the X-ray fluorescence analysis problem. Considerable experience in this laboratory with mathematical methods indicates that multiple regression analysis is the best approach to use for propellant applications. The application of multiple regression methods to propellant analysis has been described by Ailey and Myers [6]. Williams [7] gives a discussion of the general problem. Simple, and multiple linear regression methods were considered in this project. Calibration by multiple linear regression analysis is the better approach for production propellant analysis applications.

B. Regression Methods

1. Simple Linear Regression

The simplest calibration method for X-ray fluorescence analysis consists of establishing a relationship for the regression of X-ray intensity, R, from an element on its percentage, X, in a sample mixture; namely,

$$R = a + bX \quad . \tag{4}$$

As already stated, this model is of very limited use in direct propellant analysis because of its failure to account for interelement or matrix effects. When it is applicable, the ingredient percentage in an unknown sample is estimated by inverting Equation (4):

$$\hat{X} = \frac{(R - a)}{b} \quad . \tag{5}$$

Propellant analysis results using Equation (5) are valid for only a very narrow region about the calibration compositions used to determine the intercept, a, and slope, b. If the slope is zero or of negligible magnitude and the slopes for both the calibration and unknown regression lines are assumed to be equal, then the following expression can be derived:

$$\hat{X}_u = \frac{X_s R_u}{R_s} \tag{6}$$

where the subscripts u and s refer to the unknown and calibration propellants, respectively. This expression has potential use in production propellant analysis as a "go-no-go" test. Because the production propellant nominal composition is known, its actual composition can be verified by comparison against a single nominal calibration composition previously analyzed to establish R_s. If R_u agrees with R_s within an acceptable confidence region for each ingredient, then the production batch is accepted. On the other hand, if the actual propellant composition differs significantly from nominal, the determination of $\hat{X}_u$ will be inaccurate because of uncompensated matrix effects.

2. Multiple Linear Regression

Assuming that the functional relationship between the dependent and independent variables is linear over the percentage

ranges of the calibration ingredients, the statistical model for the analyses of four ingredients in a mixture when particle size is held constant is:

$$R_{ij} = B_{i0} + B_{i1} X_{1j} + B_{i2} X_{2j} + B_{i3} X_{3j} + B_{i4} X_{4j} + \epsilon_{ij} \qquad (7)$$

$$(i = 1,2,3,4)$$
$$(j = 1,2,\ldots,n)$$

where R_{ij} is the intensity ratio for the ith ingredient; X_{kj} is the percentage by weight of the kth ingredient in the jth mixture; the B_{ik} are the regression coefficients; and ϵ_{ij} is the random error associated with R_{ij}. The percentage of each ingredient appears in the model no matter which one is being determined. This accounts for mutual absorption and enhancement effects among the ingredients. The coefficients indicate the relative amounts of radiation absorption and enhancement occurring. A negative coefficient indicates absorption; a positive coefficient indicates enhancement.

Equation (7) can be used to develop a set of working expressions for estimating the ingredient concentrations. Equation (7) in matrix notation is:

$$\underline{R} = \underline{b} + B\,\hat{\underline{X}} \qquad (8)$$

where $\underline{R}$ represents the vector of intensity ratios, $\underline{b}$ the vector of intercept terms, B the matrix of regression coefficients, and $\hat{\underline{X}}$ the vector of unknown ingredient concentrations to be determined by analysis. The B_{ik} element of B is the coefficient of X_k in the ith regression equation. Inverting Equation (8) to solve for $\hat{\underline{X}}$ gives:

$$\hat{\underline{X}} = B^{-1} (\underline{R} - \underline{b}) \quad , \qquad (9)$$

assuming that B^{-1} exists. Equation (9) was then used to estimate the X_k's from X-ray intensity ratios, as calculated from Equation (3), with particle sizes held constant. Estimates of ammonium perchlorate and aluminum particle sizes at constant ingredient concentrations were also obtained with Equation (9) by replacing the $\hat{\underline{X}}$ with the particle size value, $\hat{\underline{W}}$. Equation (9) gives more accurate analyses than Equation (5), because it contains terms that correct for matrix effects. Because of the assumed linear relationship, Equation (9) is valid only when propellant ingredient percentages vary over reasonably narrow ranges.

This is perfectly acceptable for the analysis of production propellants. The actual relationship between radiation intensities and ingredient percentages for propellants is curvilinear, but this can be approximated by a linear relationship over limited concentration regions.

The b_{ik} coefficients in Equation (8) were derived by a least squares analysis which involves minimizing the sums of squares of the residual errors. For this analysis, the ingredient percentages, X_k, were chosen as the independent or concomitant variables because they can be controlled and their measurement error is small in comparison to that in the R's. From an experimental standpoint it would be simpler to reverse the role of the X's and R's to estimate the X's directly. However, because the intensities are not controlled and are measured with non-negligible error, this latter approach cannot be used without some danger. The general problem has been discussed by Berkson [8]. The inverse of the model of Equation (8) was used in a few cases during this program, but the pitfalls of using such a model are fully recognized.

The X-ray fluorescence method can also be used to determine ingredient concentrations and particle sizes when both are varied simultaneously [9]. The analysis is restricted, however, to the determination of a number of parameters equal to the number of X-ray intensity measurements made. The particle sizes of ammonium perchlorate, W_2, and aluminum, W_4, were considered here. They were determined as the weight percentages of a fine fraction in a bimodal blend of fine and coarse fractions. As reported earlier, the actual average (weight mean) particle size in the propellant can be determined by referring to an appropriate calibration curve. The main objective in this project was to determine particle size changes quantitatively that could affect the properties of production propellants.

Consider a set of multiple regression equations of the following type:

$$R_{ij} = \sum_{k=0}^{4} [B_{ik}X_{kj}] + B_{i5}W_{2j} + B_{i6}W_{4j} + \epsilon_{ij} \qquad (10)$$

$$(i = 1,2,3,4)$$

where $X_o = 1$. Equation (10) contains both particle size and concentration terms, and can be written in matrix notation as

$$\underline{R} = B_1 \underline{\hat{X}} + B_2 \underline{\hat{W}} \quad . \qquad (11)$$

The intensity ratio vector can now be corrected for either particle size or concentration to solve for one effect in the presence of the other, or to give a combined parameter determination equal to the number of intensity measurements. A complete X-ray analysis will require partial information about the propellant composition from an external source. Solving Equation (11) for concentration, $\underline{X}$, gives

$$\hat{\underline{X}} = B_1^{-1} (\underline{R} - B_2 \underline{W}) \quad , \tag{12}$$

and solving for particle size, $\underline{W}$, gives

$$\hat{\underline{W}} = B_2^{-1} (\underline{R} - B_1 \underline{X}) \quad . \tag{13}$$

As mentioned, the particle size, $\hat{\underline{W}}_i$, is expressed as the weight fraction of fine component i in a bimodal size mixture.

C. Experimental Designs

The selection or preparation of calibration mixtures for the least squares estimation of the b_{ik} coefficients in Equations (8) and (10) is critical to insure that the coefficients are accurately determined [6]. Otherwise, the analyses of unknown propellant compositions might be very inaccurate. In addition, it is desirable to use as small a number of calibration mixtures as practicable because of the amount of labor involved in preparing and analyzing them. The standards, in any event, must be representative of the type of propellant that will be analyzed with the resulting calibration equations.

The regression coefficients can be accurately and efficiently estimated if the calibration mixtures are prepared in accordance with a suitable statistical experimental design. This generally eliminates the problem of confounding of effects and high degrees of correlation among ingredient percentages which obviously must be avoided. Over the years this laboratory has evaluated many different types of experimental designs for application to the propellant analysis calibration problem. Some of these are factorial and fractional factorial designs [10], central composite designs [11], simplex lattice [12] and simplex lattice designs with reference mixtures [13,14], extreme vertices designs [15], and rotatable designs [16] recently developed that are especially applicable to mixture problems similar to the propellant analysis case.

The factorial and fractional factorial designs and the central composite design were used during this program, but in some cases another design might work as well, or better. The appropriate design must be selected by the experimenter depending on the calibration model and the objectives of the experiment.

IV. DETERMINATION OF INGREDIENT CONCENTRATIONS WITH PARTICLE SIZE CONSTANT

A. Low Rate PBAA Propellant

1. Experimental

A half fraction of a 2^4 factorial was used to prepare calibration standards for the model represented by Equation (7). The factors and factor levels are shown in Table 13, and the design data and defining contrasts are shown in Table 14. With this design, it was necessary to use the weights of ingredients as factor levels instead of their percentages. The factor levels were arbitrarily chosen to result in practical ingredient percentage ranges that were still narrow enough to permit a good fit of the linear model to the data.

TABLE 13. FACTORS AND FACTOR LEVELS FOR CALIBRATION PROPELLANT BATCHES (CONSTANT PARTICLE SIZE)

Factor	Symbol	Low Level (g)	High Level (g)
Ferric Oxide	A	4.5	5.5
Ammonium Perchlorate	B	660.0	700.0
PBAA Polymer	C	125.0	145.0
Aluminum	D	150.0	170.0

The treatment combinations in Table 14 for the first eight calibration mixtures form the principal block of the full factorial. Following convention, the high level of each factor in the treatment combination is denoted by the presence of the lower case factor symbol, and the low level by absence of the symbol. When a specific propellant composition is to be analyzed, for example a production propellant, its nominal composition should be placed at the midpoint of the design. This improves the precision of estimating the propellant ingredient percentage. The midpoint composition (Batch 9) was the one of primary interest in this example. In addition to the principal block and midpoint, three more design points represented by Batches 10, 11, and 12 were added to increase the degrees-of-freedom for estimating error.

The actual percentage compositions of the 12 calibration batches that were made in accordance with the design and tested are given in Table 15. Each batch also contained a binder component that could not be analyzed and which is therefore not shown in the table. As a consequence, the ingredient percentages for each batch are independent of each other, which is a requirement for the model used. As shown in Table 15, the bimodal ammonium perchlorate blend, and hence its particle

TABLE 14. DESIGN DATA AND DEFINING CONTRASTS FOR DETERMINING INGREDIENT CONCENTRATIONS IN PBAA PROPELLANT (PARTICLE SIZES CONSTANT)

Batch	Treatment Combination	Ferric Oxide, X_1	Ammonium Perchlorate, X_2	PBAA Polymer, X_3	Aluminum, X_4
1	ab	1	1	-1	-1
2	bc	-1	1	1	-1
3	ad	1	-1	-1	1
4	ac	1	-1	1	-1
5	cd	-1	-1	1	1
6	bd	-1	1	-1	1
7	abcd	1	1	1	1
8	(1)	-1	-1	-1	-1
9	Midpoint	0	0	0	0
10	abd	1	1	-1	1
11	bcd	-1	1	1	1
12	b	-1	1	-1	-1

Defining contrasts: I, ABCD (for Batches 1-9).

TABLE 15. COMPOSITIONS OF CALIBRATION BATCHES (WEIGHT %) FOR DETERMINING INGREDIENT CONCENTRATIONS IN PBAA PROPELLANT (PARTICLE SIZE CONSTANT)

Batch	Treatment Combination	Ferric Oxide, X_1	Ammonium Perchlorate, X_2*	PBAA Polymer, X_3	Aluminum, X_4
1	ab	0.5514	70.18	12.53	15.04
2	b	0.4426	68.84	14.26	14.75
3	ad	0.5631	67.51	12.79	17.39
4	ac	0.5624	67.52	14.83	15.34
5	cd	0.4505	66.10	14.52	17.03
6	bd	0.4425	68.86	12.30	16.72
7	abcd	0.5290	67.34	13.95	16.35
8	(1)	0.4702	69.00	13.07	15.68
9	Midpoint	0.5001	68.07	13.51	16.02
10	abd	0.5379	68.52	12.24	16.64
11	bcd	0.4321	67.26	13.93	16.34
12	b	0.4498	69.96	12.49	14.99

*Bimodal blend of 40% 15-μm ammonium perchlorate and 60% 200-μm ammonium perchlorate.

size, was held constant for all batches. The particle size of the aluminum powder was likewise held constant. Polymers cannot normally be analyzed by X-ray spectrometry. It was possible to analyze the PBAA polymer here because it contains a small percentage of sulfur (approximately 1%) in the polymer chain. However, a recalibration for PBAA polymer must be made if the polymer lot is changed.

The analytical emission lines and instrumental parameters used are given in Table 16. Peak X-ray emission line intensity measurements were made by a fixed count technique, and pulse height discrimination was used to increase the peak-to-background ratios for PBAA polymer and aluminum analyses.

2. Uncured Propellant Results

Four samples of each calibration propellant batch were analyzed. Duplicate samples were analyzed in conjunction with the uncured propellant reference standard, and this analysis was repeated. The individual intensity measurements for the four ingredients from each of the 12 calibration batches are recorded in Table 17 as the seconds required to collect the fixed counts listed in Table 16. These raw data were used to calculate the individual intensity ratios shown in Table 18. The mean X-ray intensity ratios responses, shown in Table 19, were used along with the ingredient percentages in Table 15 to derive the partial regression coefficients for the simple and multiple linear regression models used. The regression analyses were made by computer (CDC-6600) using a stepwise multiple regression program [17].

The regression data obtained by using the simple regression model of Equation (4) are given in Table 20. In addition to the least squares estimates of the coefficients, the table lists the estimated standard error of the coefficient, S_h; Student's "t" for evaluating the significance of the coefficient; the standard error, S_e, for estimating $\hat{R}_I$; and the correlation index, R_I^2. The correlation index, which should not be confused with the X-ray intensity ratio, is the fraction of the total corrected sum of squares among calibration batches that is explained by regression. It measures how well the model fits the data, and has a value of one for a perfect fit.

The fit of the simple linear model is best for the ferric oxide determination. Because iron is relatively heavy compared to the other elements analyzed, it is not affected as much by matrix effects. The simple regression model is unsuitable for ammonium perchlorate and PBAA polymer analyses because of significant matrix effects that are not compensated for by the model. The ferric oxide results for the simple regression model are plotted in Figure 6 to show the scatter of data points about the regression line. Figure 7 compares regression lines using the models of Equations (4) and (6). Analyses using Equation (6)

TABLE 16. INSTRUMENTAL PARAMETERS FOR DETERMINING PBAA PROPELLANT INGREDIENT CONCENTRATIONS (PARTICLE SIZES CONSTANT)

Ingredient	Emission Line	Analyzing Crystal	Peak Angle (deg 2θ)	Fixed Counts		Pulse Height Analysis
				Uncured Propellant	Cured Propellant	
Ferric Oxide	Iron K_α	NaCl	40.20	50,000	50,000	No
Ammonium Perchlorate	Chlorine K_α	NaCl	113.95	500,000	1,000,000	No
PBAA Polymer	Sulfur K_α	NaCl	144.75	20,000	20,000	Yes
Aluminum	Aluminum K_α	PET	144.85	100,000	100,000	Yes

NOTE: Chromium target X-ray tube operated at 40 kV and 30 mA (constant potential), samples rotated. Chlorine K_α for reference standard was measured at 114.05° 2θ.

TABLE 17. X-RAY INTENSITY MEASUREMENTS IN SECONDS FOR FIXED COUNTS* FOR UNCURED PBAA PROPELLANT ANALYSES (CONSTANT PARTICLE SIZE)

Batch	Ferric Oxide	Ammonium Perchlorate	PBAA Polymer	Aluminum
1	17.24	12.31	17.01	24.45
	15.22	13.86	20.57	24.84
	15.27	13.96	20.75	24.79
	17.21	12.31	16.91	24.50
	15.43	13.45	20.62	24.07
	15.38	13.58	20.59	25.16
2	17.19	12.22	16.99	22.78
	18.56	13.73	18.41	22.93
	18.14	13.81	18.03	22.81
	17.17	12.21	17.03	23.05
	18.71	13.84	18.34	23.27
	18.61	13.70	18.31	23.17
3	17.43	12.24	17.20	22.71
	15.31	15.26	22.02	20.17
	15.58	15.22	22.27	20.13
	17.37	12.23	17.21	22.77
	15.55	15.23	22.63	20.26
	15.63	15.23	22.84	20.50
4	17.06	12.32	17.19	24.18
	14.72	14.19	18.70	24.63
	14.68	14.18	18.57	24.80
	17.20	12.32	17.23	24.26
	14.78	14.10	18.52	24.37
	14.71	14.15	18.46	24.75
5	17.00	12.36	17.48	23.38
	18.30	15.17	19.49	20.83
	18.09	15.28	19.15	21.02
	17.06	12.32	17.19	23.53
	17.81	15.61	19.02	21.27
	18.16	15.15	19.16	21.20
6	17.17	12.30	17.27	23.13
	19.01	14.85	23.00	21.28
	18.82	14.90	22.86	21.36
	16.98	12.26	17.42	23.49
	18.77	14.77	22.81	21.07
	18.96	14.56	22.67	21.10

TABLE 17. (Concluded)

Batch	Ferric Oxide	Ammonium Perchlorate	PBAA Polymer	Aluminum
7	17.13	12.25	17.22	22.81
	15.95	14.57	19.82	21.10
	16.08	14.54	19.88	21.19
	17.21	12.28	17.41	22.82
	15.98	14.73	20.11	20.96
	16.11	14.55	20.15	20.97
8	16.95	12.13	17.52	22.58
	18.09	13.75	21.71	22.12
	17.67	13.96	21.09	21.97
	17.04	12.13	17.67	22.61
	17.80	13.80	21.46	21.92
	17.55	14.06	21.51	21.83
9	17.18	12.29	17.32	23.20
	16.73	14.62	20.75	21.89
	16.89	14.58	20.97	22.06
	17.15	12.29	17.28	23.34
	16.92	14.59	20.67	21.75
	16.87	14.52	20.53	22.18
10	17.50	12.48	17.59	23.05
	16.33	15.45	23.82	20.94
	16.19	15.25	23.72	20.97
	17.72	12.46	17.93	23.18
	16.49	15.40	24.04	21.14
	16.55	15.30	23.98	21.25
11	17.30	12.27	17.56	23.08
	19.19	14.53	20.31	21.22
	19.06	14.80	20.42	21.45
	17.32	12.28	17.79	22.97
	19.31	14.75	20.75	21.20
	19.33	14.93	20.67	21.43
12	17.15	12.30	17.43	23.93
	18.72	13.63	21.81	24.47
	18.58	13.79	21.44	24.20
	17.26	12.34	17.66	24.17
	18.18	13.95	21.52	24.13
	18.39	13.93	21.60	24.57

*Table 16 contains the fixed counts used.

TABLE 18. X-RAY INTENSITY RATIOS FOR UNCURED PBAA PROPELLANT ANALYSES (CONSTANT PARTICLE SIZE)

Batch	Ferric Oxide	Ammonium Perchlorate	PBAA Polymer	Aluminum
1	1.1327	0.8883	0.8269	0.9842
	1.1290	0.8821	0.8196	0.9864
	1.1154	0.9151	0.8199	1.0179
	1.1190	0.9065	0.8213	0.9738
2	0.9262	0.8903	0.9227	0.9934
	0.9476	0.8846	0.9422	0.9988
	0.9177	0.8824	0.9283	0.9905
	0.9226	0.8916	0.9301	0.9947
3	1.1385	0.8019	0.7810	1.1257
	1.1187	0.8040	0.7723	1.1279
	1.1170	0.8030	0.7605	1.1239
	1.1113	0.8030	0.7534	1.1108
4	1.1590	0.8685	0.9191	0.9819
	1.1621	0.8689	0.9259	0.9751
	1.1637	0.8740	0.9302	0.9956
	1.1693	0.8708	0.9335	0.9801
5	0.9290	0.8145	0.8968	1.1223
	0.9397	0.8089	0.9129	1.1124
	0.9579	0.7892	0.9038	1.1063
	0.9394	0.8130	0.8969	1.1098
6	0.9032	0.8280	0.7508	1.0870
	0.9123	0.8255	0.7555	1.[illegible]8
	0.9046	0.8299	0.7637	1.1146
	0.8956	0.8420	0.7684	1.1132
7	1.0740	0.8409	0.8690	1.0808
	1.0653	0.8427	0.8663	1.0766
	1.0770	0.8337	0.8657	1.0887
	1.0683	0.8441	0.8640	1.0882
8	0.9370	0.8820	0.8068	1.0207
	0.9592	0.8686	0.8306	1.0279
	0.9573	0.8792	0.8232	1.0314
	0.9709	0.8626	0.8216	1.0358
9	1.0269	0.8407	0.8348	1.0598
	1.0172	0.8431	0.8260	1.0516
	1.0136	0.8423	0.8358	1.0728
	1.0166	0.8464	0.8416	1.0522

TABLE 18. (Concluded)

Batch	Ferric Oxide	Ammonium Perchlorate	PBAA Polymer	Aluminum
10	1.0716	0.8080	0.7383	1.1006
	1.0809	0.8181	0.7415	1.0989
	1.0746	0.8089	0.7458	1.0965
	1.0707	0.8144	0.7477	1.0909
11	0.9015	0.8443	0.8645	1.0878
	0.9077	0.8289	0.8593	1.0758
	0.8969	0.8323	0.8572	1.0837
	0.8960	0.8223	0.8608	1.0717
12	0.9161	0.9024	0.7992	0.9779
	0.9230	0.8921	0.8128	0.9889
	0.9494	0.8847	0.8206	1.0016
	0.9386	0.8861	0.8177	0.9836

TABLE 19. MEAN X-RAY INTENSITY RATIOS FOR UNCURED PBAA PROPELLANT ANALYSES (CONSTANT PARTICLE SIZE)

Batch	Ferric Oxide R_1	Ammonium Perchlorate R_2	PBAA Polymer R_3	Aluminum R_4
1	1.1240	0.8980	0.8219	0.9906
2	0.9285	0.8872	0.9308	0.9944
3	1.1214	0.8030	0.7668	1.1221
4	1.1635	0.8706	0.9272	0.9832
5	0.9415	0.8064	0.9026	1.1127
6	0.9039	0.8314	0.7596	1.0994
7	1.0712	0.8404	0.8662	1.0836
8	0.9561	0.8731	0.8206	1.0290
9	1.0186	0.8431	0.8346	1.0591
10	1.0744	0.8124	0.7432	1.0967
11	0.9005	0.8320	0.8606	1.0798
12	0.9318	0.8913	0.8126	0.9880

TABLE 20. SIMPLE REGRESSION DATA FOR UNCURED PBAA PROPELLANT ANALYSES (CONSTANT PARTICLE SIZE)

Ingredient	Coefficient Level	Coefficient	S_b	t	S_e	R^2
Ferric Oxide	b_{10}	0.10722				
	b_{11}	1.82900	0.08074	22.65296	0.01386	0.98088
Ammonium Perchlorate	b_{20}	-0.56622				
	b_{22}	0.02073	0.00621	3.33816	0.02447	0.52745
PBAA Polymer	b_{30}	-0.01354				
	b_{33}	0.06364	0.00797	7.98494	0.02427	0.86446
Aluminum	b_{40}	0.09166				
	b_{44}	0.06001	0.00449	13.36525	0.01283	0.94702

$$\hat{R}_i = b_{io} + b_{ii}X_i$$

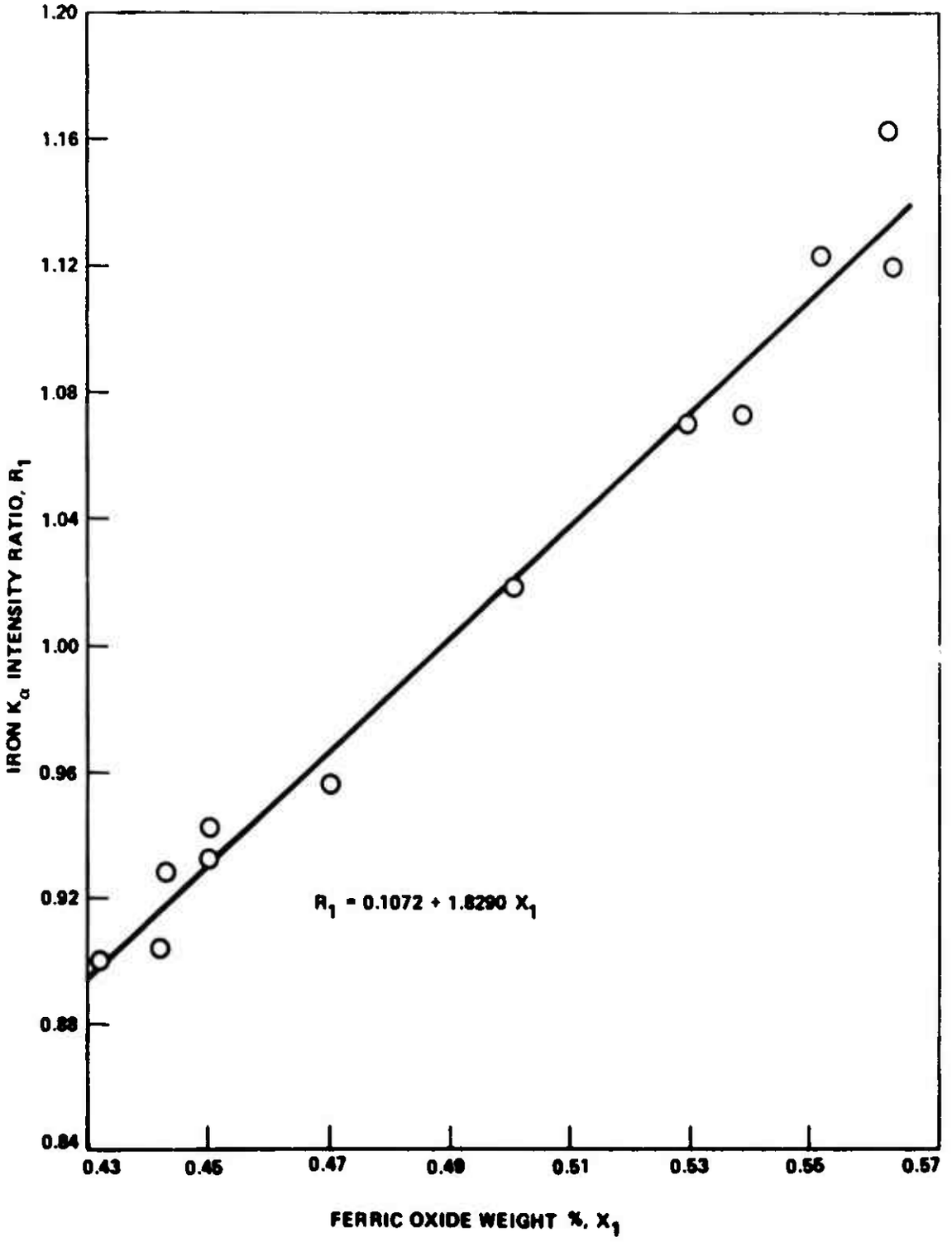

Figure 6. Simple calibration curve for ferric oxide concentration in uncured PBAA propellants.

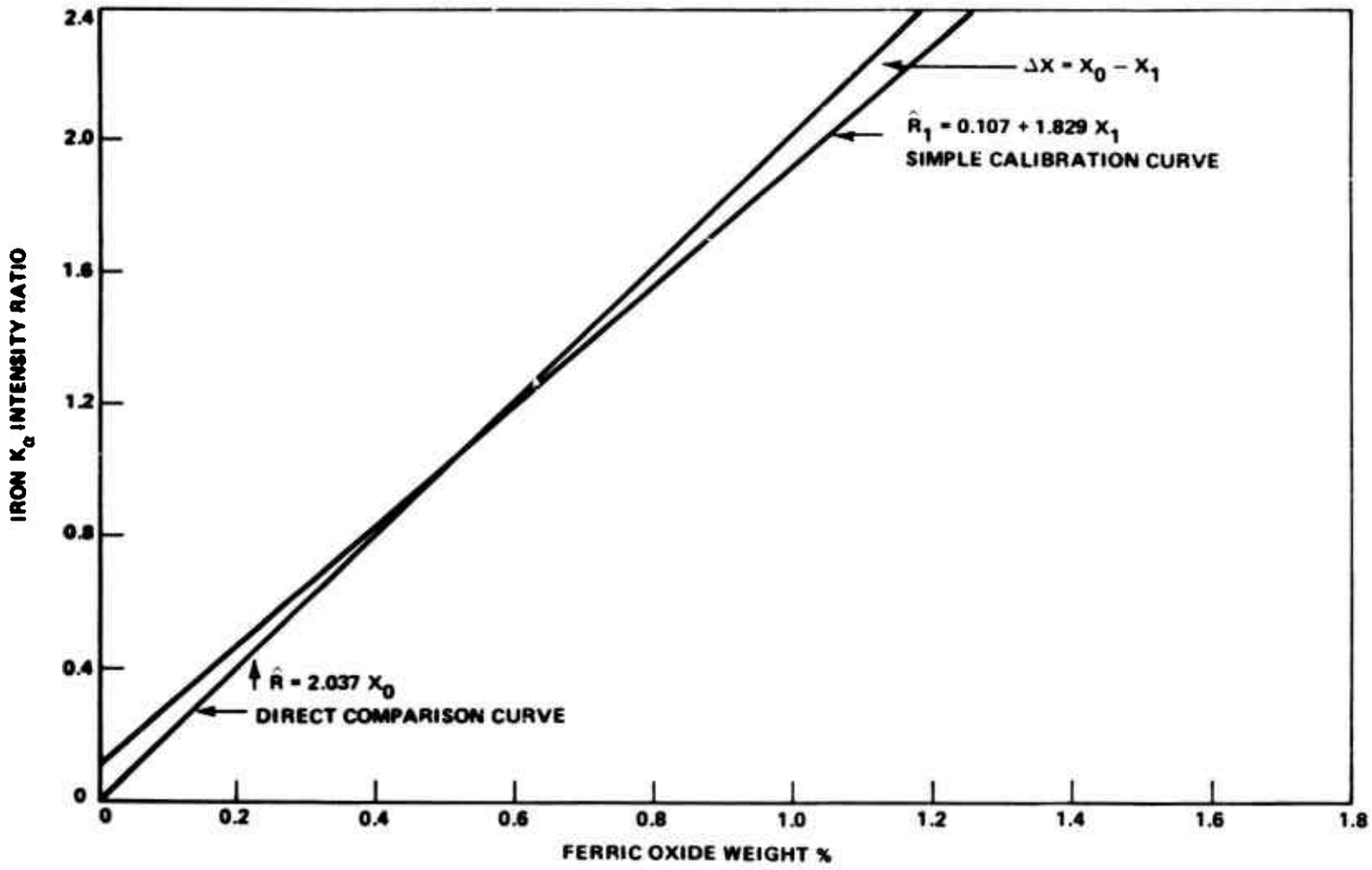

Figure 7. Simple and direct calibration curves for determining nominal 0.5 weight% ferric oxide in uncured PBAA propellant.

are often referred to as direct comparison analyses, because the unknown is compared directiy with the known composition (standard) that is being controlied in practice. The error of the determination becomes greater as the unknown ferric oxide percentage varies from the 0.5% weight nominai value. The same reasoning appiies to the determination of the other ingredients except that the added effects of matrix interactions must aiso be considered. The ammonium perchiorate data from Table 20 are plotted in Figure 8. The large scatter of data about the regression line was indicated by the large value of S_e and the smaii vaiue of R^2 in Table 20. The inverted equation coefficients for estimating ingredient percentages, as well as the reiative and root-mean-square errors (RMSE) for estimating the ingredient percentages are shown in Tabie 2i.

TABLE 2i. SIMPLE EQUATIONS FOR ESTIMATING INGREDIENT CONCENTRATIONS IN UNCURED PBAA PROPELLANTS (CONSTANT PARTICLE SIZE)

$$\hat{X}_i = d_{io} + d_{ii}R_i \quad .$$

Ingredient Estimated	Measured Intensity Ratio	Coefficient Level	Coefficient	Relative Error (%)	RMSE
Ferric Oxide, $\hat{X}_1$		d_{10}	-0.05862		
	R_1	d_{11}	0.54674	i.i57	0.00691
Ammonium Perchlorate, $\hat{X}_2$		d_{20}	27.31403		
	R_2	d_{22}	48.23926	1.234	i.07700
PBAA Poiymer, $\hat{X}_3$		d_{30}	0.2i275		
	R_3	d_{33}	i5.71338	2.122	0.34785
Aluminum, $\hat{X}_4$		d_{40}	-i.52741		
	R_4	d_{44}	16.66388	0.922	0.19519

Far more accurate estimates of ingredient percentages can be made usIng the iinear multiple regression modei of Equation (7) which has terms to compensate for matrix effects. The data for the multiple regression response function resulting from the use of Equation (7) are given in Table 22. The standard errors, S_e, and the correlation indices, R_1^2, show an improvement over the simple response function data in Table 20 for all ingredients. The improvement was greatest, however, for the PBAA polymer and ammonium perchlorate determinations.

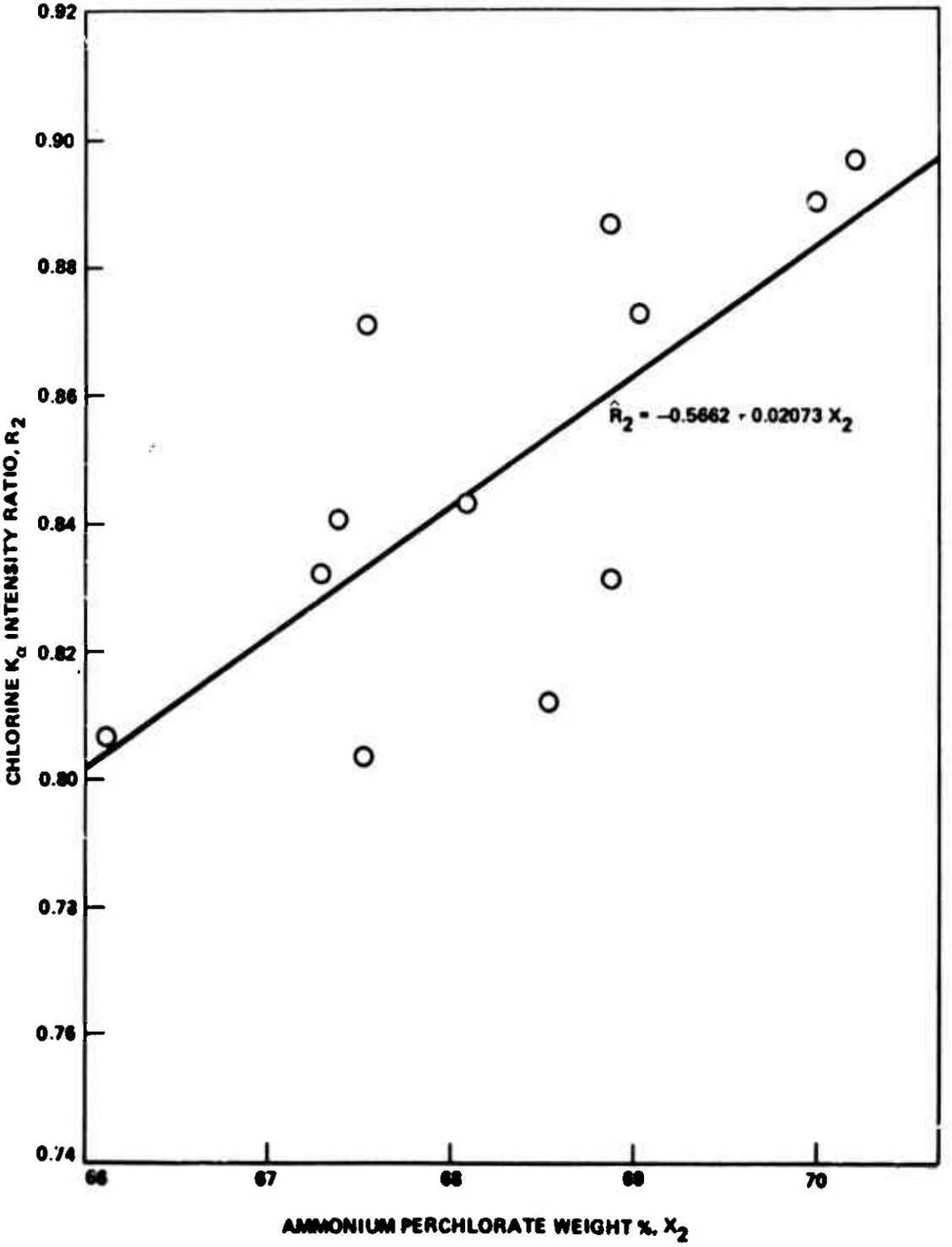

Figure 8. Simple calibration curve for ammonium perchlorate concentration in uncured PBAA propellants.

TABLE 22. MULTIPLE REGRESSION DATA FOR UNCURED PBAA PROPELLANT ANALYSES (CONSTANT PARTICLE SIZE)

$$R_1 = b_{10} + b_{11}X_1 + b_{12}X_2 + b_{13}X_3 + b_{14}X_4$$

Ingredient	Coefficient Level	Coefficient	S_b	t	S_e	R^2
Ferric Oxide	b_{10}	0.15411			0.00768	0.99589
	b_{11}	1.85730	0.04526	41.03623		
	b_{12}	-0.00074	0.01592	-0.04648		
	b_{13}	0.00919	0.01576	0.58312		
	b_{14}	-0.00832	0.01646	-0.50546		
Ammonium Perchlorate	b_{20}	-1.43740			0.00776	0.96675
	b_{21}	0.01832	0.04573	0.40061		
	b_{22}	0.03020	0.01609	1.87694		
	b_{23}	0.02561	0.01592	1.60866		
	b_{24}	-0.00790	0.01663	-0.47504		
PBAA Polymer	b_{30}	-1.51670			0.01130	0.97944
	b_{31}	-0.07426	0.06658	-1.11534		
	b_{32}	0.02008	0.02342	0.85738		
	b_{33}	0.08024	0.02318	3.46160		
	b_{34}	-0.00328	0.02421	-0.13548		
Aluminum	b_{40}	0.60788			0.01265	0.96398
	b_{41}	-0.13257	0.07454	-1.77850		
	b_{42}	-0.00442	0.02623	-0.16850		
	b_{43}	-0.00641	0.02595	-0.24701		
	b_{44}	0.05605	0.02711	2.06750		

The regression equations, in algebraic form, for estimating the $\hat{R}_i$'s with all the X_k's present are as follows:

$$\hat{R}_1 = 0.154 + 1.857\ X_1 - 0.00074\ X_2 + 0.00919\ X_3 - 0.00832\ X_4$$

$$\hat{R}_2 = -1.437 + 0.0183\ X_1 + 0.0302\ X_2 + 0.0256\ X_3 - 0.0079\ X_4 \qquad (14)$$

$$\hat{R}_3 = 1.517 - 0.0743\ X_1 + 0.0201\ X_2 + 0.0802\ X_3 - 0.00328\ X_4$$

$$\hat{R}_4 = 0.608 - 0.1326\ X_1 - 0.00442\ X_2 - 0.00641\ X_3 + 0.05605\ X_4 \quad .$$

The corrected sums of squares and cross products obtained during the regression analysis are listed in Tables 23(A) and 23(B).

TABLE 23(A). CORRECTED SUMS OF SQUARES AND CROSS PRODUCTS (a_{kl}) FOR UNCURED PBAA PROPELLANT ANALYSES (CONSTANT PARTICLE SIZE)

$a_{11} = 0.02947$	$a_{12} = -0.01256$	$a_{13} = -0.04654$	$a_{14} = 0.05013$
$a_{21} = -0.01256$	$a_{22} = 15.55322$	$a_{23} = -8.00854$	$a_{24} = -7.35425$
$a_{31} = -0.04654$	$a_{32} = -8.00854$	$a_{33} = 9.27685$	$a_{34} = -1.01920$
$a_{41} = 0.05013$	$a_{42} = -7.35425$	$a_{43} = -1.01920$	$a_{44} = 8.17828$

TABLE 23(B). INVERSE OF a_{kl}'s (c_{kl}) FOR UNCURED PBAA PROPELLANT ANALYSES (CONSTANT PARTICLE SIZE)

$c_{11} = 34.72988$	$c_{12} = 1.00642$	$c_{13} = 1.13464$	$c_{14} = 0.83355$
$c_{21} = 1.00642$	$c_{22} = 4.29894$	$c_{23} = 4.19776$	$c_{24} = 4.38275$
$c_{31} = 1.13464$	$c_{32} = 4.19776$	$c_{33} = 4.20892$	$c_{34} = 4.29237$
$c_{41} = 0.83355$	$c_{42} = 4.38275$	$c_{43} = 4.29237$	$c_{44} = 4.59324$

The inverse working equations for estimating ingredient percentages from measured X-ray intensity ratios are shown in Table 24. In algebraic form they are as follows:

$$\hat{X}_1 = -0.1438 + 0.5406\ R_1 + 0.07935\ R_2 - 0.0803\ R_3 + 0.0867\ R_4$$

$$\hat{X}_2 = 38.26 - 0.5767\ R_1 + 42.57\ R_2 - 13.11\ R_3 + 5.148\ R_4$$

$$\hat{X}_3 = 8.902 + 0.6984\ R_1 - 10.48\ R_2 + 15.69\ R_3 - 0.4547\ R_4 \qquad (15)$$

$$\hat{X}_4 = -7.152 + 1.313\ R_1 - 2.345\ R_2 + 0.5705\ R_3 + 18.40\ R_4 \quad .$$

Using Equations (15), the percentages of all four ingredients can be determined with a relative error of less than 1%. This type of accuracy would provide for excellent control of propellant compositions during a manufacturing operation. The estimated ingredient percentages for each propellant batch, using Equations (15), and the absolute (residual) errors of the estimates are shown in Table 25.

The estimated coefficients in Equations (14) can be tested by standard statistical methods to ascertain whether they are significantly different from zero. Those that are not can be omitted from the equations during the least squares analysis presumably to improve the precision of estimating the R_{ij}'s. The stepwise multiple regression computer program readily performs this operation. The resulting equations, giving the smallest calculated errors of estimation and containing only statistically significant coefficients, are called the best set for estimating the R_{ij}'s. This best set of regression equations cannot always be inverted, however, and even when they can, there is no assurance that they will produce a better set of working equations for estimating the X_k's than the set of Equations (15). The best sets of multiple regression data for this experiment are shown in Table 26. Comparison of these data with those in Table 22 for the full model shows that the best sets provide only a slight improvement.

All of the coefficients except that for the analyte in each of the Equations (14) can be interpreted as correction factors for the effects of sample matrix ingredients on the X-ray intenaity ratio. This can be illustrated by considering the equation for $\hat{R}_2$ (ammonium perchlorate) in Table 26. If the $\hat{R}_2$'s are adjusted for the departure of the individual X_3's from the mean $\bar{X}_3$ over all calibration standarda, the equation becomes

TABLE 24. EQUATIONS FOR ESTIMATING INGREDIENT CONCENTRATIONS IN UNCURED PBAA PROPELLANTS (CONSTANT PARTICLE SIZE)

$$X_i = d_{i0} + d_{i1}R_1 + d_{i2}R_2 + d_{i3}R_3 + d_{i4}R_4$$

Ingredient Estimated	Measured Intensity Ratio	Coefficient Level	Coefficient	Relative Error (%)	RSME
Ferric Oxide, X_1		d_{10}	-0.14381	0.467	0.00253
	R_1	d_{11}	0.54061		
	R_2	d_{12}	0.07935		
	R_3	d_{13}	-0.08034		
	R_4	d_{14}	0.08670		
Ammonium Perchlorate, X_2		d_{20}	38.26196	0.255	0.23721
	R_1	d_{21}	-0.57673		
	R_2	d_{22}	32.56902		
	R_3	d_{23}	-13.11162		
	R_4	d_{24}	5.14778		
PBAA Polymer, X_3		d_{30}	8.90163	0.861	0.13843
	R_1	d_{31}	0.69836		
	R_2	d_{32}	-10.48292		
	R_3	d_{33}	15.69262		
	R_4	d_{34}	-0.55369		
Aluminum, X_4		d_{40}	-7.15234	0.896	0.16969
	R_1	d_{41}	1.31310		
	R_2	d_{42}	2.35481		
	R_3	d_{43}	0.52056		
	R_4	d_{44}	18.40104		

TABLE 25. ESTIMATED CONCENTRATIONS AND RESIDUAL ERRORS FOR INGREDIENTS IN UNCURED PBAA PROPELLANTS

Batch	Ferric Oxide		Ammonium Perchlorate		PBAA Polymer		Aluminum	
	Weight (%)	Error	Weight (%)	Error	Weight (%)	Error	Weight (%)	Error
1	0.5549	0.0035	70.16	-0.02	12.72	0.19	15.13	0.09
2	0.4400	-0.0026	68.41	-0.43	14.40	0.14	14.98	0.23
3	0.5618	-0.0013	67.52	0.01	12.79	0	17.29	-0.10
4	0.5650	0.0026	67.56	0.04	14.69	-0.14	15.04	-0.30
5	0.4531	0.0026	65.94	-0.16	14.76	0.24	16.96	-0.07
6	0.4451	0.0026	68.83	-0.03	12.24	-0.06	16.65	-0.07
7	0.5263	-0.0027	67.64	0.30	13.94	-0.01	16.66	0.31
8	0.4656	-0.0046	69.42	0.42	12.83	-0.24	15.55	-0.13
9	0.4985	-0.0016	68.07	0	13.39	-0.12	16.13	0.11
10	0.5368	-0.0011	68.13	-0.39	12.30	0.06	16.77	0.13
11	0.4335	0.0014	67.43	0.17	13.82	-0.11	16.34	0
12	0.4510	0.0012	70.10	0.14	12.51	0.02	14.80	-0.19

TABLE 26. BEST SETS OF MULTIPLE REGRESSION DATA FOR UNCURED PBAA PROPELLANT ANALYSES (CONSTANT PARTICLE SIZE)

$$\hat{R}_i = b_{i0} + b_{i1}X_1 + b_{i2}X_2 + b_{i3}X_3 + b_{i4}X_4$$

Ingredient	Coefficient Level	Coefficient	S_b	t	S_e	R^2
Ferric Oxide	b_{10}	0.08175			0.00719	0.99589
	b_{11}	1.85750	0.04220	44.01658		
	b_{13}	0.00992	0.00238	4.16806		
	b_{14}	-0.00756	0.00254	-2.97637		
Ammonium Perchlorate	b_{20}	-2.15740			0.00703	0.96487
	b_{22}	0.03762	0.00239	15.74058		
	b_{23}	0.03280	0.00310	10.58064		
PBAA Polymer	b_{30}	-1.82470			0.01058	0.97940
	b_{31}	-0.07366	0.06221	-1.18405		
	b_{32}	0.02321	0.00362	6.41160		
	b_{33}	0.08331	0.00470	17.72553		
Aluminum	b_{40}	0.14262			0.01138	0.96255
	b_{41}	-0.12865	0.06660	-1.93168		
	b_{44}	0.06079	0.00400	15.19750		

$$\text{ADJ } \hat{R}_2 = \hat{R}_2 - 0.03280\ (X_3 - \overline{X}_3) = -2.157 + 0.03762\ X_2 + 0.03280\ \overline{X}_3 \quad . \tag{16}$$

The regression line represented by Equation (16) and the ammonium perchlorate data points for the calibration batches are given in Figure 9. The marked reduction in data scatter about the regression line for ammonium perchlorate by applying a matrix correction for the PBAA polymer concentration, X_3, is evident by comparing Figures 8 and 9.

Another linear model that might be considered is one that includes two-factor (first order) interactions such as that shown in Table 27. This model was fitted to the data to determine whether the resulting response function would give a more precise estimate of the $\hat{R}_i$ than Equations (14). These regression equations cannot be inverted in a straightforward manner to allow estimation of the ingredient percentages. A significant two-factor interaction means that nonparallelism exists between the regression lines or planes involved. Over the relatively narrow ingredient concentration ranges that would be used for the analysis of production propellants, the two-factor interactions can generally be disregarded.

3. Analysis of Variance

An analysis of variance [18] for the uncured PBAA propellant results (Table 28) was made to evaluate the various sources of error, and to permit later resolution of error variance components. The total sum of squares for variation among the propellant batches has been partitioned into the residual sum of squares, $(SS_E)_1$, and the sum of squares for regression, $(SSReg)_i$. The sum of squares for regression were determined as follows:

$$(SSReg)_i = \sum_{k=1}^{4} b_{ik}\ a_{ikR} \tag{17}$$

where a_{ikR} is the corrected sums of cross products of the R_{ij} with X_{kj} from the raw data. The a_{ikR} were obtained from the corrected sum of cross products (or the sum of squares when $1 = k$) listed in Table 23(A). The residual sums of squares were calculated from

$$(SS_E)_i = \sum_{j=1}^{n} (R_{ij} - \hat{R}_{ij})^2 \quad . \tag{18}$$

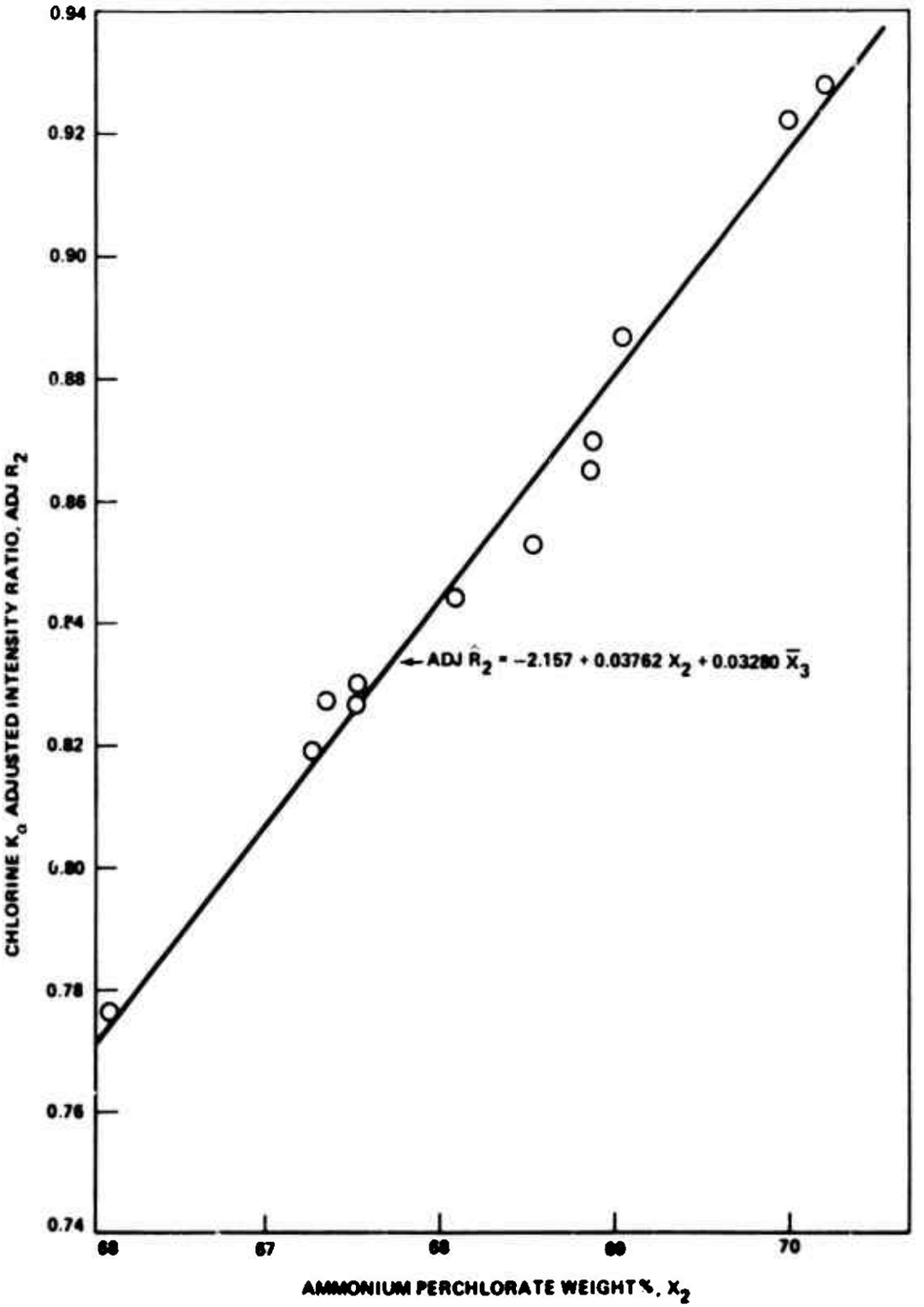

Figure 9. Adjusted calibration curve for ammonium perchlorate concentration in uncured PBAA propellant.

TABLE 27. MULTIPLE REGRESSION DATA WITH CROSS PRODUCTS FOR UNCURED PBAA PROPELLANT ANALYSES (CONSTANT PARTICLE SIZE)

$$\dot{R}_i = b_{i0} + b_{i1}X_1 + \ldots + b_{i4}X_4 + b_{i5}X_1X_2 + \ldots + b_{i10}X_3X_4$$

Ingredient	Coefficient Level	Coefficient	S_b	t	S_e	R^2
Ferric Oxide	b_{10}	-0.26659			0.00606	0.99744
	b_{11}	3.13040	0.62807	4.98415		
	b_{14}	0.06194	0.01950	3.17641		
	b_{17}	-0.07942	0.03908	-2.03224		
	b_{19}	-0.00058	0.00013	-4.46153		
Ammonium Perchlorate	b_{20}	-1.18490			0.00609	0.97954
	b_{22}	0.03941	0.01336	2.94985		
	b_{23}	-0.05136	0.03742	-1.37252		
	b_{24}	-0.06994	0.03130	-2.23450		
	b_{210}	0.00537	0.00248	2.16532		
PBAA Polymer	b_{30}	-12.00300			0.00548	0.99586
	b_{32}	0.17024	0.03305	5.15098		
	b_{33}	0.08857	0.01124	7.87989		
	b_{34}	0.61861	0.12963	4.77212		
	b_{36}	-0.00410	0.00244	-1.68032		
	b_{39}	-0.00901	0.00187	-4.81818		
Aluminum	b_{40}	-1.07180			0.00998	0.97756
	b_{41}	1.34190	0.63011	2.12962		
	b_{43}	0.07213	0.02422	2.97811		
	b_{46}	-0.11051	0.04712	-2.34528		
	b_{49}	0.00112	0.00007	16.11100		

TABLE 28. ANALYSIS OF VARIANCE FOR UNCURED PBAA PROPELLANT ANALYSES (CONSTANT PARTICLE SIZE)

Source of Variation	Degrees of Freedom	Ferric Oxide		Ammonium Perchlorate		PBAA Polymer		Aluminum	
		Sum of Squares	Mean Square	Sum of Squares	Mean Square	Sum of Squares	Mean Square	Sum of Squares	Mean Square
Among B's	11								
Regression (4)		0.400422	0.100106	0.049014	0.012253	0.170274	0.042568	0.119896	0.029974
Residual (7)		0.001650	0.000236	0.001686	0.000240	0.003574	0.000510	0.004480	0.000640
Between T's	1	0.000004	0.000004	0	0	0.000027	0.000027	0.000221	0.000221
BxT (Exp Error)	11	0.001946	0.000176	0.001172	0.000106	0.000896	0.000081	0.001407	0.000127
Sampling Error	24	0.001416	0.000059	0.001081	0.000045	0.000953	0.000040	0.001969	0.000082
Total	47	0.405438		0.052953		0.175724		0.127973	

The least squares analysis minimized this expression. The standard error, $(S_E)_i$, was obtained from the residual sum of squares:

$$(S_E)_i = \left[\frac{(SS_E)_i}{(n - p - 1)} \right]^{1/2} \qquad (19)$$

where n is the number of calibration standards analyzed (12 in this case), p is the number of degrees of freedom for regression, and n - p - 1 is the number of degrees of freedom for residual error. One degree of freedom is required for each term in the regression model. Consequently, it is desirable to analyze a large number of calibration batches so that there will be adequate degrees of freedom remaining for estimating the residual mean squares and standard errors.

The best estimate of experimental error here is considered to be the interaction between calibration batches, B, and sample pairs, T. The sampling error was calculated from the 24 duplicate sample analyses and represents sample repeatability with the instrumental operating conditions essentially fixed.

The validity of the linearity assumption and the selected model can be checked by testing the significance of the residual mean squares. The residual errors for both PBAA polymer and aluminum analyses are significant at the 5% ($\alpha = 0.05$) significance level. This significance might be partly due to the fact that the BXT interaction is an underestimate of the true random experimental error. The variation among batches, B, is significant for all ingredients. This is an expected result because the compositions were purposely varied by the experimental design.

4. Cured Propellant Results

X-ray fluorescence spectrometry is of primary interest for the rapid, accurate analyses of uncured propellants during their manufacture. At that stage, substandard compositions can either be corrected or discarded without serious consequences. Nevertheless, there are often times when problems arise during production or motor storage and surveillance that an analysis of the cured propellant is either necessary or very desirable. For this reason, techniques were also developed during this program for the analysis of cured PBAA propellants. Similar techniques can also be applied to other types of cured propellants.

The raw intensity measurements and the individual and average X-ray intensity ratios for analyses of the 12 calibration batches (Table 15) are recorded in Tables 29, 30, and 31. It is interesting to compare the intensities of analytical emission lines from uncured and cured propellants having the same compositions as shown in Tables 17 and 29. The concentrations of ferric oxide and PBAA polymer are

TABLE 29. X-RAY INTENSITY MEASUREMENTS IN SECONDS FOR FIXED COUNTS* FOR CURED PBAA PROPELLANT ANALYSES (CONSTANT PARTICLE SIZE)

Batch	Ferric Oxide	Ammonium Perchlorate	PBAA Polymer	Aluminum
1	22.25	14.13	19.74	16.66
	19.73	14.39	26.92	15.16
	20.01	14.31	26.80	15.36
	22.13	14.05	19.98	16.57
	19.98	14.28	27.00	15.40
	20.04	14.26	27.15	15.61
2	22.67	14.43	21.01	18.76
	24.78	14.75	26.13	18.02
	25.06	14.80	25.92	17.82
	22.65	14.38	20.86	18.76
	24.97	14.73	26.19	17.90
	24.68	14.72	26.32	17.84
3	22.78	14.44	21.08	18.92
	20.71	14.91	32.32	15.83
	20.61	15.12	31.58	15.57
	22.48	14.39	21.21	18.62
	20.76	15.02	31.88	15.46
	20.15	15.13	31.71	15.21
4	22.78	14.45	21.89	18.81
	19.86	15.21	27.15	16.67
	19.72	15.57	25.52	16.59
	22.86	14.42	21.56	18.77
	19.48	15.37	25.42	16.66
	19.76	15.19	25.30	16.77
5	22.71	14.53	20.75	17.07
	23.62	15.71	25.23	13.82
	23.75	15.60	25.50	13.98
	22.47	14.49	20.64	17.19
	24.03	15.34	25.76	14.43
	23.98	15.47	25.72	14.24
7	22.56	14.48	20.90	17.04
	21.13	15.14	26.78	14.67
	20.81	15.20	26.85	14.66
	22.63	14.43	20.61	17.08
	20.94	15.27	26.56	14.60
	20.88	15.17	26.92	14.88

TABLE 29. (Concluded)

Batch	Ferric Oxide	Ammonium Perchlorate	PBAA Polymer	Aluminum
9	22.76	14.44	20.83	17.19
	22.41	14.99	28.22	15.33
	22.28	15.02	28.24	15.35
	22.43	14.39	20.92	17.14
	22.44	14.92	28.02	15.53
	22.58	14.78	28.22	15.42
10	22.67	14.43	20.59	18.74
	21.12	14.78	31.68	16.27
	21.43	14.79	31.29	16.32
	22.53	14.41	20.78	18.97
	21.25	14.84	30.61	16.39
	21.03	14.90	30.78	16.35
11	22.72	14.44	21.60	18.62
	24.89	15.24	28.39	15.85
	25.07	15.21	28.41	15.89
	22.79	14.42	21.20	18.79
	25.69	15.00	29.03	16.30
	25.36	15.14	28.40	16.08
12	22.95	14.40	21.84	18.82
	24.70	14.55	31.68	17.88
	24.96	14.40	31.53	17.76
	22.66	14.35	21.79	18.72
	24.85	14.51	31.10	17.73
	24.81	14.52	31.94	17.80

*Table 16 contains fixed counts used.

TABLE 30. X-RAY INTENSITY RATIOS FOR CURED PBAA PROPELLANT ANALYSES (CONSTANT PARTICLE SIZE)

Batch	Ferric Oxide	Ammonium Perchlorate	PBAA Polymer	Aluminum
1	1.1277	0.9819	0.7333	1.0989
	1.1119	0.9874	0.7366	1.0846
	1.1076	0.9839	0.7400	1.0760
	1.1043	0.9853	0.7359	1.0615
2	0.9148	0.9783	0.8040	1.0411
	0.9046	0.9750	0.8106	1.0527
	0.9071	0.9762	0.7965	1.0480
	0.9176	0.9766	0.7926	1.0514
3	1.1000	0.9685	0.6522	1.1952
	1.1053	0.9550	0.6675	1.2152
	1.0828	0.9580	0.6653	1.2044
	1.1158	0.9508	0.6688	1.2241
4	1.1468	0.9503	0.8062	1.1284
	1.1552	0.9281	0.8578	1.1338
	1.1735	0.9382	0.8482	1.1266
	1.1569	0.9493	0.8522	1.1193
5	0.9615	0.9249	0.8224	1.2352
	0.9562	0.9314	0.8137	1.2210
	0.9351	0.9446	0.8012	1.1913
	0.9370	0.9366	0.8025	1.2072
7	1.0681	0.9564	0.7804	1.1616
	1.0846	0.9526	0.7784	1.1623
	1.0807	0.9450	0.7760	1.1699
	1.0838	0.9512	0.7656	1.1478
9	1.0156	0.9633	0.7381	1.1213
	1.0215	0.9614	0.7376	1.1199
	0.9996	0.9645	0.7466	1.1037
	0.9932	0.9739	0.7413	1.1113
10	1.0733	0.9760	0.6499	1.1519
	1.0579	0.9756	0.6580	1.1483
	1.0602	0.9710	0.6789	1.1544
	1.0713	0.9671	0.6751	1.1572

TABLE 30. (Concluded)

Batch	Ferric Oxide	Ammonium Perchlorate	PBAA Polymer	Aluminum
11	0.9127	0.9476	0.7607	1.1746
	0.9063	0.9494	0.7603	1.1718
	0.8871	0.9613	0.7303	1.1528
	0.8986	0.9524	0.7465	1.1685
12	0.9291	0.9897	0.6894	1.0526
	0.9195	1.0000	0.6927	1.0597
	0.9119	0.9848	0.7006	1.0558
	0.9133	0.9883	0.6822	1.0517

TABLE 31. MEAN X-RAY INTENSITY RATIOS FOR CURED PBAA PROPELLANT ANALYSES (CONSTANT PARTICLE SIZE)

Batch	Ferric Oxide R_1	Ammonium Perchlorate R_2	PBAA Polymer R_3	Aluminum R_4
1	1.1129	0.9846	0.7364	1.0802
2	0.9110	0.9765	0.8009	1.0483
3	1.1010	0.9581	0.6634	1.2097
4	1.1581	0.9415	0.8411	1.1270
5	0.9474	0.9344	0.8100	1.2137
7	1.0793	0.9513	0.7751	1.1604
9	1.0075	0.9658	0.7409	1.1140
10	1.0657	0.9724	0.6655	1.1530
11	0.9012	0.9527	0.7494	1.1669
12	0.9184	0.9907	0.6912	1.0550

higher and the concentrations of ammonium perchlorate and aluminum are lower in the uncured propellant surface. Thus, the true ingredient concentrations in the propellant surface are known only for the cured samples. This phenomenon with the uncured propellant is due in large part to the interfacial tension between the liquid polymer and the Mylar film on the sample holder. A practical consequence is that theoretical calibration procedures which depend on knowing the true ingredient percentage in the analyzed sample surface are not applicable to uncured propellant analysis.

Simple regression equations for cured propellant analysis are given in Table 32 along with several statistical parameters already defined. As before, the best fit of the model to the data was found for ferric oxide. If the highest degree of accuracy is not required, a simple calibration of this type is adequate for ferric oxide determinations. The calibration curve for ferric oxide in Figure 10, obtained from another experiment, shows that the simple calibration procedure for ferric oxide can be used over relatively wide concentration ranges. The simple inverse equations for estimating ingredient concentrations are given in Table 33. Ammonium perchlorate can be more accurately analyzed in cured propellant by this simple calibration procedure than in uncured propellant.

Multiple regression equations for cured propellant analysis are shown in Table 34. All ingredients can be analyzed with a high degree of precision using the model of Equation (7). The corrected sums of squares and cross products and their inverse, derived during the regression analysis, are given in Tables 35(A) and 35(B). The analysis of variance, similar to that for the uncured propellant analysis, is shown in Table 36. Only 10 of the 12 calibration batches were analyzed in the cured state because of problems encountered with the curing of two batches. This accounts for the nine degrees-of-freedom among batches.

The inverse working equations for estimating ingredient percentages are shown in Table 37 along with the estimated relative and root-mean-square errors. The relative errors for all ingredients are less than 1%. The tabulated ingredient percentage errors are in Table 38. The best sets of multiple regression equations for cured propellant analyses are given in Table 39. These sets of equations result in only a slight improvement in the estimation precision for the $\hat{R}_{ij}$'s when compared with the regression equations in Table 34.

B. High-Rate HTPB Propellant

1. Experimental

Most composite propellants contain similar types, but not necessarily the same, components. Therefore, in general, X-ray spectometric techniques developed for one propellant type can be

TABLE 32. SIMPLE REGRESSION DATA FOR CURED PBAA PROPELLANT ANALYSES (CONSTANT PARTICLE SIZE)

$$\hat{R}_i = b_{i0} + b_{ii}X_i$$

Ingredient	Coefficient Level	Coefficient	S_b	t	S_e	R^2
Ferric Oxide	b_{10}	0.13986				
	b_{11}	1.75410	0.11546	15.19227	0.01849	0.96650
Ammonium Perchlorate	b_{20}	0.01859				
	b_{22}	0.01386	0.00156	8.88461	0.00592	0.90832
PBAA Polymer	b_{30}	-0.06736				
	b_{33}	0.06033	0.00879	6.86348	0.02462	0.85491
Aluminum	b_{40}	0.15555				
	b_{44}	0.06112	0.00692	8.83236	0.01904	0.90690

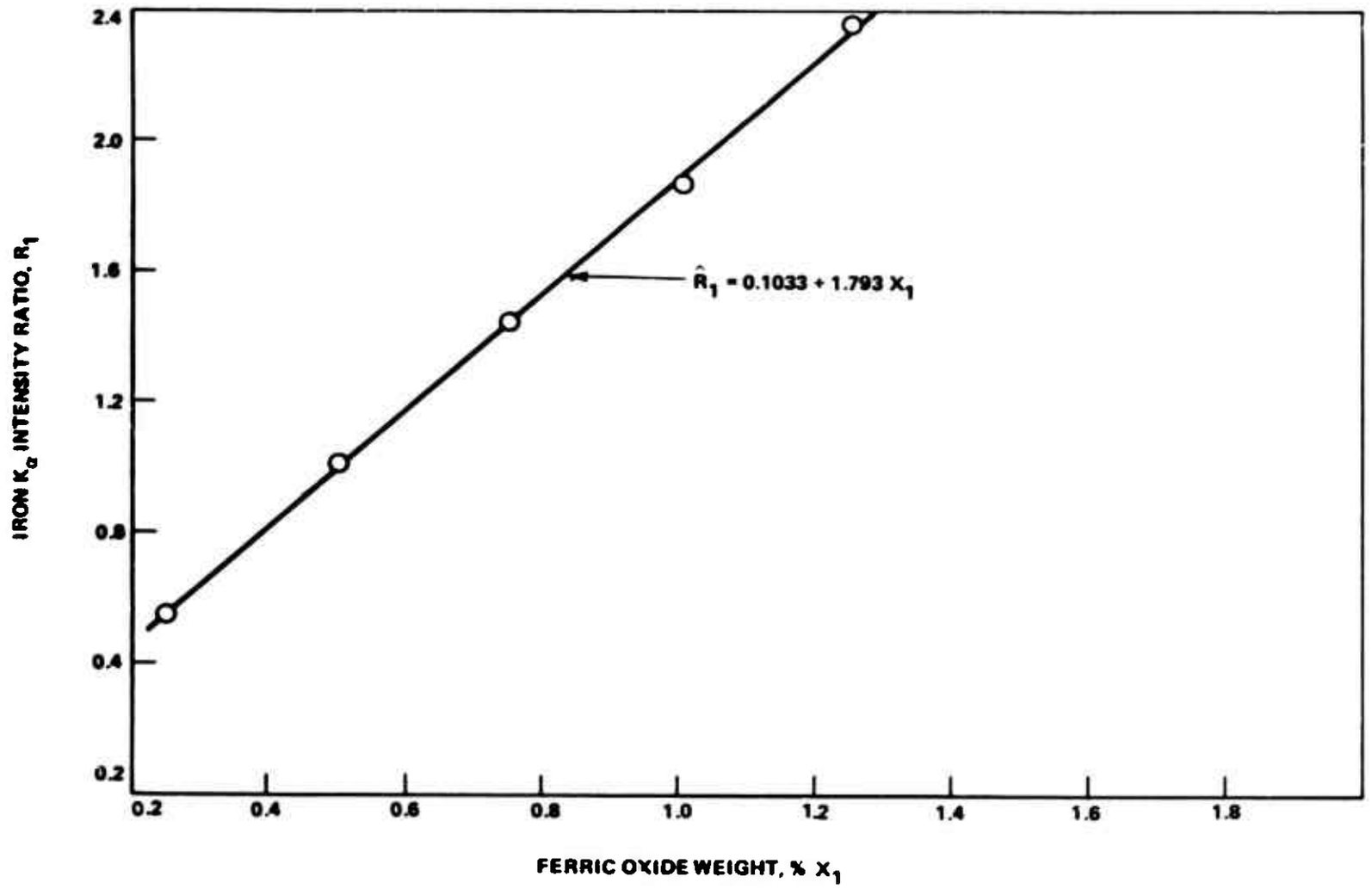

Figure 10. Calibration curve for ferric oxide concentration in cured PBAA propellant (wide concentration range).

TABLE 33. SIMPLE EQUATIONS FOR ESTIMATING INGREDIENT CONCENTRATIONS IN CURED PBAA PROPELLANTS (CONSTANT PARTICLE SIZE)

$$\hat{X}_i = d_{i0} + d_{ii}R_i$$

Estimated Ingredient	Measured Intensity Ratio	Coefficient Level	Coefficient	Relative Error (%)	RMSE
Ferric Oxide, X_1		d_{10}	-0.79730		
	R_1	d_{11}	0.57009	1.610	0.00944
Ammonium Perchlorate, X_2		d_{20}	-1.34126		
	R_2	d_{22}	72.15007	0.426	0.38210
PBAA Polymer, X_3		d_{30}	1.11652		
	R_3	d_{33}	16.57550	1.878	0.36469
Aluminum, X_4		d_{40}	-2.54499		
	R_4	d_{44}	16.36125	1.527	0.27857

TABLE 34. MULTIPLE REGRESSION DATA FOR CURED PBAA PROPELLANT ANALYSES (CONSTANT PARTICLE SIZE)

$$R_1 = b_{i0} + b_{i1}X_1 + b_{i2}X_2 + b_{i3}X_3 + b_{i4}X_4$$

Ingredient	Coefficient level	Coefficient	S_b	t	S_e	R^2
Ferric oxide	b_{10}	3.85130			0.01240	0.99059
	b_{11}	1.87300	0.08793	21.30103		
	b_{12}	-0.04004	0.03886	-1.03036		
	b_{13}	-0.02176	0.03593	-0.60562		
	b_{14}	-0.04689	0.04104	-1.14254		
Ammonium Perchlorate	b_{20}	-0.87140			0.00408	0.97282
	b_{21}	-0.07917	0.02893	-2.73660		
	b_{22}	0.02342	0.01278	1.83255		
	b_{23}	0.00550	0.01182	0.46531		
	b_{24}	0.01274	0.01350	0.94370		
PBAA Polymer	b_{30}	-0.76552			0.02026	0.93855
	b_{31}	0.11275	0.14375	0.78435		
	b_{32}	0.00961	0.06353	0.15126		
	b_{33}	0.07019	0.05874	1.19492		
	b_{34}	-0.00915	0.06710	-0.13636		
Aluminum	b_{40}	1.48140			0.01533	0.96221
	b_{41}	0.11875	0.10882	1.09125		
	b_{42}	-0.01626	0.04809	-0.33811		
	b_{43}	0.00021	0.04447	0.00472		
	b_{44}	0.04358	0.05079	0.85804		

TABLE 35(A). CORRECTED SUMS OF SQUARES AND CROSS PRODUCTS (a_{kl}) FOR CURED PBAA PROPELLANT ANALYSES (CONSTANT PARTICLE SIZE)

a_{11} = 0.02563	a_{12} = 0.04647	a_{13} = -0.11970	a_{14} = 0.08083
a_{21} = 0.04647	a_{22} = 14.46875	a_{23} = -6.96069	a_{24} = -7.56897
a_{31} = -0.11970	a_{32} = -6.96069	a_{33} = 7.85014	a_{34} = -0.32336
a_{41} = 0.08083	a_{42} = -7.56897	a_{43} = -0.32336	a_{44} = 7.55875

TABLE 35(B). INVERSE OF a_{kl}'s (c_{kl}) FOR CURED PBAA PROPELLANT ANALYSES (CONSTANT PARTICLE SIZE)

c_{11} = 50.31830	c_{12} = -8.25086	c_{13} = -6.92344	c_{14} = -9.09629
c_{21} = -8.25806	c_{22} = 9.82710	c_{23} = 9.01271	c_{24} = 10.31419
c_{31} = -6.92344	c_{32} = 9.01271	c_{33} = 8.40297	c_{34} = 9.45842
c_{41} = -9.09629	c_{42} = 10.31419	c_{43} = 9.45842	c_{44} = 10.96234

applied to another type with relatively minor modifications. Of course, a separate calibration must be performed for each specific propellant whose composition will be monitored and controlled during production. High rate propellants [19,20] in contrast to low rate propellants, contain ultrafine ammonium perchlorate having a weight median diameter of 1 μm or smaller, and a more effective ballistic modifier to enhance burning rate. Most composite propellants under development also use a state-of-the-art HTPB binder system. This binder provides improved structural integrity over earlier binders such as the PBAA type.

From an X-ray fluorescence analysis standpoint, the HTPB binder cannot be determined because it has no detectable element and the determination of ammonium perchlorate and aluminum are complicated by the fact that the ultrafine ammonium perchlorate tends to form agglomerates during propellant mixing [20]. These agglomerates, which can vary in size among propellant batches, affect the precision of the aluminum determination because the AlK_{α} emission line intensity is sensitive to the agglomerate size.

TABLE 36. ANALYSIS OF VARIANCE FOR CURED PBAA PROPELLANT ANALYSES (CONSTANT PARTICLE SIZE)

Source of Variation	Degrees of Freedom	Ferric Oxide		Ammonium Perchlorate		PBAA Polymer		Aluminum	
		Sum of Squares	Mean Squares	Sum of Squares	Mean Squares	Sum of Squares	Mean Squares	Sum of Squares	Mean Squares
Among B's	9								
Regression (4)		0.323375	0.080843	0.011901	0.002975	0.125454	0.031363	0.119843	0.029960
Residual (5)		0.003073	0.000614	0.000333	0.000066	0.008214	0.001642	0.004707	0.000941
Between T's	1	0.000456	0.000456	0	0	0	0	0.000541	0.000541
BXT (Exp Error)	9	0.001303	0.000144	0.000525	0.000058	0.001902	0.000211	0.001354	0.000150
Sampling Error	20	0.001478	0.000073	0.000680	0.000034	0.001961	0.000098	0.001388	0.000069
Total	39	0.329685		0.013439		0.137531		0.127833	

TABLE 37. EQUATIONS FOR ESTIMATING INGREDIENT CONCENTRATIONS IN CURED PBAA PROPELLANTS (CONSTANT PARTICLE SIZE)

$$X_i = d_{i0} + d_{i1}R_1 + d_{i2}R_2 + d_{i3}R_3 + d_{i4}R_4$$

Ingredient Estimated	Measured Intensity Ratio	Coefficient Level	Coefficient	Relative Error (%)	RMSE
Ferric Oxide, X_1		d_{10}	-1.53757	0.950	0.00572
	R_1	d_{11}	0.55778		
	R_2	d_{12}	1.12022		
	R_3	d_{13}	0.08425		
	R_4	d_{14}	0.29031		
Ammonium Perchlorate, X_2		d_{20}	38.91085	0.280	0.22246
	R_1	d_{21}	2.50823		
	R_2	d_{22}	41.14054		
	R_3	d_{23}	-2.41824		
	R_4	d_{24}	-9.83672		
PBAA Polymer, X_3		d_{30}	6.05390	1.324	0.22395
	R_1	d_{31}	-1.31468		
	R_2	d_{32}	-5.82529		
	R_3	d_{33}	14.26669		
	R_4	d_{34}	3.28737		
Aluminum, X_4		d_{40}	-15.31444	0.788	0.15722
	R_1	d_{41}	-0.57791		
	R_2	d_{42}	12.32482		
	R_3	d_{43}	-1.19899		
	R_4	d_{44}	18.46987		

TABLE 38. ESTIMATED CONCENTRATIONS AND RESIDUAL ERRORS FOR INGREDIENTS IN CURED P8AA PROPELLANTS (CONSTANT PARTICLE SIZE)

	Ferric Oxide		Ammonium Perchlorate		PBAA Polymer		Aluminum	
Batch	Weight (%)	Error	Weight (%)	Error	Weight (%)	Error	Weight (%)	Error
1	0.5618	0.0104	69.80	-0.37	12.93	0.40	15.24	0.21
2	0.4363	-0.0063	69.12	0.28	14.06	-0.20	14.60	-0.16
3	0.5569	-0.0062	67.59	0.07	12.48	-0.31	17.40	0.02
4	0.5611	-0.0013	67.43	-0.09	14.77	-0.07	15.43	0.08
5	0.4582	0.0077	65.83	-0.27	14.93	0.41	17.10	0.07
7	0.5323	0.0033	67.47	0.13	13.98	0.03	16.29	-0.07
9	0.4921	-0.0080	68.42	0.35	13.35	-0.16	15.69	-0.32
10	0.5369	-0.0010	68.64	0.12	12.29	0.05	16.55	-0.09
11	0.4342	0.0021	67.08	-0.19	13.86	-0.07	16.56	0.22
12	0.4490	-0.0008	69.92	-0.04	12.42	-0.08	15.02	0.03

TABLE 39. BEST SETS OF MULTIPLE REGRESSION DATA FOR CURED PBAA PROPELLANT ANALYSES (CONSTANT PARTICLE SIZE)

$$\dot{R}_i = h_{i0} + b_{i1}X_1 + b_{i2}X_2 + b_{i3}X_3 + b_{i4}X_4$$

Ingredient	Coefficient Level	Coefficient	S_b	t	S_e	R^2
Ferric Oxide	b_{10}	1.58510			0.01175	0.98984
	b_{11}	1.85500	0.07851	23.62756		
	b_{12}	-0.01670	0.00471	-3.54564		
	b_{14}	-0.02240	0.00661	-3.38880		
Ammonium Perchlorate	b_{20}	0.29217			0.00404	0.96794
	b_{21}	-0.06860	0.02644	-2.59455		
	b_{22}	0.01144	0.00142	8.05633		
	b_{23}	-0.00549	0.00199	-2.75879		
PBAA Polymer	b_{30}	-1.46590			0.01820	0.93060
	b_{32}	0.01746	0.00632	2.76265		
	b_{33}	0.07581	0.00858	8.83566		
Aluminum	b_{40}	1.50280			0.01400	0.96221
	b_{41}	0.11892	0.09354	1.27132		
	b_{42}	-0.01648	0.00561	-2.93761		
	b_{44}	0.04335	0.00787	5.50825		

A central composite experimental design [11] was used to evaluate applicability of the X-ray fluorescence method to high-rate propellant analysis. For this report, however, the design has been broken down into three separate experiments consisting of two factorial designs and the full central composite design. The compositions of the calibration batches for the first experiment are shown in Table 40. Each propellant batch also contains HTPB binder. This is a full 2^3 factorial design with independent ingredient concentrations. The liquid ballistic modifier in this case contained sulfur; therefore, it could be determined in the propellant. The ammonium perchlorate oxidizer was composed of a bimodal blend (55/45 by weight) of nominal 0.5- and 90-μm sizes.

Experiment -2, as shown in Table 41, was also a 2^3 factorial design. The ingredient percentages were the same as for Experiment -1 except that the ammonium perchlorate consisted of a 75/25 by weight bimodal blend of 0.5- to 90-μm ammonium perchlorate.

TABLE 40. COMPOSITIONS OF CALIBRATION BATCHES (WEIGHT %) FOR DETERMINING INGREDIENT CONCENTRATIONS IN HIGH RATE HTPB PROPELLANT (EXPERIMENT -1, PARTICLE SIZE CONSTANT)

Batch	35-μm Aluminum, X_1	Ballistic Modifier, X_2	Ammonium Perchlorate, X_3*
1	12.80	6.20	70.65
2	12.80	9.80	68.85
3	15.20	6.20	68.85
4	12.80	6.20	72.45
5	15.20	9.80	68.85
6	12.80	9.80	72.45
7	15.20	6.20	72.45
8	15.20	9.80	70.65

*Bimodal blend of 45% - 0.5-μm and 55% - 90-μm ammonium perchlorate.

NOTE: Remainder of propellant composition is HTPB binder.

TABLE 41. COMPOSITIONS OF CALIBRATION BATCHES (WEIGHT %) FOR DETERMINING INGREDIENT CONCENTRATIONS IN HIGH RATE HTPB PROPELLANT (EXPERIMENT -2, PARTICLE SIZE CONSTANT)

Batch	35-μm Aluminum, X_1	Ballistic Modifier, X_2	Ammonium Perchlorate*, X_3
1	12.80	6.20	70.65
2	12.80	9.80	68.85
3	15.20	6.20	68.85
4	12.80	6.20	72.45
5	15.20	9.80	68.85
6	12.80	9.80	72.45
7	15.20	9.80	70.65

*Bimodal blend of 75% - 0.5-μm and 25% - 90-μm ammonium perchlorate.

NOTE: Remainder of propellant composition is HPTB binder.

The analytical emission lines and the instrumental operating conditions used are given in Table 42. A fixed time measurement technique was used. Pulse height analysis was required only for the determination of aluminum. Only uncured propellant samples were analyzed. They were prepared and analyzed in the same manner as described for the low-rate PBAA propellant in Section II.

2. Results and Discussion

The average X-ray intensity ratios for the three analyzed ingredients in each calibration batch are shown in Tables 43 and 44 for Experiments -1 and -2, respectively. Regression analyses were made using these X-ray intensity responses and the composition data in Tables 40 and 41.

The regression data for the multiple linear regression model with all components present are shown in Tables 45 and 46 for Experiment -1 and in Table 47 for Experiment -2. The precision for estimating the $\hat{R}_i$'s is less than it is for low-rate propellant analysis. The correlation indices for aluminum and ammonium perchlorate determinations

TABLE 42. INSTRUMENTAL PARAMETERS FOR DETERMINING HIGH RATE HTPB PROPELLANT INGREDIENT CONCENTRATIONS (PARTICLE SIZE CONSTANT)

Ingredient	Emission Line	Analyzing Crystal	Peak Angle (deg 2θ)	Fixed Time (sec)	Pulse Height Analysis
Aluminum	Aluminum K_{α}	PET	145.10	50	Yes
Ballistic Modifier	Sulfur K_{α}	PET	75.92	50	No
Ammonium Perchlorate	Chlorine K_{β}	PET	60.55	50	No

NOTE: Chromium target X-ray tube operated at 40 kV and 30 mA (constant potential).

TABLE 43. MEAN X-RAY INTENSITY RATIOS* FOR UNCURED HIGH RATE HTPB PROPELLANT ANALYSES (EXPERIMENT -I, PARTICLE SIZE CONSTANT)

Batch	Aluminum, R_1	Ballistic Modifier, R_2	Ammonium Perchlorate, R_3
1	0.288	1.243	0.747
2	0.274	1.936	0.726
3	0.353	1.255	0.715
4	0.264	1.255	0.767
5	0.366	1.976	0.691
6	0.282	1.974	0.727
7	0.191	1.093	0.816
8	0.323	1.946	0.716

*Each ratio is the mean of three sample determinations.

TABLE 44. MEAN X-RAY INTENSITY RATIOS* FOR UNCURED HIGH RATE HTPB PROPELLANT ANALYSES (EXPERIMENT -2, PARTICLE SIZE CONSTANT)

Batch	Aluminum, R_1	Ballistic Modifier, R_2	Ammonium Perchlorate, R_3
1	0.112	1.014	0.843
2	0.096	1.582	0.817
3	0.143	0.989	0.837
4	0.133	1.061	0.797
5	0.132	1.541	0.802
6	0.163	1.696	0.736
7	0.151	1.575	0.780

*Each ratio is the mean of three sample determinations.

indicate an unacceptable fit of the model to the data. The model itself is believed to be adequate. The relatively poor fit for these ingredients is attributed to the adverse influence of the ultrafine ammonium perchlorate agglomeration in the propellant. This agglomeration problem was compounded in these experiments by the propellant processing procedure used. Shear stress during mixing was kept high by the controlled addition of the solids in an attempt to break up agglomerates. This was later found to make the agglomerate formation problem worse. At the present time, with improved procedures, high-rate propellants can be processed to give substantially better results than were obtained in these experiments. However, the overall precision for high-rate propellant analysis by X-ray spectrometry is still less than that for low-rate propellant analysis, particularly for the aluminum determination.

A model that includes first-order interaction terms was also considered in Experiment -1. The regression analysis data are presented in Table 46. This model appears to be superior to the one that contains only main effect terms (as in Table 45). But, the goodness-of-fit might be misleading because there is only one degree-of-freedom remaining for estimating the residual error. If all of the degrees-of-freedom (seven in this case) had been used for regression, then the correlation index would necessarily have a value of one. That is, the regression planes would have been forced through all of the points. Because of the lack of fit in most cases, the regression equations were not inverted to obtain working equations for estimating ingredient percentages.

TABLE 45. MULTIPLE REGRESSION DATA FOR UNCURED HIGH RATE HTPB PROPELLANT ANALYSES (EXPERIMENT -1, PARTICLE SIZE CONSTANT)

$$\hat{R}_i = b_{io} + b_{i1}X_1 + b_{i2}X_2 + b_{i3}X_3$$

Ingredient	Coefficient Level	Coefficient	S_b	t	S_e	R^2
Aluminum	b_{10}	1.66219				
	b_{11}	0.00522	0.01532	0.3404	0.04959	0.54830
	b_{12}	0.00517	0.01022	0.5063		
	b_{13}	-0.02101	0.01232	-1.7050		
Ballistic Modifier	b_{20}	1.27830				
	b_{21}	-0.01992	0.01835	-1.0853	0.05939	0.98756
	b_{22}	0.20367	0.01223	16.6467		
	b_{23}	-0.01478	0.01476	-1.0015		
Ammonium Perchlorate	b_{30}	-0.19182				
	b_{31}	0.00220	0.00865	0.2575	0.02770	0.70946
	b_{32}	-0.00945	0.00571	-1.6555		
	b_{33}	0.01379	0.00688	2.0044		

TABLE 46. MULTIPLE REGRESSION DATA WITH CROSS PRODUCTS FOR UNCURED HIGH-RATE HTPB PROPELLANT ANALYSES (EXPERIMENT -1, PARTICLE SIZE CONSTANT)

$$R_I = b_{10} + b_{11}X_1 + \ldots + b_{13}X_3 + b_{14}X_1X_2 + \ldots + b_{16}X_2X_3$$

Ingredient	Coefficient Level	Coefficient	S_b	t	S_e	R^2
Aluminum	b_{10}	-6.54495				
	b_{11}	0.079843	0.08913	0.89580		
	b_{12}	-0.45603	0.06442	-7.07901		
	b_{13}	0.10630	0.02136	4.97659	0.00465	0.99901
	b_{14}	0.00705	0.00093	7.58065		
	b_{15}	-0.01202	0.00120	-10.01667		
	b_{16}	0.00513	0.00080	6.41250		
Ballistic Modifier	b_{20}	-11.67577				
	b_{21}	1.08567	0.37710	2.87900		
	b_{22}	-0.20973	0.27254	-0.76954		
	b_{23}	0.17951	0.09037	1.98639	0.01968	0.99966
	b_{24}	0.00694	0.00394	1.76142		
	b_{25}	-0.01643	0.00509	-3.22790		
	b_{26}	0.00447	0.00339	1.31858		
Ammonium Perchlorate	b_{30}	3.80441				
	b_{31}	-0.42430	0.05742	-7.38941		
	b_{32}	0.28530	0.04150	6.87470		
	b_{33}	-0.04817	0.01376	-3.50073	0.00300	0.99915
	b_{34}	-0.00341	0.00060	-5.68333		
	b_{35}	0.00642	0.00077	8.33766		
	b_{36}	-0.00349	0.00051	-6.84314		

TABLE 47. MULTIPLE REGRESSION DATA FOR UNCURED HIGH RATE HTPB PROPELLANT ANALYSES (EXPERIMENT -2, PARTICLE SIZE CONSTANT)

$$\dot{R}_i = b_{i0} + b_{i1}X_1 + b_{i2}X_2 + b_{i3}X_3$$

Ingredient	Coefficient Level	Coefficient	S_b	t	S_e	R^2
Aluminum	b_{10}	-1.05439			0.01430	0.80267
	b_{11}	0.01554	0.00545	2.85138		
	b_{12}	0.00173	0.00308	0.56169		
	b_{13}	0.01360	0.00431	3.15545		
Ballistic Modifier	b_{20}	-1.46056			0.03001	0.99540
	b_{21}	-0.01275	0.01144	-1.11451		
	b_{22}	0.16465	0.00647	25.44822		
	b_{23}	0.02313	0.00904	2.55863		
Ammonium Perchlorate	b_{30}	2.3359			0.01453	0.92035
	b_{31}	-0.00637	0.00554	-1.14982		
	b_{32}	-0.01316	0.00313	-4.20447		
	b_{33}	-0.01900	0.00437	-4.34783		

V. DETERMINATION OF PARTICLE SIZES WITH INGREDIENT CONCENTRATIONS CONSTANT

A. General Considerations

The X-ray emission line intensities from elements in a propellant sample are sensitive not only to the percentages of the corresponding ingredients but also to the average particle sizes of the ingredients. The fact that in-situ particle size measurements of propellant solid ingredients could be made by X-ray spectrometry was recognized and applied on a semiquantitative basis by this command several years ago [1]. Normally, particle size or grain effects are considered to be a disturbing effect in X-ray spectrometric analysis; samples are treated either to minimize or eliminate the effects. In contrast, for propellant analysis, the ability to measure solids particle sizes in finished propellants is an important feature of the X-ray fluorescence method. The reason for this is that the solids particle sizes can have a pronounced influence on propellant ballistic, mechanical, and rheological properties. In fact, during the tailoring of propellant properties the particle sizes of the solids, particularly ammonium perchlorate and aluminum, are carefully chosen along with other components to provide the required propellant properties. Moreover, the particle sizes, specifically the particle size distribution, of these solids must be closely controlled during propellant manufacture.

The importance and implications of particle size effects in X-ray spectrometry, both qualitatively and quantitatively, have been well-reported in the literature [21,22]. These and other published methods, however, are not directly applicable to composite propellant analysis. Jenkins [23] gives a discussion of particle size effects in X-ray spectrometry and their origin. The particle size effects in propellants arise because, as the particle size of a component of a bimodal or multimodal blend changes, its concentration in the analyzed propellant surface also changes relative to the other size components. As the average particle size of the component decreases, its concentration, and hence its analytical emission line intensity, increases. Conversely, as the average particle size of the component increases, the analytical emission line intensity decreases. It was reported in earlier work [24] that the ClK_{α} emission line intensity from ammonium perchlorate in propellant is linearly related to the ammonium perchlorate weight mean diameter. Also, the ClK_{α} intensity is a linear function of the percentage of a fine ammonium perchlorate fraction in a bimodal blend of fine and coarse size fractions.

The effective depth of penetration of the emission line in the analyzed propellant surface also plays an important role with respect to particle size effects, because it determines the volume of propellant analyzed. The effective depth of penetration for long wavelength radiation such as ClK_{α}, SK_{α}, and AlK_{α} is of the order of 50 μm or less,

becoming smaller as the wavelength increases. If the effective depth of penetration is less than the diameters of the particles being measured, then particle size effects are especially pronounced.

Another factor to he considered is particle shielding. For example, AlK_α radiation may have to pass through ammonium perchlorate particles before it is measured. Consequently, as the ammonium perchlorate particle size decreases, the measured AlK_α intensity from aluminum particles also decreases, even though the aluminum particle size is held constant. Furthermore, the magnitude of this effect depends on the mass absorption coefficient of the matrix (and matrix particles) for the measured radiation. Because of its high absorption by ammonium perchlorate and its small effective penetration depth, AlK_α radiation is very sensitive to ammonium perchlorate particle size changes. It can be used to measure ammonium perchlorate weight median sizes down to at least 1 μm. The chlorine K_α radiation, on the other hand, is not sensitive to ammonium perchlorate particle size change below a weight median diameter of approximately 5 μm.

The purpose of this experiment was to develop quantitative procedures for determining ammonium perchlorate and aluminum particle size variations in uncured and cured propellants. These variations can occur through a weighing error or uncontrolled alteration of the particles during propellant processing. The percentage of a fine fraction in a bimodal blend of sizes was used here as a measure of particle size variations. The actual weight (volume) mean diameters of the particles, if desired, can readily be obtained for a specific propellant formulation by establishing the linear intensity-particle diameter relationship. This is not required for the analysis and control of production propellant compositions.

B. Low-Rate PBAA Propellant

1. Experimental

The experimental design used was a 2^2 factorial with two additional design points as shown in Tables 48 and 49. The two additional points have the same composition as the midpoint of the design shown in Table 15. The low level for each ingredient was composed of the larger average particle size and consequently the high level was composed of the smaller average particle size. Only the average particle sizes of ammonium perchlorate and aluminum were varied, with all ingredient percentages held constant. The average particle size of ammonium perchlorate was varied by changing the ratio of nominal 20- and 200-μm particle size fractions. The average aluminum particle size was varied by using two different aluminum powders having nominal sizes of 9- and 32-μm weight median diameters. The analytical conditions and instrumental parameters for this experiment are listed in Table 50.

TABLE 48. FACTORS AND FACTOR LEVELS FOR PBAA PROPELLANT PARTICLE SIZE CALIBRATION BATCHES (CONSTANT CONCENTRATIONS)

Factor	Symbol	Low Level*	High Level*
Ammonium Perchlorate	E	20% - 20 μm	60% - 20 μm
		80% - 200 μm	20% - 200 μm
Aluminum	F	0% - 9 μm	100% - 9 μm
		100% - 32 μm	0% - 32 μm

*Weight percent on a total ingredient basis.

2. Uncured Propellant Results

The individual X-ray intensity ratios for analyses of the calibration standards are recorded in Table 51; the average values used in the regression analysis are recorded in Table 52. Despite the fact that only ammonium perchlorate and aluminum particle sizes were varied, all of the ingredient emission line intensities were measured to evaluate the effects of the particle size variations on all ingredient determinations.

The regression equations for estimating the R_i's with the ammonium perchlorate, W_2, and aluminum, W_4, particle size fine fractions as the independent variables are given in Table 53. A good fit of the model to the data was found for all ingredients. The magnitudes and signs of the partial regression coefficients indicate the effects of the particle size variations on each estimated analytical emission line, $\hat{R}_i$. A negative coefficient means that the particular emission line intensity decreases as the average particle size decreases. Conversely, a positive coefficient means that the intensity increases as the average particle size decreases (high fine-fraction percentage). For example, as the particle size of ammonium perchlorate decreases, the ClK_α line intensity increases; whereas the SK_α, AlK_α, and FeK_α line intensities decrease. Likewise, when the aluminum particle size decreases, the AlK_α emission line intensity increases, and the emission line intensities from the other elements decrease. This is a general phenomenon. The high correlation index, R_i^2, shows that the intensity-particle size (weight % fine-fraction) relationship is well represented by a linear model.

TABLE 49. COMPOSITIONS OF CALIBRATION BATCHES FOR PARTICLE SIZE ANALYSIS (WEIGHT %) (CONSTANT CONCENTRATIONS)

Batch	Treatment Combination	Ferric Oxide, X_1	Ammonium Perchlorate, X_2	FBAA Polymer, X_3	Aluminum, X_4	20-μm Ammonium Perchlorate, W_2	9-μm Aluminum, W_4
1	-	0.4997	67.89	13.60	16.07	40.00	100.00
2	-	0.5004	68.00	13.60	16.01	40.00	100.00
3	t	0.4999	67.98	13.60	16.00	19.98	100.00
4	et	0.5003	68.02	13.61	16.01	59.99	100.00
5	(1)	0.4999	67.98	13.60	16.00	20.00	0
6	e	0.5004	67.97	13.58	16.01	59.99	0

TABLE 50. INSTRUMENTAL PARAMETERS FOR AMMONIUM PERCHLORATE AND ALUMINUM PARTICLE SIZE DETERMINATIONS (CONSTANT CONCENTRATIONS)

Ingredient	Emission Line	Analyzing Crystal	Peak Angle (deg 2θ)	Fixed Counts		Pulse Height Analysis
				Uncured Propellant	Cured Propellant	
Ferric Oxide	Iron K_α	NaCl	40.20	500,000	200,000	No
Ammonium Perchlorate	Chlorine K_α	NaCl	113.95	500,000	500,000	No
PBAA Polymer	Sulfur K_α	NaCl	144.78	20,000	20,000	Yes
Aluminum	Aluminum K_α	EDDT	142.82	20,000	50,000	Yes

NOTE: Tungsten target X-ray tube operated at 45 kV and 40 mA (constant potential), samples rotated. Chlorine K_α for reference standard was measured at 114.05° 2θ.

TABLE 51. X-RAY INTENSITY RATIOS FOR UNCURED PBAA PROPELLANT PARTICLE SIZE ANALYSES (CONSTANT CONCENTRATIONS)

Batch	Ferric Oxide	Ammonium Perchlorate	PBAA Polymer	Aluminum
1	1.0368	0.8180	0.8456	1.1829
	1.0357	0.8199	0.8556	1.1818
	1.0379	0.8319	0.8403	1.1533
	1.0449	0.8147	0.8675	1.1660
2	1.0384	0.8182	0.8502	1.1608
	1.0362	0.8203	0.8429	1.1766
	1.0392	0.8251	0.8470	1.1694
	1.0419	0.8219	0.8466	1.1517
3	1.1801	0.5904	0.9676	1.3864
	1.1576	0.5778	0.9308	1.4256
	1.1636	0.5829	0.9370	1.3726
	1.1514	0.5895	0.9203	1.3833
4	0.9260	1.0265	0.7657	0.9754
	0.9318	1.0023	0.7723	0.9712
	0.9386	1.0339	0.7667	0.9775
	0.9218	1.0500	0.7475	0.9614
5	1.1848	0.9516	1.3721	0.7298
	1.1520	0.9494	1.3181	0.7402
	1.1692	0.9673	1.3526	0.7622
	1.1749	0.9572	1.3424	0.7563
6	0.9503	1.3925	1.0069	0.4709
	0.9615	1.3702	0.9981	0.4562
	0.9382	1.4177	0.9928	0.4863
	0.9400	1.4047	0.9853	0.4846

TABLE 52. MEAN X-RAY INTENSITY RATIOS FOR UNCURED PBAA PROPELLANT PARTICLE SIZE ANALYSES (CONSTANT CONCENTRATIONS)

Batch	Ferric Oxide R_1	Ammonium Perchlorate R_2	PBAA Polymer R_3	Aluminum R_4
1	1.0388	0.8211	0.8522	1.1715
2	1.0389	0.8214	0.8467	1.1646
3	1.1632	0.5851	0.9389	1.3920
4	0.9296	1.0282	0.7630	0.9714
5	1.1702	0.9564	1.3463	0.7471
6	0.9475	1.3963	0.9958	0.4745

The best sets of multiple regrassion data with the first order interaction W_2W_4 includad are given in Table 54. These equations, except for ammonium perchlorate, reduce the error of estimating R_i's when compared with the equations in Table 53, but they cannot be inverted in a streight-forward manner for estimating W_2 and W_4. Tables 55 end 56 list equations for estimating W_2 and W_4 from the measured intensitias, R_i. Although the root-mean-squere errors ara small, the equations, as pointed out earlier, must be used with caution beceuse the intensities which ara not controlled were used as the independent variables for the leest squares anelysis. The particle siza estimates in weight fractions for the individual celibration batches, using the best sets of equations, are given in Table 57. A truer test of the velidity of the estimation equations would be to analyze propellants not included in the calibration. It should be mentioned that the equations in Table 53 can be inverted to give adequate working equations for astimating particle sizes.

The various intensity-particle size relationships are shown graphically as two-way plots in Figures 11 through 16. In practice, the in-situ measurement of ammonium perchlorate particle size is of primary interest. As illustrated in Figures 11 and 12, both ClK_α and AlK_α intensities are very sensitive to ammonium perchlorate particle size changes. The AlK_α radiation is actually more sensitive to the ammonium perchlorate size change than the ClK_α radiation in most applications. Therefore, the AlK_α line is the one of choice for

TABLE 53. MULTIPLE REGRESSION DATA FOR UNCURED PBAA PROPELLANT PARTICLE SIZE ANALYSES (CONSTANT CONCENTRATIONS)

$$\hat{R}_i = b_{i0} + b_{i1} (W_2 \times 10^{-2}) + b_{i2} (W_4 \times 10^{-2})$$

Ingredient	Coefficient Level	Coefficient	S_b	t	S_e	R^2
Ferric Oxide	b_{10}	1.28700	0.00651	197.69585	0.00532	0.99838
	b_{11}	-0.57039	0.01329	-42.91873		
	b_{12}	-0.01624	0.00460	-3.53043		
Ammonium Perchlorate	b_{20}	0.73490	0.01026	71.62768	0.00838	0.99943
	b_{21}	1.10380	0.02095	52.68735		
	b_{22}	-0.36237	0.00726	-49.91322		
PBAA Polymer	b_{30}	1.43420	0.06184	23.19210	0.05050	0.96428
	b_{31}	-0.65795	0.12624	-5.21189		
	b_{32}	-0.32087	0.04373	-7.33752		
Aluminum	b_{40}	0.95738	0.05324	17.98234	0.04347	0.98970
	b_{41}	-0.86656	0.10868	-7.97350		
	b_{42}	0.56405	0.03765	14.98140		

TABLE 54. BEST SETS OF MULTIPLE REGRESSION DATA FOR UNCURED PBAA PROPELLANT PARTICLE SIZE ANALYSES (CONSTANT CONCENTRATIONS)

$$\hat{R}_i = b_{i0} + b_{i1} (W_2 \times 10^{-2}) + b_{i2} (W_4 \times 10^{-2}) + b_{i3} (W_2 W_4 \times 10^{-4})$$

Ingredient	Coefficient Level	Coefficient	S_b	t	S_e	R^2
Ferric Oxide	b_{10}	1.27870	0.00494	258.84615	0.00454	0.99882
	b_{11}	-0.55115	0.01222	-45.10229		
	b_{13}	-0.03845	0.00903	-4.25802		
Ammonium Perchlorate	b_{20}	0.73490	0.01026	71.62768	0.00838	0.99943
	b_{21}	1.10380	0.02095	52.68735		
	b_{22}	-0.36237	0.00726	-49.91322		
PBAA Polymer	b_{30}	1.52160	0.00464	327.93103	0.00293	0.99993
	b_{31}	-0.87647	0.01036	-84.60135		
	b_{32}	-0.49557	0.00639	-77.55399		
	b_{33}	0.43683	0.01466	29.79740		
Aluminum	b_{40}	0.88343	0.01604	55.07668	0.01014	0.99962
	b_{41}	-0.68167	0.03588	-18.99860		
	b_{42}	0.71187	0.02211	32.19674		
	b_{43}	-0.36959	0.05073	-7.28543		

TABLE 55. EQUATIONS FOR ESTIMATING AMMONIUM PERCHLORATE SIZE FRACTIONS (W_2) IN UNCURED PBAA PROPELLANTS (CONSTANT CONCENTRATIONS)

$$\hat{W}_2 \times 10^{-2} = d_{20} + d_{21}R_1 + d_{22}R_2 + d_{23}R_3 + d_{24}R_4$$

Intensity Ratios	Coefficient Level	Coefficient	RMSE
	d_{20}	-2.46759	0.03464
R_2	d_{22}	1.82788	
R_4	d_{24}	1.17431	
	d_{20}	1.73962	0.00516
R_1	d_{21}	-1.31374	
R_2	d_{22}	0.15815	
R_3	d_{23}	-0.11565	
	d_{20}	1.46859	0.00538
R_1	d_{21}	-1.41677	
R_2	d_{22}	0.28957	
R_4	d_{24}	0.14740	
	d_{20}	5.19576	0.00663
R_2	d_{22}	-1 51767	
R_3	d_{23}	-1.59034	
R_4	d_{24}	-1.87968	
	d_{20}	2.06579	0.00497
R_1	d_{21}	-1.18976	
R_3	d_{23}	-0.25482	
R_4	d_{24}	-0.17739	

TABLE 56. EQUATIONS FOR ESTIMATING ALUMINUM SIZE FRACTIONS (W_4) IN UNCURED PBAA PROPELLANTS (CONSTANT CONCENTRATIONS)

$$\hat{W}_4 \times 10^{-2} = d_{40} + d_{41}R_1 + d_{42}R_2 + d_{43}R_3 + d_{44}R_4$$

Intensity Ratios	Coefficient Level	Coefficient	RMSE
	d_{40}	-5.48833	0.10630
R_2	d_{42}	2.80821	
R_4	d_{44}	3.57703	
	d_{40}	7.32703	0.00550
R_1	d_{41}	-4.00174	
R_2	d_{42}	-2.27786	
R_3	d_{43}	-0.35226	
	d_{40}	6.50145	0.00561
R_1	d_{41}	-4.31555	
R_2	d_{42}	-1.87756	
R_4	d_{44}	0.44900	
	d_{40}	17.85463	0.02107
R_2	d_{42}	-7.38253	
R_3	d_{43}	-4.84428	
R_4	d_{44}	-5.72560	
	d_{40}	2.62927	0.1020
R_1	d_{41}	-5.78744	
R_3	d_{43}	1.65222	
R_4	d_{44}	2.55495	

TABLE 57. ESTIMATED SIZE FRACTIONS OF AMMONIUM PERCHLORATE AND ALUMINUM IN CALIBRATION BATCHES OF UNCURED PBAA PROPELLANT (CONSTANT CONCENTRATIONS) (SEE TABLES 55 AND 56 FOR ESTIMATION EQUATIONS)

Variable	Actual	$R_2 - R_4$		$R_1 - R_2 - R_3$		$R_1 - R_2 - R_4$		$R_2 - R_3 - R_4$		$R_1 - R_3 - R_4$	
		Estimated	Error	Estimated	Error	Estimated	Error	Estimated	Error	Estimated	Error
Ammonium Perchlorate Fraction, $W_2 \times 10^{-2}$	0.400	0.4090	+0.0090	0.4062	+0.0062	0.4073	0.0073	0.3923	-0.0077	0.4049	0.0049
	0.400	0.4014	+0.0014	0.4068	+0.0068	0.4062	0.0062	0.4135	0.0135	0.4074	0.0074
	0.1998	0.2365	+0.0367	0.1954	-0.0044	0.1952	-0.0046	0.1981	-0.0017	0.1957	-0.0041
	0.5999	0.5526	-0.0473	0.5927	-0.0072	0.5925	-0.0074	0.5959	-0.0040	0.5930	-0.0069
	0.2000	0.1579	-0.0421	0.1978	-0.0021	0.1978	-0.0022	0.1989	-0.0011	0.1979	-0.0021
	0.5999	0.6419	+0.0420	0.6005	+0.0006	0.6005	0.0006	0.6011	0.0012	0.6006	0.0007
Aluminum Fraction, $W_4 \times 10^{-2}$	1.0000	1.0080	+0.0080	0.9995	-0.0005	1.0028	0.0028	0.9570	-0.0430	1.0184	0.0184
	1.0000	0.9841	-0.0159	1.0003	0.0003	0.9987	-0.0013	1.0209	0.0209	0.9911	-0.0089
	1.0000	1.1340	+0.1340	1.0087	0.0087	1.0081	0.0081	1.0168	0.0168	1.0051	0.0051
	1.0000	0.8738	-0.1262	0.9961	-0.0039	0.9954	-0.0046	1.0059	0.0059	0.9918	-0.0082
	0	-0.1302	-0.1302	-0.0086	-0.0086	-0.0089	-0.0089	-0.0055	-0.0055	-0.0100	-0.0100
	0	0.1301	+0.1301	0.0040	0.0040	0.0039	0.0039	0.0057	0.0057	0.0033	0.0033

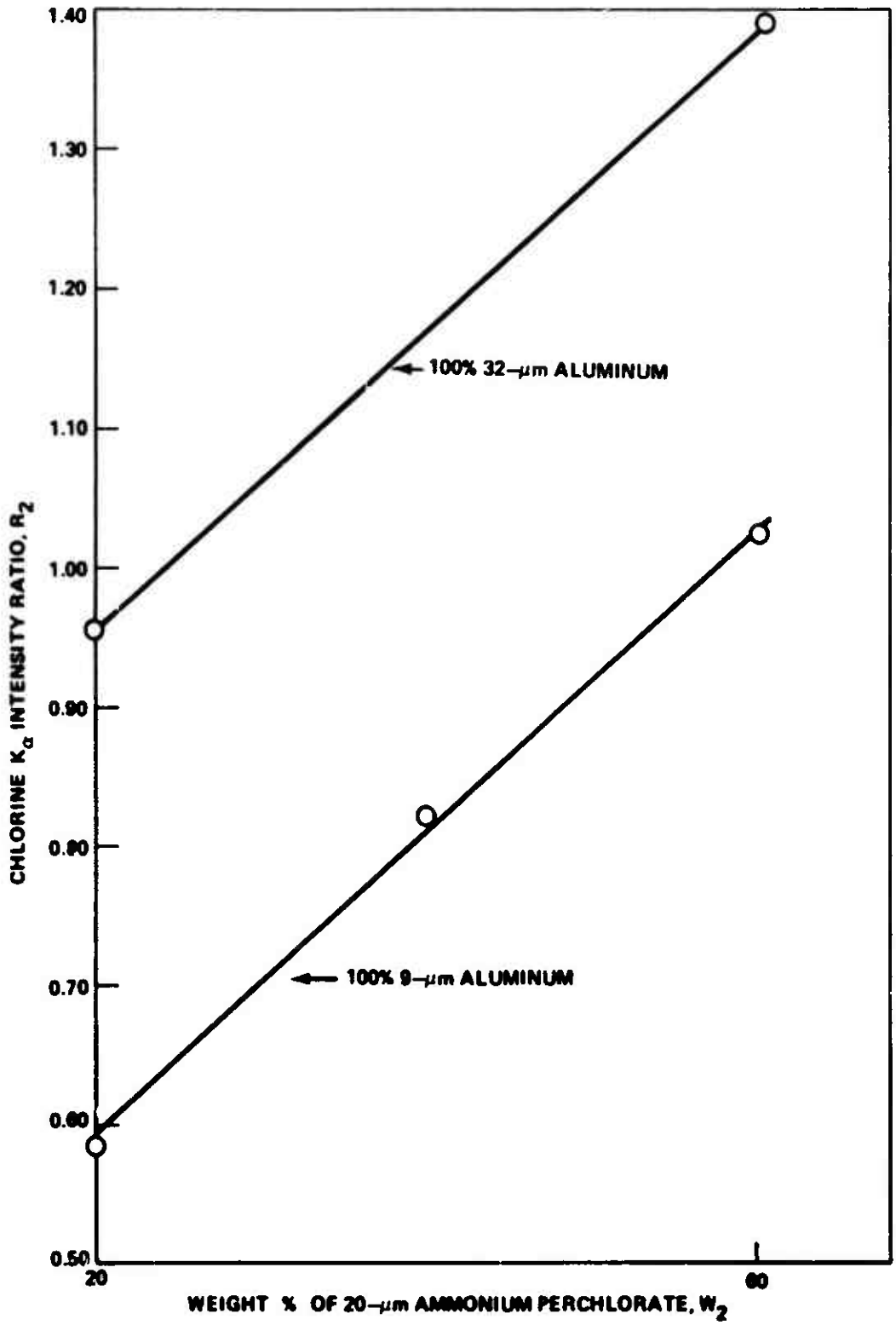

Figure 11. Chlorine K_α intensity as a function of ammonium perchlorate particle size fractions for constant aluminum particle size (uncured PBAA propellant).

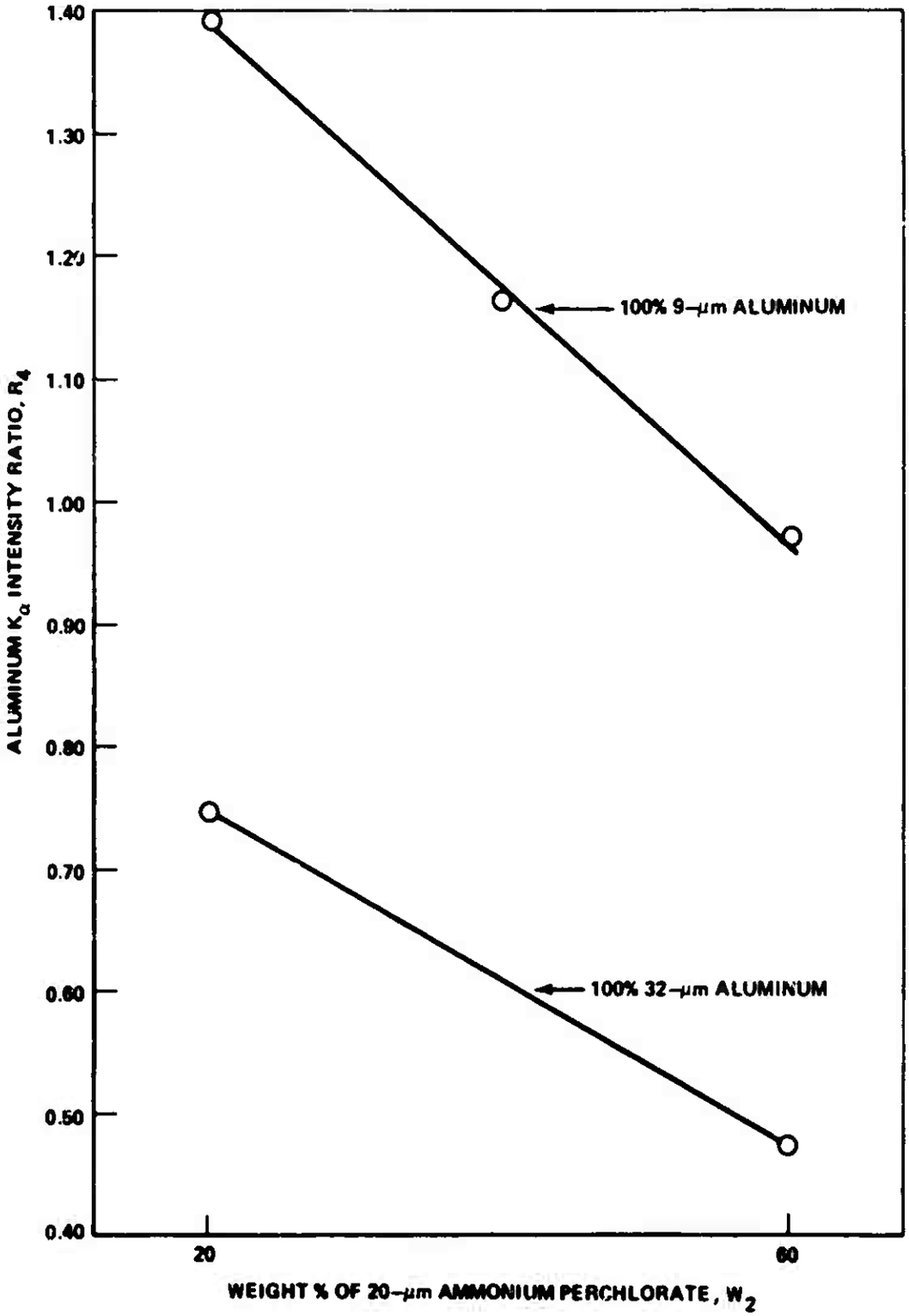

Figure 12. Aluminum K_α intensity as a function of ammonium perchlorate particle size fractions for constant aluminum particle size (uncured PBAA propellant).

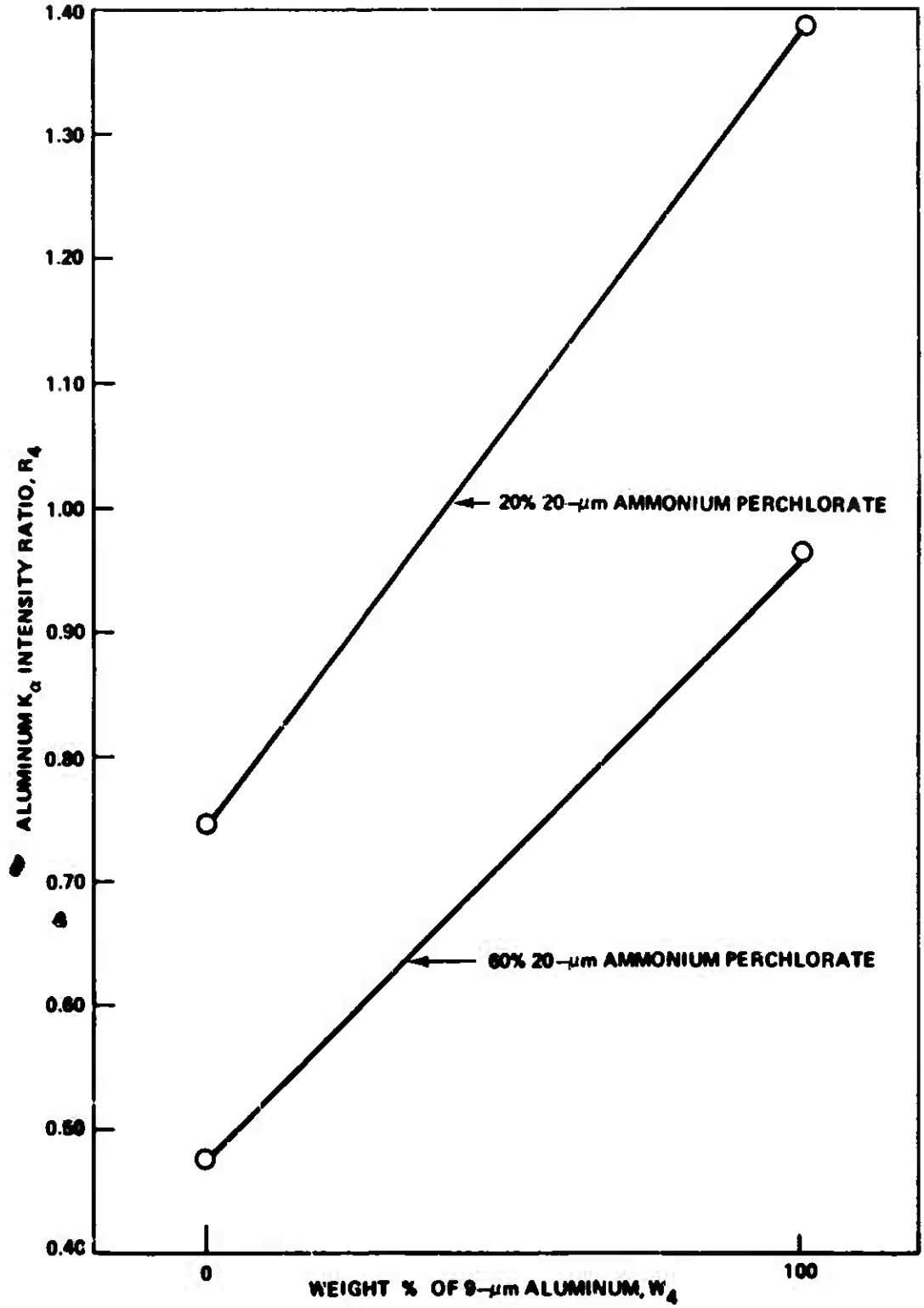

Figure 13. Aluminum K_α intensity as a function of aluminum particle size fractions for constant ammonium perchlorate particle size (uncured PBAA propellant).

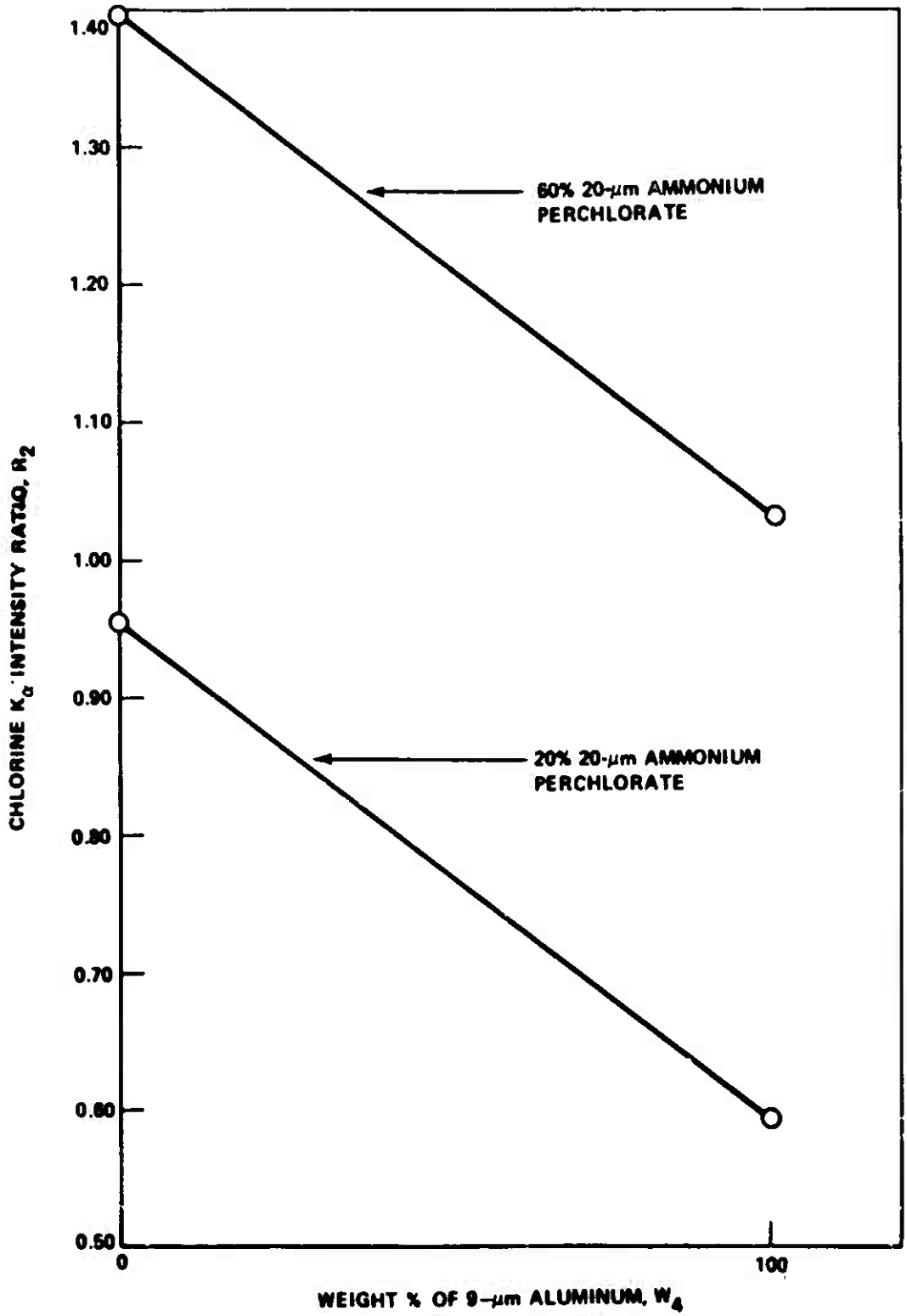

Figure 14. Chlorine K_α intensity as a function of aluminum particle size fractions for constant ammonium perchlorate particle size (uncured PBAA propellant).

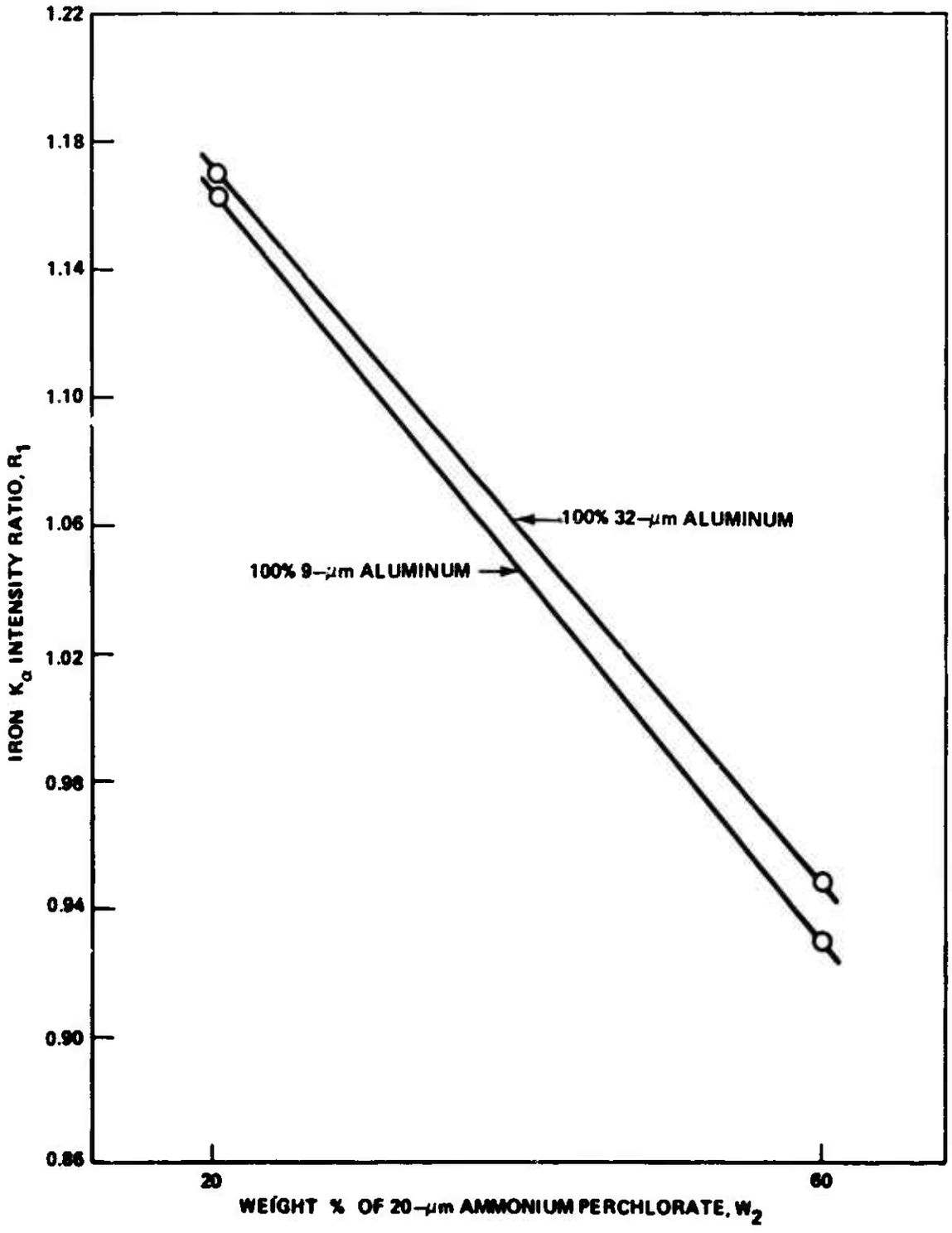

Figure 15. Iron K_α intensity as a function of ammonium perchlorate particle size fractions for constant aluminum particle size (uncured PBAA propellant).

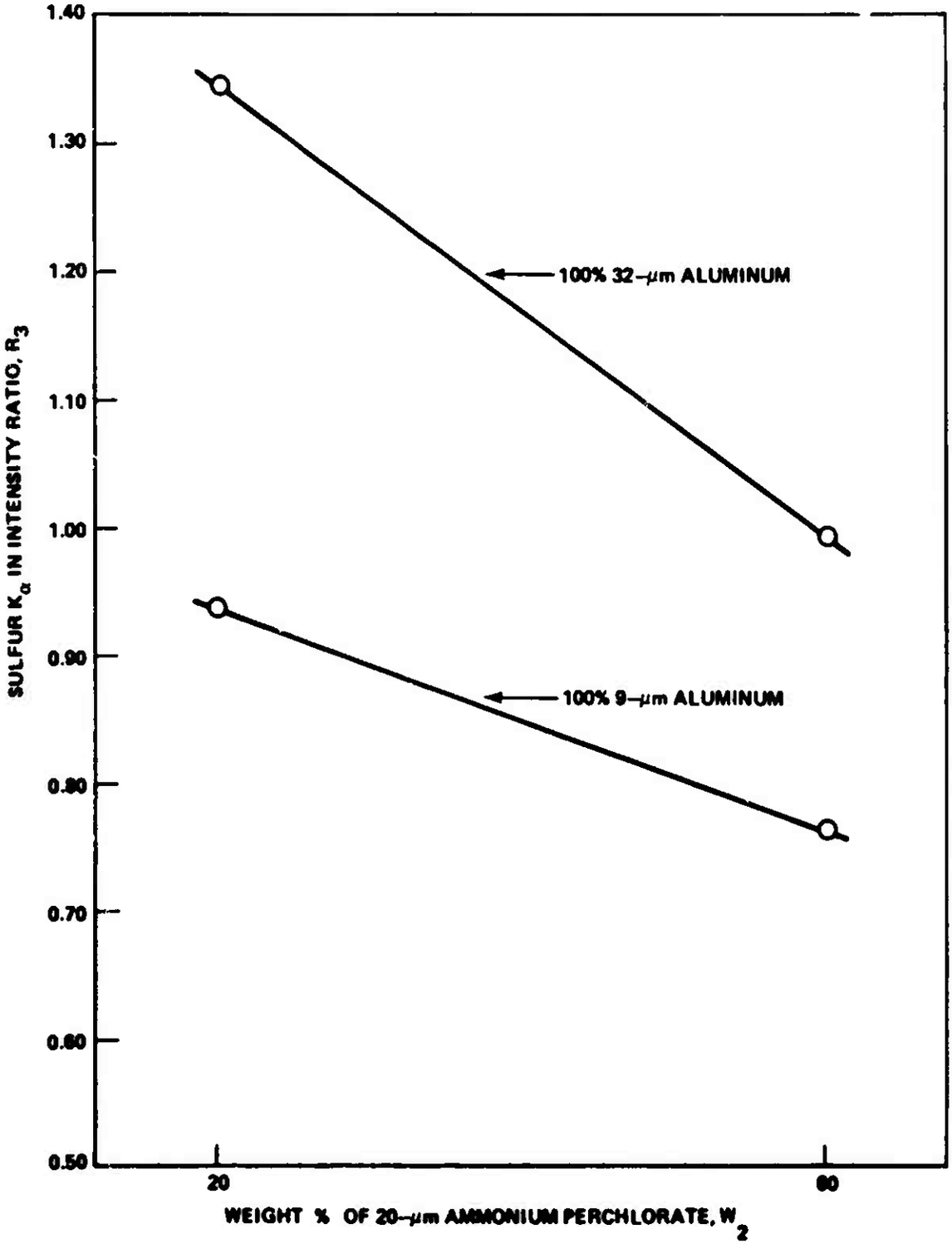

Figure 16. Sulfur K_α intensity as a function of ammonium perchlorate particle size fractions for constant aluminum particle size (uncured PBAA propellant).

ammonium perchlorate particle size measurements when the aluminum particle size is held constant. Figure 12 shows that, because of a significant interaction between aluminum and ammonium perchlorate particle sizes, the AlK_α intensity measurement becomes more sensitive to ammonium perchlorate size changes as the particle size of the aluminum powder itself decreases. There also appears to be significant interactions in Figures 13 and 16. Notice that the FeK_α and SK_α line intensities in Figures 15 and 16 are affected less by the particle size changes than the AlK_α and ClK_α lines. The aluminum particle size change has little effect, in particular, on the FeK_α emission line intensity, as shown in Figure 15 because of the large penetration depth of FeK_α radiation relative to the aluminum particle size, and the small absorption coefficient of aluminum for FeK_α radiation.

3. Cured Propellant Results

The cured propellant results are similar to those for uncured propellant, except that the magnitudes of the relative particle size effects are different because the compositions of the analyzed surfaces of cured and uncured propellants are entirely different, as has already been explained. The composition of the cured propellant surface accurately represents the composition of the bulk of the propellant.

Individual and average X-ray intensity ratio measurements for the cured propellant analyses are recorded in Tables 58 and 59, respectively. The multiple regression equations for estimating R_i with W_2 and W_4 as independent variables are shown in Table 60. Except for ammonium perchlorate, the standard errors, S_e, for estimating R_i are smaller than those for uncured propellant analysis (Table 53). The signs of the partial regression coefficients are the same in each case. The magnitude of the particle size effects on emission line intensities, however, is significantly smaller for cured propellant analysis. Thus, the measurements are less sensitive to ammonium perchlorate and aluminum particle size changes when analyzing cured propellants.

The best sets of multiple regression data including the W_2W_4 interaction term are given in Table 61. The equations for estimating W_2 and W_4 are given in Tables 62 and 63, and the resulting particle size estimates using these equations are given in Table 64. As for uncured propellant, the least squares analysis was made using the W_2 and W_4 as the dependent variables and the measured intensity ratios as the independent variables.

TABLE 58. X-RAY INTENSITY RATIOS FOR CURED PBAA PROPELLANT PARTICLE SIZE ANALYSES (CONSTANT CONCENTRATIONS)

Batch	Ferric Oxide	Ammonium Perchlorate	PBAA Polymer	Aluminum
1	1.0055	0.9586	0.7308	1.1955
	1.0062	0.9624	0.7310	1.1654
	1.0138	0.9586	0.7238	1.1793
	1.0055	0.9623	0.7162	1.1520
2	1.0007	0.9694	0.7119	1.1700
	1.0068	0.9612	0.7191	1.1851
	1.0117	0.9667	0.7114	1.1704
	0.9986	0.9733	0.7104	1.1584
3	1.0330	0.9504	0.7284	1.2553
	1.0323	0.9556	0.7158	1.2277
	1.0379	0.9577	0.7115	1.2274
	1.0358	0.9567	0.7236	1.2227
4	0.9728	0.9793	0.6994	1.1015
	0.9760	0.9760	0.7065	1.1110
	0.9824	0.9770	0.7013	1.0899
	0.9760	0.9765	0.6992	1.0998
5	1.0366	1.0460	0.9621	1.0817
	1.0438	1.0325	0.9811	1.0948
	1.0554	1.0325	0.9938	1.0856
	1.0488	1.0417	0.9806	1.0827
6	0.9850	1.0869	0.8863	1.0265
	0.9748	1.0944	0.8769	0.9976
	0.9831	1.0903	0.8752	1.0250
	0.9761	1.0916	0.8794	1.0038

TABLE 59. MEAN X-RAY INTENSITY RATIOS FOR CURED PBAA PROPELLANT PARTICLE SIZE ANALYSES (CONSTANT CONCENTRATIONS)

Batch	Ferric Oxide R_1	Ammonium Perchlorate R_2	PBAA Polymer R_3	Aluminum R_4
1	1.0078	0.9605	0.7254	1.1730
2	1.0044	0.9676	0.7132	1.1710
3	1.0348	0.9551	0.7198	1.2333
4	0.9768	0.9772	0.7016	1.1006
5	1.0462	1.0382	0.9794	1.0862
6	0.9798	1.0908	0.8794	1.0132

The intensity-particle size (weight percent fine-fraction) results for cured propellant analysis are shown graphically in Figures 17 through 22. The data can be interpreted in the same manner as was done for the uncured propellants. The most evident difference between uncured and cured propellant results, when the graphs are compared to the same scale, is the lower sensitivity attainable with cured propellant analysis. Small particle size changes can be detected with a higher degree of precision and accuracy when analyzing uncured propellants.

C. High-Rate HTPB Propellant Results

The low-rate PBAA propellant experiments were not repeated with high-rate propellants, because the principles involved and the qualitative intensity-particle size relationships for the two types of propellants are very similar. Consequently the experimental and regression procedures described for the low-rate propellant can be applied equally well to the high-rate propellant. The major difference between the two types of propellants from a particle size analysis standpoint is the ultrafine ammonium perchlorate used in the high-rate propellant. This ultrafine ammonium perchlorate normally has a weight median diameter of 0.5 to 1 μm.

It has been demonstrated that when ultrafine ammonium perchlorate is processed in composite propellants of the type described here it forms agglomerates in the propellant [20]. Normally, the weight mean diameter of the agglomerates is in the range of 5 to 10 μm. The agglomerates can affect propellant properties and the precision and accuracy of propellant spectrometric analyses. The X-ray spectrometric

TABLE 60. MULTIPLE REGRESSION DATA FOR CURED PBAA PROPELLANT PARTICLE SIZE ANALYSES (CONSTANT CONCENTRATIONS)

$$\hat{R}_i = b_{i0} + b_{i1} (W_2 \times 10^{-2}) + b_{i2} (W_4 \times 10^{-2})$$

Ingredient	Coefficient Level	Coefficient	S_b	t	S_e	R^2
Ferric Oxide	b_{10}	1.07520	0.00344	312.55813	0.00281	0.99364
	b_{11}	-0.15550	0.00702	-22.15099		
	b_{12}	-0.00705	0.00243	-2.90123		
Ammonium Perchlorate	b_{20}	1.02720	0.01146	89.63350	0.00935	0.98235
	b_{21}	0.09336	0.02339	3.99144		
	b_{22}	-0.09940	0.00810	-12.27160		
PBAA Polymer	b_{30}	0.98848	0.03019	32.74196	0.02465	0.97268
	b_{31}	-0.14772	0.06162	-2.39727		
	b_{32}	-0.21440	0.02135	-10.04215		
Aluminum	b_{40}	1.15250	0.02142	53.80485	0.01749	0.97019
	b_{41}	-0.25714	0.04372	-5.88151		
	b_{42}	0.11977	0.01514	7.91083		

TABLE 61. BEST SETS OF MULTIPLE REGRESSION DATA FOR CURED PBAA PROPELLANT PARTICLE SIZE ANALYSES (CONSTANT CONCENTRATIONS)

$$\dot{R}_i = b_{i0} + b_{i1} (W_2 \cdot 10^{-2}) + b_{i2} (W_4 \cdot 10^{-2}) + b_{i3} (W_2 W_4 \cdot 10^{-4})$$

Ingredient	Coefficient Level	Coefficient	S_b	t	S_e	R^2
Ferric Oxide	b_{10}	1.07940	0.00271	398.30258	0.00172	0.99813
	b_{11}	-0.16604	0.00607	-27.35420		
	b_{12}	-0.01548	0.00374	-4.13903		
	b_{13}	0.02108	0.00858	2.45687		
Ammonium Perchlorate	b_{20}	1.01190	0.00609	166.15763	0.00385	0.99806
	b_{21}	0.13153	0.01362	9.65712		
	b_{22}	-0.06888	0.00839	-8.20977		
	b_{23}	-0.07630	0.01925	-3.96363		
PBAA Polymer	b_{30}	1.0294	0.01363	75.52457	0.00862	0.99782
	b_{31}	-0.25006	0.03047	-8.20676		
	b_{32}	-0.29623	0.01878	-15.77369		
	b_{33}	0.20459	0.04308	4.74907		
Aluminum	b_{40}	1.12270	0.00592	189.64527	0.00374	0.99923
	b_{41}	-0.18255	0.01323	-13.79818		
	b_{42}	0.17940	0.00815	22.01226		
	b_{43}	-0.14911	0.01871	-7.96953		

TABLE 62. EQUATIONS FOR ESTIMATING AMMONIUM PERCHLORATE SIZE FRACTIONS (W_2) IN CURED PBAA PROPELLANTS (CONSTANT CONCENTRATIONS)

$$\hat{W}_2 \times 10^{-2} = d_{20} + d_{21}R_1 + d_{22}R_2 + d_{23}R_3 + d_{24}R_4$$

Intensity Ratios	Coefficient Level	Coefficient	RMSE
	d_{20}	16.52225	0.13675
R_2	d_{22}	-8.32892	
R_4	d_{24}	-6.91237	
	d_{20}	7.95476	0.00430
R_1	d_{21}	-7.29558	
R_2	d_{22}	-0.61157	
R_3	d_{23}	0.52355	
	d_{20}	7.10588	0.00544
R_1	d_{21}	-5.61735	
R_2	d_{22}	-0.34525	
R_4	d_{24}	-0.61735	
	d_{20}	4.26451	0.01507
R_2	d_{22}	0.54618	
R_3	d_{23}	-1.75242	
R_4	d_{24}	-2.68393	
	d_{20}	6.00542	0.00877
R_1	d_{21}	-3.44175	
R_3	d_{23}	-0.67871	
R_4	d_{24}	-1.41777	

TABLE 63. EQUATIONS FOR ESTIMATING ALUMINUM SIZE FRACTIONS (W_4) IN CURED PBAA PROPELLANTS (CONSTANT CONCENTRATIONS)

$$\hat{W}_4 \times 10^{-2} = d_{40} + d_{41}R_1 + d_{42}R_2 + d_{43}R_3 + d_{44}R_4$$

Intensity Ratios	Coefficient Level	Coefficient	RMSE
	d_{40}	25.85048	0.19339
R_2	d_{42}	-17.88178	
R_4	d_{44}	-6.49235	
	d_{40}	9.47954	0.00392
R_1	d_{41}	-1.55671	
R_2	d_{42}	-5.70588	
R_3	d_{43}	-1.96760	
	d_{40}	12.66980	0.01208
R_1	d_{41}	-7.86383	
R_2	d_{42}	-6.70677	
R_4	d_{44}	2.32029	
	d_{40}	8.69213	0.00558
R_2	d_{42}	-5.45885	
R_3	d_{43}	-2.45324	
R_4	d_{44}	-0.57269	
	d_{40}	-8.70761	0.07225
R_1	d_{41}	34.39916	
R_3	d_{43}	-13.18458	
R_4	d_{44}	-13.22761	

TABLE 64. ESTIMATED SIZE FRACTIONS OF AMMONIUM PERCHLORATE AND ALUMINUM IN CALIBRATION BATCHES OF CURED PBAA PROPELLANT (CONSTANT CONCENTRATIONS)

Variable	Actual	$R_2 - R_4$		$R_1 - R_2 - R_3$		$R_1 - R_2 - R_4$		$R_2 - R_3 - R_4$		$R_1 - R_3 - R_4$	
		Estimated	Error	Estimated	Error	Estimated	Error	Estimated	Error	Estimated	Error
Ammonium Perchlorate Fraction, $W_2 \times 10^{-2}$	0.4000	0.4141	+0.0141	0.3946	-0.0054	0.3889	-0.0111	0.3697	-0.0303	0.3814	-0.0186
	0.4000	0.3688	-0.0312	0.4087	0.0087	0.4068	0.0068	0.4033	0.0033	0.4043	0.0043
	0.1998	0.0423	-0.1575	0.1980	-0.0018	0.2019	0.0021	0.2147	0.0149	0.2068	0.0070
	0.5999	0.7755	+0.1756	0.5981	-0.0018	0.6020	0.0021	0.6148	0.0149	0.6069	0.0070
	0.2000	0.3670	+0.1670	0.2000	0	0.2000	0	0.1999	-0.0001	0.2000	0
	0.5999	0.4334	-0.1664	0.5999	0	0.5999	0	0.5998	-0.0001	0.5999	0
Aluminum Fraction, $W_4 \times 10^{-2}$	1.0000	1.0595	+0.0595	1.0029	0.0029	1.0245	0.0245	0.9976	-0.0024	0.8798	-0.1202
	1.0000	0.9455	-0.0545	0.9917	-0.0083	0.9990	-0.0010	0.9899	-0.0101	0.9501	-0.0499
	1.0000	0.7646	-0.2354	1.0027	0.0027	0.9883	-0.0117	1.0062	0.0062	1.0848	0.0848
	1.0000	1.2309	+0.2309	1.0027	0.0027	0.9883	-0.0117	1.0063	0.0063	1.0849	0.0849
	0	0.2336	+0.2336	0	0	0	0	0	0	0	0
	0	-0.2330	-0.2330	0	0	0	0	0	0	0	0

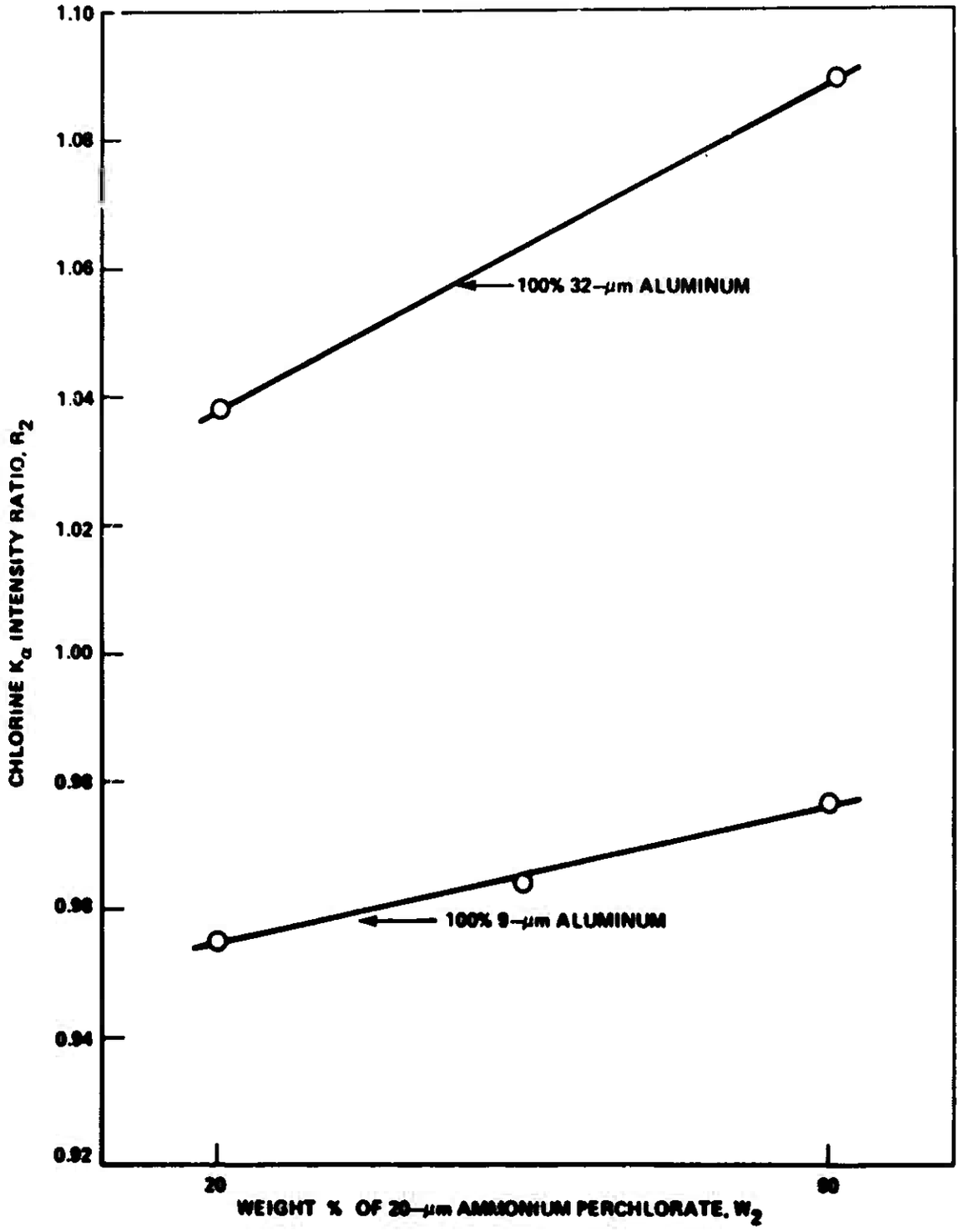

Figure 17. Chlorine K_α intensity as a function of ammonium perchlorate particle size fractions for constant aluminum particle size (cured PBAA propellant).

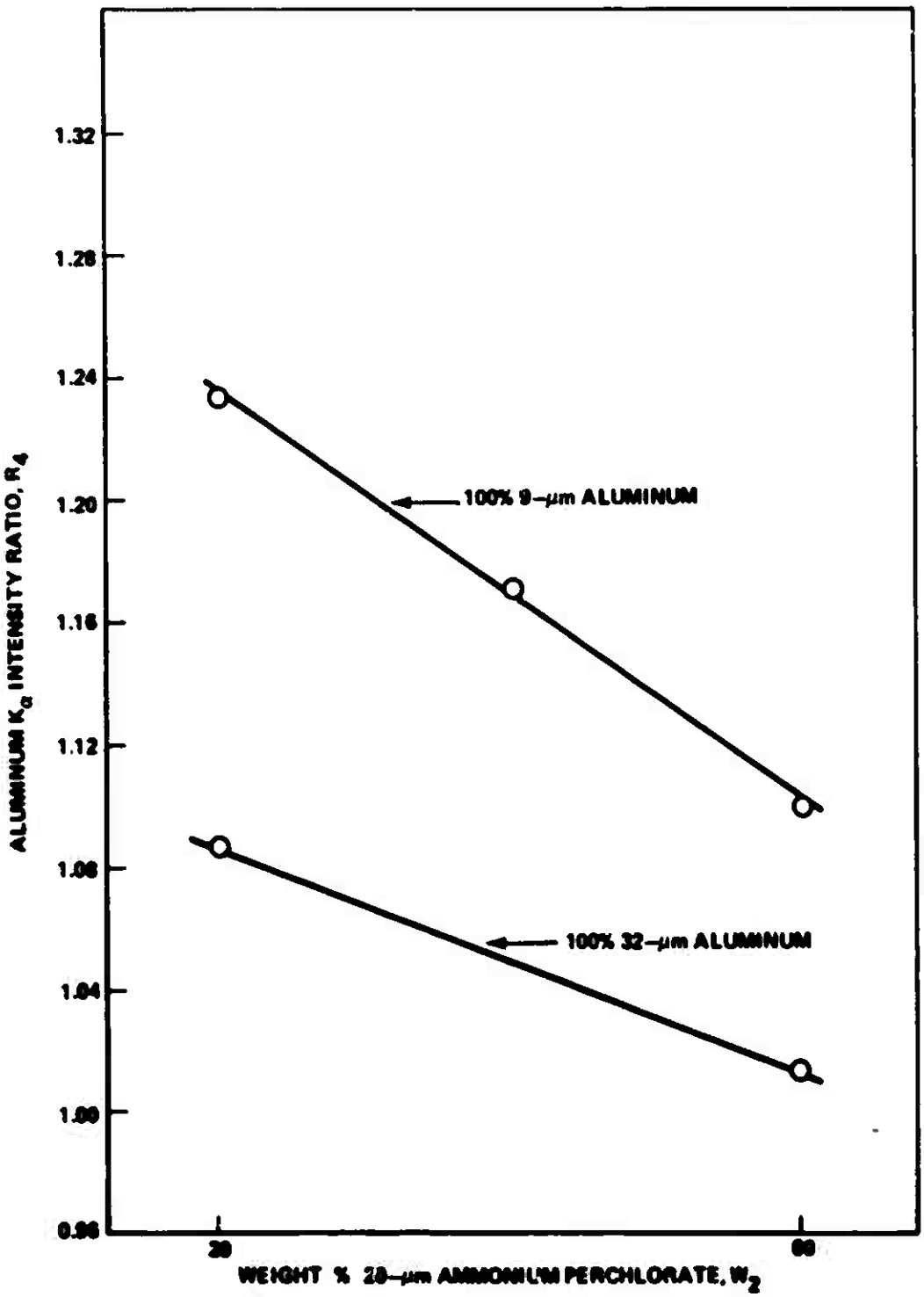

Figure 18. Aluminum K_α intensity as a function of ammonium perchlorate particle size fractions for constant aluminum particle size (cured PBAA propellant).

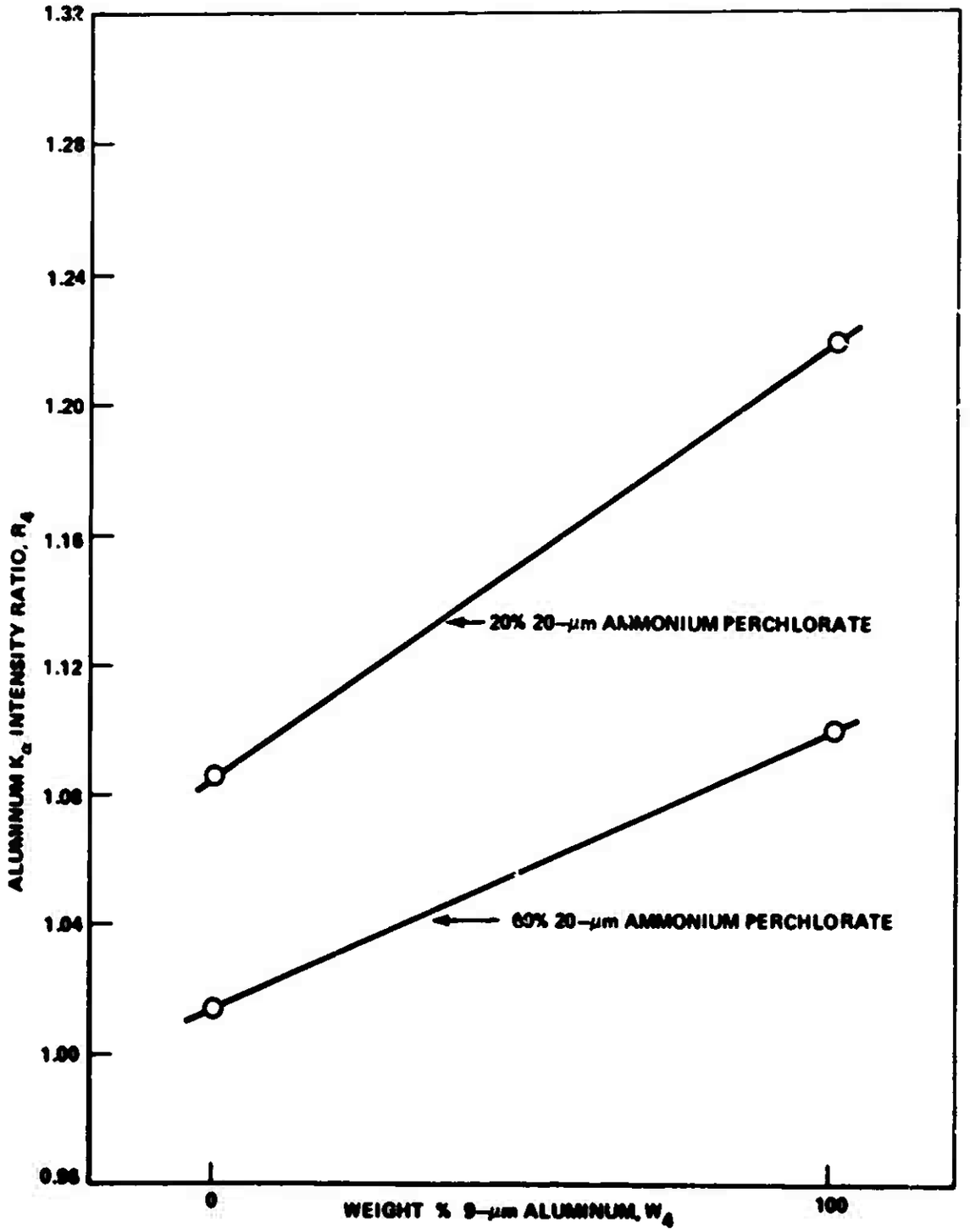

Figure 19. Aluminum K_α intensity as a function of aluminum particle size fractions for constant ammonium perchlorate particle size (cured PBAA propellant).

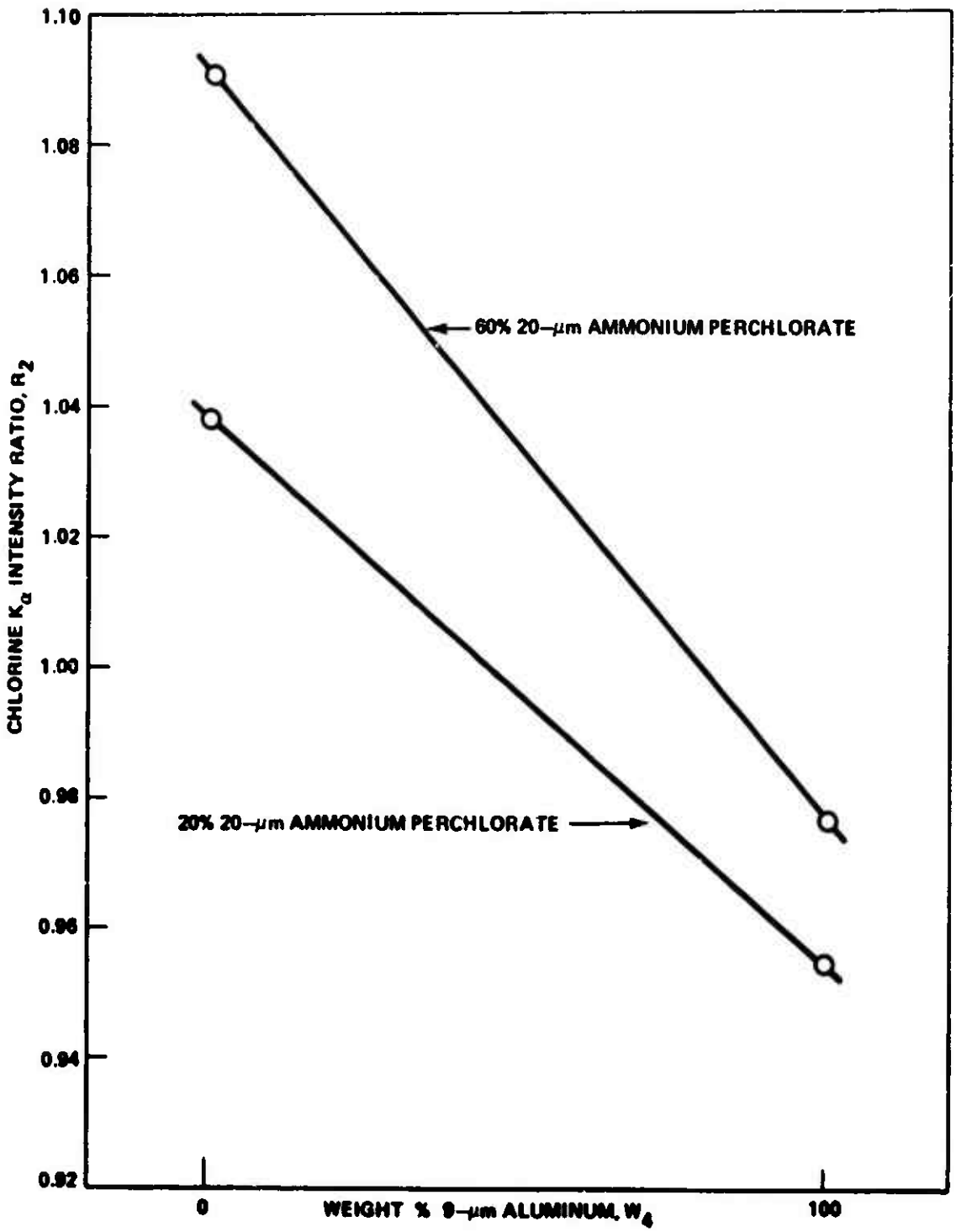

Figure 20. Chlorine K_α intensity as a function of aluminum particle size fractions for constant ammonium perchlorate particle size (cured PBAA propellant).

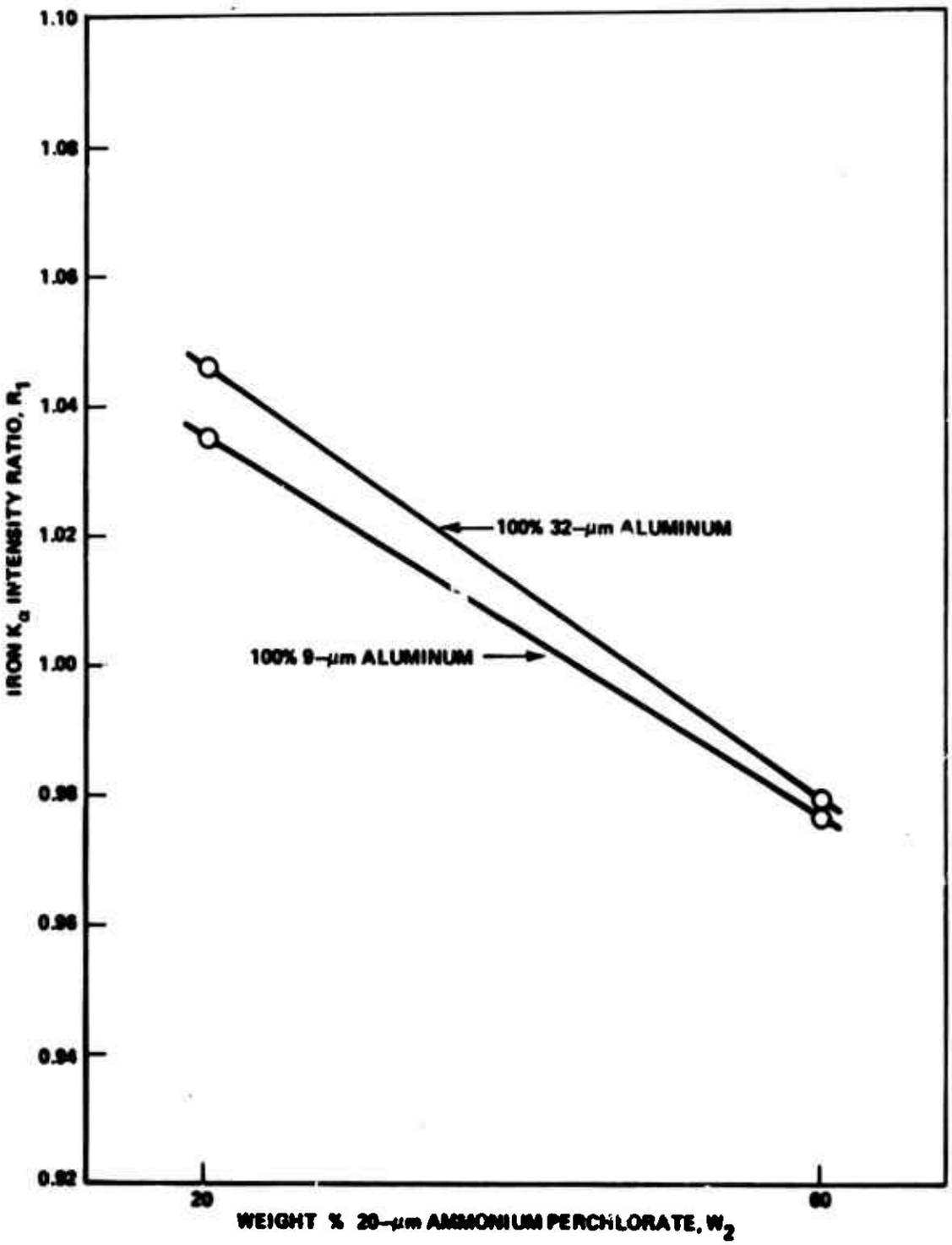

Figure 21. Iron K_α intensity as a function of ammonium perchlorate particle size fractions for constant aluminum particle size (cured PBAA propellant).

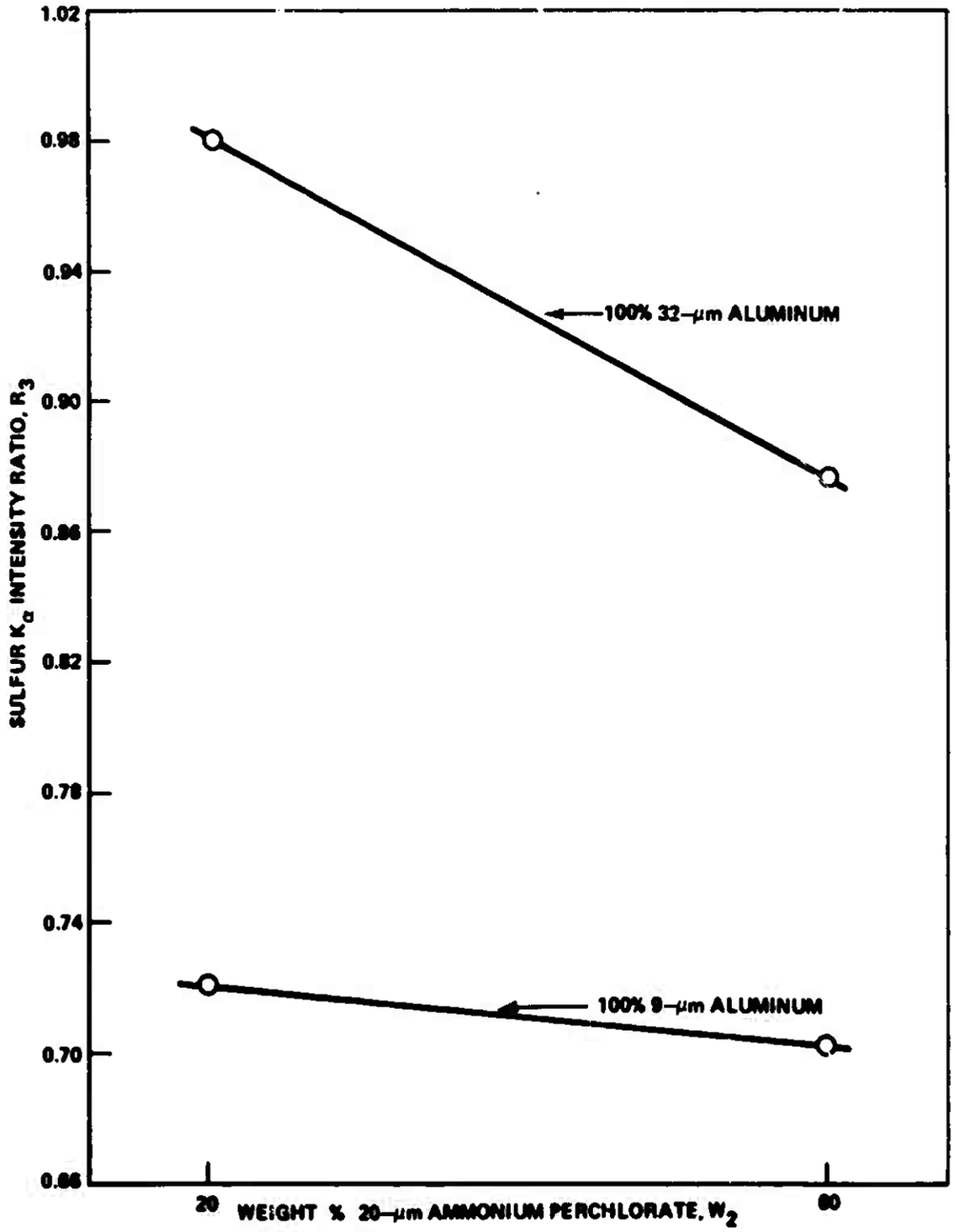

Figure 22. Sulfur K_α intensity as a function of ammonium perchlorate particle size fractions for constant aluminum particle size (cured PBAA propellant).

technique described here is the only known one for detecting and measuring ultrafine ammonium perchlorate agglomeration in high-rate propellants. Accordingly, it is a very valuable tool for monitoring and controlling the compositions of these propellants in a manufacturing situation.

The influence of ultrafine ammonium perchlorate agglomeration on X-ray spectrometric particle size measurements is illustrated in Figure 23. For this example the recommended AlK_α radiation as well as ClK_α radiation were used to detect the ammonium perchlorate particle size change quantitatively. The propellant contained a bimodal blend of nominal 1- and 70-μm ammonium perchlorate. The ratio of this blend was purposely varied, but all ingredient percentages were held constant. The plot for ClK_α radiation is linear whereas that for AlK_α radiation is curvilinear. The curvilinear relationship is caused by the influence of increasing ultrafine ammonium perchlorate agglomeration, as the ultrafine ammonium perchlorate percentage is increased, on the AlK_α intensity. The AlK_α radiation with its short effective penetration depth and high sensitivity for small ultrafine ammonium perchlorate particles detects the agglomeration effect as a departure from linearity. The ClK_α radiation, on the other hand, is insensitive to the ultrafine ammonium perchlorate agglomerates, but is sensitive to the large change in weight mean diameter of the ammonium perchlorate resulting from varying the bimodal blend ratio. Consequently, the relationship using ClK_α radiation is linear. The relationship with AlK_α radiation would also be linear if the percentage of ultrafine ammonium perchlorate agglomeration remained constant as the total ultrafine ammonium perchlorate percentage increased. In any event the AlK_α intensity will increase as the ultrafine ammonium perchlorate agglomerate size increases. Thus, the X-ray fluorescence method will readily detect an abnormal ultrafine ammonium perchlorate agglomeration condition in high rate propellants, and thereby prevent substandard propellant from being used.

Ultrafine ammonium perchlorate agglomerstion affects the precision of X-rsy spectrometric analyses of high rste propellants alluded to in Section IV.B. The AlK_α intensity measurement precision is strongly affected because of its sensitivity to the agglomeration and the fact that the agglomeration creates a locally inhomogeneous condition in the analyzed propellant surface. The ClK_α measurement precision is normally not affected, as indicated in Figure 23, unless the agglomerstion condition is very severe. This was the case for the data in Tsbles 46, 47, and 48. High-rate propellsnt processing procedures hsve now been improved to the point where ClK_α intensity messurements can be made with a high degree of precision, but the ultrsfine ammonium perchlorate agglomeration and its influence on AlK_α intensity measurements still persists.

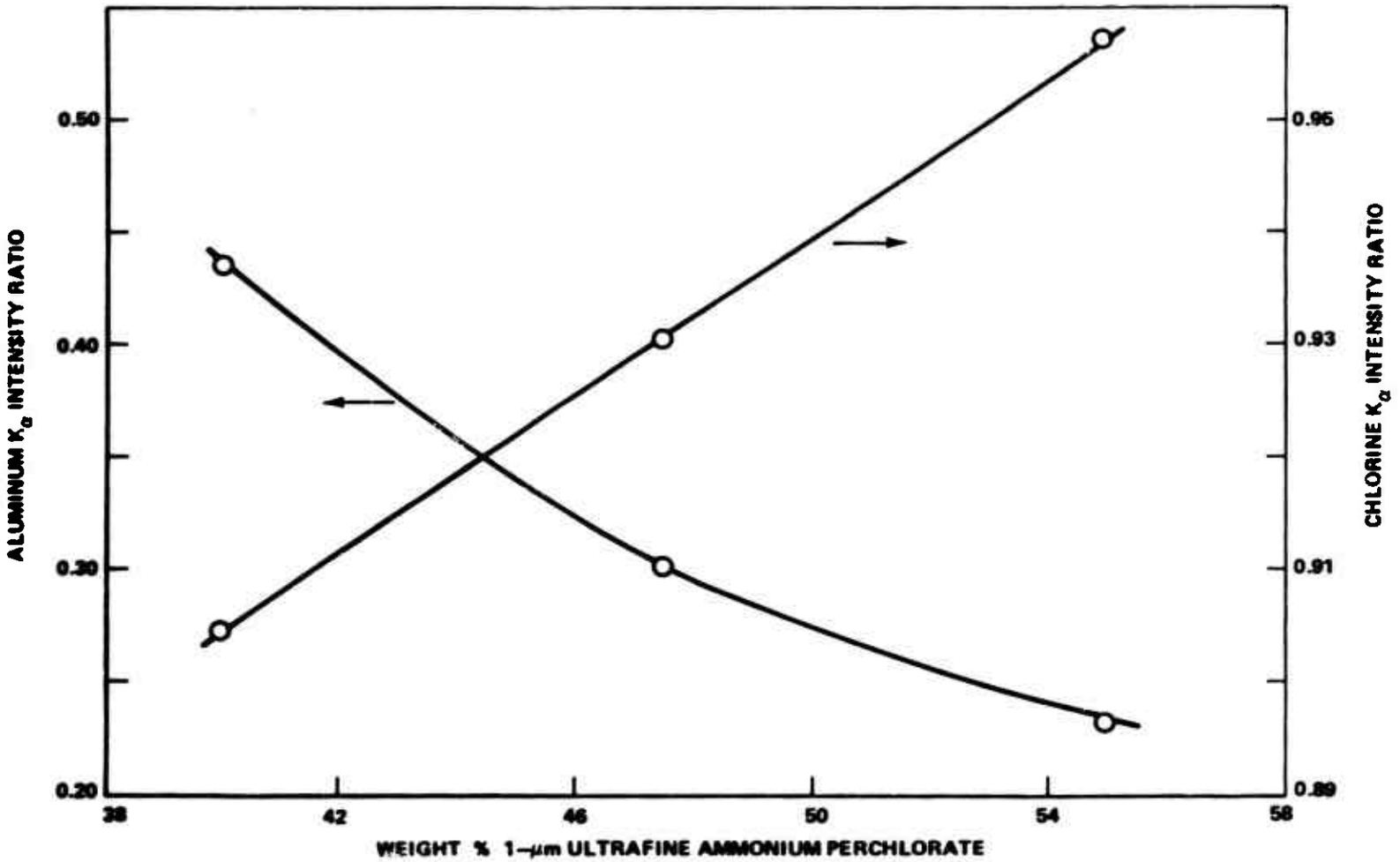

Figure 23. X-ray fluorescence analysis of ammonium perchlorate particle size in high rate propellant.

VI. SIMULTANEOUS DETERMINATION OF INGREDIENT CONCENTRATIONS AND PARTICLE SIZES

A. Low Rate PBAA Propellant

1. Experimental

It would be desirable in the X-ray spectrometric analysis of propellants to be able to determine not only ingredient percentages and particle size variations but also a simultaneous variation of these parameters. Such a simultaneous variation might be expected to occur during an actual propellant manufacturing situation. This part of the project was done, therefore, to demonstrate the methodology required. No attempt was made to analyze unknown propellants in which ingredient percentages and particle sizes were simultaneously varied, but extension of the principles to this application will be apparent. The primary limitation in this case is the total number of variables that can be determined. As explained earlier, the total number is equal to the number of different ingredients (emission lines) that can be determined. Consequently, it is often necessary to have separate and independent information about the propellant composition to supplement the X-ray fluorescence analysis and provide a complete determination.

A 1/8 fraction of a 2^6 factorial design was chosen for the preparation of calibration batches required for the multiple regression analysis. The factors and factor levels are given in Table 65, and the design data and defining contracts are given in Table 66. The particle size of ammonium perchlorate was varied by changing the ratio of a bimodal blend of nominal 20- and 200-μm size fractions; whereas the particle size of aluminum was varied by changing the blend ratio of nominal 9- and 32-μm sizes. The actual compositions of the resulting nine calibration batches, including the midpoint of the design, are shown in Table 67. The instrumental parameters for this determinstion are recorded in Table 68.

2. Uncured Propellant Results

Four replicate samples of each calibration batch were analyzed. The individual X-ray intensity ratios for each of the four ingredients are listed in Table 69. The mean intensity ratios used in the regression analysis are listed in Table 70.

Multiple regression data for uncured propellant analysis with terms for all ingredient concentrations and particle sizes present are shown in Table 71. The relatively small standard errors and large correlation indices indicate that the model is a good estimate of the true relationship. The best sets of multiple regression equations are shown in Table 72. Except for the ferric oxide determination, the particle size variables, W_2 and W_4, are in all sets. The aluminum particle size as previously shown, has very little effect on iron K_α radiation; hence, this variable is not in the best set for ferric oxide.

TABLE 65. FACTORS AND FACTOR LEVELS FOR CALIBRATION BATCHES (VARIABLE CONCENTRATIONS AND PARTICLE SIZES)

Factor	Symbol	Low Level (g)	High Level (g)
Ferric Oxide	A	4.5	5.5
Ammonium Perchlorate	B	660.0	700.0
PBAA Polymer	C	125.0	145.0
Aluminum	D	150.0	170.0
Ammonium Perchlorate Particle Size	E	*30.0% - 20 μm 70.0% - 200 μm	40.0% - 20 μm 60.0% - 200 μm
Aluminum Particle Size	F	*80% - 9 μm 20% - 32 μm	100% - 9 μm 0% - 32 μm

*Weight percent on a total ingredient basis.

An analysis of variance for these results is given in Table 73. This analysis is similar to that given in Section IV.A, and can be interpreted in the same manner. The residual errors in this experiment are significant at the 5% significance level for ferric oxide, ammonium perchlorate, and PBAA polymer determinations.

3. Cured Propellant Results

Individual X-ray intensity ratios for cured propellant determinations are recorded in Table 74; the mean values are recorded in Table 75. The multiple regression equations with all independent variables present in the model are shown in Table 76. The results compare favorably with those for uncured propellant analysis. The best sets of multiple regression equations for cured propellant analysis are shown in Table 77. Terms for aluminum and ammonium perchlorate particle size effects are present in all sets. Like uncured propellant analyses, the best sets of equations provide only a small improvement in the estimation of intensity ratios when compared with the complete linear model.

An analysis of variance for the cured propellant results is given in Table 78. The residual errors for ferric oxide and ammonium perchlorate determinations are significant at the 5% significance level.

TABLE 66. DESIGN DATA AND DEFINING CONTRASTS

Batch	Treatment Combination	Ferric Oxide X_1	Ammonium Perchlorate X_2	PBAA Polymer X_3	Aluminum X_4	20-μm Ammonium Perchlorate Fraction W_2	9-μm Aluminum Fraction W_4
1	abef	1	1	-1	-1	1	1
2	cdef	-1	-1	1	1	1	1
3	(1)	-1	-1	-1	-1	-1	-1
4	ace	1	-1	1	-1	1	-1
5	bde	-1	1	-1	1	1	-1
6	abcd	1	1	1	1	-1	-1
7	adf	1	-1	-1	1	-1	1
8	bcf	-1	1	1	-1	-1	1
9	Midpoint	0	0	0	0	0	0

Defining contrasts: I, ADE, BCE, ACF, BDF, ABCD, ABEF, CDEF.

TABLE 67. COMPOSITIONS OF CALIBRATION BATCHES (WEIGHT %) FOR COMBINED INGREDIENT PARTICLE SIZE AND CONCENTRATION DETERMINATIONS

Batch	Treatment Combination	Ferric Oxide X_1	Ammonium Perchlorate X_2	PBAA Polymer X_3	Aluminum X_4	20-μm Ammonium Perchlorate W_2	9-μm Aluminum W_4
1	abef	0.5514	70.18	12.53	15.04	40.00	100.00
2	cdef	0.4505	66.10	14.52	17.03	40.00	100.00
3	(1)	0.4694	68.86	13.04	15.65	30.00	79.99
4	ace	0.5616	67.38	14.80	15.31	40.00	80.00
5	bde	0.4419	68.72	12.27	16.70	40.00	79.98
6	abcd	0.5291	67.34	13.95	16.36	30.00	79.99
7	adf	0.5615	67.38	12.76	17.36	30.00	100.00
8	bcf	0.4418	68.73	14.24	14.73	30.00	100.00
9	Midpoint	0.5007	68.07	13.51	16.02	35.00	89.99

TABLE 68. INSTRUMENTAL PARAMETERS FOR COMBINED INGREDIENT PARTICLE SIZE AND CONCENTRATION DETERMINATIONS (PBAA PROPELLANT)

Ingredient	Emission Line	Analyzing Crystal	Peak Angle (deg 2θ)	Fixed Counts		Pulse Height Analysis
				Uncured Propellant	Cured Propellant	
Ferric Oxide	Iron K_α	NaCl	40.20	50,000	50,000	No
Ammonium Perchlorate	Chlorine K_α	NaCl	113.95	500,000	1,000,000	No
PBAA Polymer	Sulfur K_α	NaCl	144.78	20,000	20,000	Yes
Aluminum	Aluminum K_α	PET	144.45	100,000	100,000	Yes

TABLE 69. X-RAY INTENSITY RATIOS FOR UNCURED PBAA PROPELLANT ANALYSES (VARIABLE CONCENTRATIONS AND PARTICLE SIZES)

Batch	Ferric Oxide	Ammonium Perchlorate	P8AA Polymer	Aluminum
1	1.1327	0.8883	0.8269	0.9842
	1.1290	0.8821	0.8196	0.9864
	1.1154	0.9151	0.8199	1.0179
	1.1190	0.9065	0.8213	0.9738
2	0.9290	0.8145	0.8968	1.1223
	0.9397	0.8089	0.9129	1.1124
	0.9579	0.7892	0.9038	1.1063
	0.9394	0.8130	0.8969	1.1098
3	0.9889	0.8171	0.9297	1.0089
	0.9959	0.8061	0.9418	1.0110
	1.0141	0.8181	0.9305	1.0098
	1.0188	0.8125	0.9454	1.0211
4	1.1629	0.9154	0.9831	0.8972
	1.1684	0.9196	0.9930	0.8840
	1.1696	0.9156	0.9852	0.8995
	1.1503	0.9106	0.9822	0.9006
5	0.9194	0.8871	0.8111	0.9854
	0.9194	0.8818	0.8052	0.9805
	0.9232	0.8871	0.8122	0.9788
	0.9094	0.8818	0.7903	0.9825
6	1.1560	0.7746	1.0092	1.0699
	1.1497	0.7649	1.0022	1.0602
	1.1577	0.7707	1.0219	1.0607
	1.1384	0.7694	0.9660	1.0734
7	1.1954	0.6994	0.8288	1.1832
	1.2032	0.6997	0.8567	1.1948
	1.1838	0.7136	0.8347	1.1950
	1.2225	0.6936	0.8507	1.1854
8	1.0072	0.7893	0.9755	1.0178
	1.0012	0.7998	0.9991	1.0275
	1.0012	0.7955	0.9728	1.0200
	1.0072	0.7916	0.9744	1.0239
9	1.0869	0.8018	0.9222	1.0430
	1.0718	0.8024	0.9082	1.0503
	1.0798	0.8076	0.9136	1.0549
	1.0575	0.8116	0.8997	1.0409

TABLE 70. MEAN X-RAY INTENSITY RATIOS FOR UNCURED PBAA PROPELLANT ANALYSES (VARIABLE CONCENTRATIONS AND PARTICLE SIZES)

Batch	Ferric Oxide R_1	Ammonium Perchlorate R_2	PBAA Polymer R_3	Aluminum R_4
1	1.1240	0.8980	0.8219	0.9906
2	0.9415	0.8064	0.9026	1.1127
3	1.0044	0.8134	0.9368	1.0127
4	1.1628	0.9153	0.9859	0.8953
5	0.9178	0.8844	0.8047	0.9818
6	1.1504	0.7699	0.9998	1.0660
7	1.2012	0.7016	0.8427	1.1896
8	1.0042	0.7940	0.9804	1.0223
9	1.0740	0.8058	0.9109	1.0473

B. High Rate Propellant Results

The compositions of the calibration batches for Experiment 3 of the high-rate propellant analyses are given in Table 79. These compositions in combination with those in Tables 40 and 41 form a complete central composite design with four variables. The fourth variable is the percentage of 0.5-μm ammonium perchlorate in the propellant.

The mean X-ray intensity for each of the three ingredients, calculated from duplicate sample determinations, is given in Table 80. All samples were analyzed using the instrumental conditions shown in Table 42.

A complete quadratic polynomial model, as shown in Table 81, was fitted to the data. The model gives a good fit to the data for each of the three ingredients, but it cannot be inverted in a straightforward manner for estimating ingredient percentages and particle sizes. A polynomial model was used for this experiment because of the relatively wide ingredient concentration and particle size ranges used. A linear model would not be an accurate representation of the true curvilinear relationships involved.

TABLE 71. MULTIPLE REGRESSION DATA FOR UNCURED PBAA PROPELLANT ANALYSES (VARIABLE CONCENTRATIONS AND PARTICLE SIZES)

$$\hat{R}_1 = b_{10} + b_{11}X_1 + b_{12}X_2 + b_{13}X_3 + b_{14}X_4 + b_{15}X_5 + b_{16}X_6$$

Ingredient	Coefficient Level	Coefficient	S_b	t	S_e	R^2
Ferric oxide	b_{10}	-5.851180			0.02005	0.99034
	b_{11}	1.93200	0.16009	12.06821		
	b_{12}	0.05104	0.10835	0.47106		
	b_{13}	0.06237	0.11205	0.55662		
	b_{14}	0.05010	0.11236	0.44588		
	b_{15}	-0.00582	0.00152	-3.82895		
	b_{16}	0.00024	0.00076	0.31578		
Ammonium Perchlorate	b_{20}	2.82710			0.01199	0.99222
	b_{21}	-0.03948	0.09571	-0.41259		
	b_{22}	-0.01436	0.06478	-0.22167		
	b_{23}	-0.02355	0.06699	-0.35155		
	b_{24}	-0.05424	0.06718	-0.80738		
	b_{25}	0.01072	0.00091	11.78021		
	b_{26}	-0.00218	0.00046	-4.73913		
PBAA Polymer	b_{30}	-8.55030			0.00830	0.99658
	b_{31}	0.11398	0.06625	1.72045		
	b_{32}	0.09433	0.04584	2.05779		
	b_{33}	0.15863	0.04643	3.41751		
	b_{34}	0.07888	0.05659	1.39414		
	b_{35}	-0.00882	0.00063	-10.82539		
	b_{36}	-0.00245	0.00042	-5.84625		
Aluminum	b_{40}	-8.19590			0.01298	0.98113
	b_{41}	0.08418	0.1814	0.45986		
	b_{42}	0.08280	0.12434	0.66622		
	b_{43}	0.08462	0.12854	0.65888		
	b_{44}	0.14812	0.12879	1.15008		
	b_{45}	-0.00815	0.00125	-6.52114		
	b_{46}	0.00417	0.00087	4.79410		

TABLE 72. BEST SETS OF MULTIPLE REGRESSION DATA FOR UNCURED PBAA PROPELLANT ANALYSES (VARIABLE CONCENTRATIONS AND PARTICLE SIZE)

$$R_1 = b_{10} + b_{11}X_1 + b_{12}X_2 + b_{13}X_3 + b_{14}X_4 + b_{15}W_2 + b_{16}W_4$$

Ingredient	Coefficient level	Coefficient	S_b	t	S_e	R^2
Ferric oxide	b_{10}	0.17092			0.01455	0.98729
	b_{11}	1.89500	0.09992	18.96517		
	b_{13}	0.01028	0.00563	1.82593		
	b_{15}	-0.00556	0.00103	-5.39805		
Ammonium Perchlorate	b_{20}	1.39650			0.00887	0.99158
	b_{23}	-0.00869	0.00351	-2.47578		
	b_{24}	-0.03936	0.00352	-11.18181		
	b_{25}	0.01064	0.00063	16.88888		
	b_{26}	-0.00222	0.00031	-7.16129		
PBAA Polymer	b_{30}	-8.45030			0.00830	0.99679
	b_{31}	0.11398	0.06625	1.72045		
	b_{32}	0.09337	0.04484	2.08229		
	b_{33}	0.15847	0.04617	3.43251		
	b_{34}	0.07888	0.04650	1.69634		
	b_{35}	-0.00682	0.00063	-10.82539		
	b_{36}	-0.00245	0.00032	-7.65625		
Aluminum	b_{40}	-0.10228			0.01612	0.97623
	b_{44}	0.06428	0.00644	9.98107		
	b_{45}	-0.00773	0.00115	-6.72173		
	b_{46}	0.00438	0.00058	7.55172		

TABLE 73. ANALYSIS OF VARIANCE FOR UNCURED PBAA PROPELLANT ANALYSES (VARIABLE CONCENTRATIONS AND PARTICLE SIZES)*

Source of Variation	Degrees of Freedom	Ferric Oxide		Ammonium Perchlorate		PBAA Polymer		Aluminum	
		Sum of Squares	Mean Square	Sum of Squares	Mean Square	Sum of Squares	Mean Square	Sum of Squares	Mean Square
Among B's	8	3330.313	416.289	1477.877	184.735	1717.385	214.673	2240.940	280.118
Regression (6)		3298.153	549.692	1466.382	244.397	1711.877	285.313	2198.691	366.448
Residual (2)		32.160	16.080	11.495	5.748	5.508	2.754	42.249	21.124
Between T's	1	0.020	0.020	0.703	0.703	2.806	2.806	0.346	0.346
BXT (Exp Error)	8	11.616	1.452	8.042	1.005	2.169	0.271	2.955	0.369
Sampling Error	18	19.578	1.088	7.995	0.444	32.544	1.808	16.229	0.902
Total	35	3361.527		1494.617		1754.904		2260.471	

*All values multiplied by 10^4.

TABLE 74. X-RAY INTENSITY RATIOS FOR CURED PBAA PROPELLANT ANALYSES (VARIABLE CONCENTRATIONS AND PARTICLE SIZES)

Batch	Ferric Oxide	Ammonium Perchlorate	P8AA Polymer	Aluminum
1	1.1277	0.9819	0.7333	1.0989
	1.1119	0.9874	0.7366	1.0846
	1.1076	0.9839	0.7400	1.0760
	1.1043	0.9853	0.7359	1.0615
2	0.9615	0.9249	0.8224	1.2352
	0.9562	0.9314	0.8137	1.2210
	0.9351	0.9446	0.8012	1.1913
	0.9370	0.9366	0.8025	1.2072
3	0.9750	0.9577	0.7858	1.1722
	0.9814	0.9648	0.7834	1.1499
	0.9916	0.9568	0.7978	1.1529
	0.9659	0.9620	0.7861	1.1426
4	1.1647	0.9511	0.8845	1.0853
	1.1689	0.9480	0.8813	1.0910
	1.1506	0.9493	0.8918	1.0838
	1.1524	0.9468	0.8914	1.0852
5	0.9000	0.9572	0.7117	1.2052
	0.8949	0.9572	0.7202	1.1959
	0.9097	0.9633	0.7024	1.1818
	0.8995	0.9686	0.6987	1.1607
6	1.0913	0.9374	0.8327	1.1864
	1.0907	0.9313	0.8405	1.2016
	1.0894	0.9363	0.8188	1.2038
	1.0936	0.9431	0.8126	1.1773
7	1.1469	0.9246	0.6984	1.3055
	1.1623	0.9163	0.7134	1.3025
	1.1534	0.9304	0.7086	1.3030
	1.1534	0.9237	0.7032	1.2864
8	0.9726	0.9360	0.8457	1.0974
	0.9776	0.9348	0.8484	1.0953
	0.9760	0.9343	0.8409	1.1107
	0.9676	0.9398	0.8318	1.0977
9	1.0511	0.9457	0.7764	1.1744
	1.0541	0.9407	0.7918	1.1842
	1.0414	0.9493	0.7720	1.1618
	1.0434	0.9551	0.7772	1.1460

TABLE 75. MEAN X-RAY INTENSITY RATIOS FOR CURED PBAA PROPELLANT ANALYSES (VARIABLE CONCENTRATIONS AND PARTICLE SIZES)

Batch	Ferric Oxide R_1	Ammonium Perchlorate R_2	PBAA Polymer R_3	Aluminum R_4
1	1.1129	0.9846	0.7364	1.0802
2	0.9474	0.9344	0.8100	1.2137
3	0.9785	0.9603	0.7883	1.1544
4	1.1592	0.9488	0.8872	1.0863
5	0.9010	0.9616	0.7082	1.1859
6	1.0912	0.9370	0.8262	1.1923
7	1.1540	0.9238	0.7059	1.2994
8	0.9734	0.9362	0.8417	1.1003
9	1.0475	0.9477	0.7794	1.1666

VII. PRECISION AND ACCURACY

Precision data for low-rate PBAA propellant analyses were given in the analysis of variance Tables 28, 36, 73, and 78. To optimize the precision of the procedure for a particular application, however, the analyst needs to assess the magnitudes of the various sources of error. The methodology for resolving the error variances with specific applications to the uncured and cured PBAA propellant analyses reported here is detailed in Appendix A. Possible sources of error based on the experimental procedure described in Section II are as follows:

a) Counting error.

b) Sampling error for replicate samples.

c) Error between pairs (or groups) of samples analyzed at different times.

d) Error associated with the reference standard measurement and determination of X-ray intensity ratios.

e) Instrumental, mechanical, and electronic variations.

TABLE 76. MULTIPLE REGRESSION DATA FOR CURED PBAA PROPELLANT ANALYSES (VARIABLE CONCENTRATIONS AND PARTICLE SIZES)

$$R_i = b_{i0} + b_{i1}X_1 + b_{i2}X_2 + b_{i3}X_3 + b_{i4}X_4 + b_{i5}W_2 + b_{i6}W_4$$

Ingredient	Coefficient Level	Coefficient	S_b	t	S_e	R^2
Ferric Oxide	b_{10}	4.72240			0.01093	0.99665
	b_{11}	1.76250	0.08724	20.20288		
	b_{12}	-0.04725	0.05905	-0.80016		
	b_{13}	-0.03524	0.06106	-0.57713		
	b_{14}	-0.05470	0.06123	-0.89335		
	b_{15}	-0.00188	0.00083	-2.26506		
	b_{16}	0.00079	0.00042	1.88095		
Ammonium Perchlorate	b_{20}	-0.85551			0.01112	0.90873
	b_{21}	0.02143	0.08875	0.24146		
	b_{22}	0.02172	0.06007	0.36157		
	b_{23}	0.00967	0.06212	0.15566		
	b_{24}	0.00991	0.06229	0.15909		
	b_{25}	0.00173	0.00085	2.03529		
	b_{26}	-0.00040	0.00042	-0.95238		
PBAA Polymer	b_{30}	-0.74645			0.00740	0.99641
	b_{31}	0.03239	0.05907	0.54833		
	b_{32}	0.01230	0.03998	0.30765		
	b_{33}	0.07091	0.04134	1.71528		
	b_{34}	-0.00759	0.04146	-0.18306		
	b_{35}	-0.00078	0.00056	-1.39285		
	b_{36}	-0.00144	0.00028	-5.14285		
Aluminum	b_{40}	6.31160			0.00451	0.99897
	b_{41}	-0.01612	0.03599	-0.44790		
	b_{42}	-0.06261	0.02436	-2.57019		
	b_{43}	-0.06814	0.02519	-2.70504		
	b_{44}	0.00635	0.02526	0.25138		
	b_{45}	-0.00415	0.00034	-12.20588		
	b_{46}	0.00098	0.00017	5.76470		

TABLE 77. BEST SETS OF MULTIPLE REGRESSION DATA FOR CURED PBAA PROPELLANT ANALYSES (VARIABLE CONCENTRATIONS AND PARTICLE SIZES)

$$R_i = b_{i1}X_1 + b_{i2}X_2 + b_{i3}X_3 + b_{i4}X_4 + b_{i5}W_2 + b_{i6}W_4$$

Ingredient	Coefficient Level	Coefficient	S_b	t	S_e	R^2
Ferric Oxide	b_{10}	1.36970			0.00980	0.99596
	b_{11}	1.78820	0.06734	26.55479		
	b_{12}	-0.01326	0.00375	-3.53600		
	b_{14}	-0.01950	0.00489	-3.98773		
	b_{15}	-0.00206	0.00069	-2.98550		
	b_{16}	0.00070	0.00035	2.00000		
Ammonium Perchlorate	b_{20}	0.08382			0.00715	0.90569
	b_{22}	0.01227	0.00213	5.76056		
	b_{25}	0.00178	0.00051	3.49019		
	b_{26}	-0.00037	0.00025	-1.48000		
PBAA Polymer	b_{30}	0.47804			0.00562	0.99586
	b_{33}	0.05818	0.00222	26.20720		
	b_{34}	-0.02033	0.00223	-9.11659		
	b_{35}	-0.00072	0.00040	-1.80000		
	b_{36}	-0.00140	0.00020	-7.00000		
Aluminum	b_{40}	6.90130			0.00344	0.99879
	b_{42}	-0.06869	0.00132	-52.03787		
	b_{43}	-0.07439	0.00171	-43.50292		
	b_{45}	-0.00412	0.00024	-17.16666		
	b_{46}	0.00099	0.00012	8.25000		

TABLE 78. ANALYSIS OF VARIANCE FOR CURED PBAA PROPELLANT ANALYSES (VARIABLE CONCENTRATIONS AND PARTICLE SIZES)*

Source of Variation	Degrees of Freedom	Ferric Oxide		Ammonium Perchlorate		P8AA Polymer		Aluminum	
		Sum of Squares	Mean Square	Sum of Squares	Mean Square	Sum of Squares	Mean Square	Sum of Squares	Mean Square
Among 8's	8	2851.084	356.386	108.419	13.552	1219.832	152.479	1570.902	196.363
Regression (6)		2841.533	473.589	98.535	16.422	1215.454	202.576	1569.276	261.546
Residual (2)		9.551	4.776	9.884	4.942	4.378	2.189	1.626	0.813
Between T's	1	3.796	3.796	1.814	1.814	3.198	3.198	18.318	18.318
8XT (Exp Error)	8	7.342	0.918	2.118	0.265	9.600	1.200	13.834	1.729
Sampling Error	18	7.542	0.419	2.737	0.152	5.259	0.292	18.878	1.049
Total	35	2869.764		115.087		1237.889		1621.932	

*All values multiplied by 10^4.

TABLE 79. RESIDUAL COMPOSITIONS* FOR DETERMINING COMBINED INGREDIENT PARTICLE SIZES AND CONCENTRATIONS IN HIGH-RATE HTPB PROPELLANT (WEIGHT %, EXPERIMENT-3)

Batch	35-μm Aluminum X_1	Ballistic Modifier X_2	Ammonium Perchlorate** X_3
1	14.00	8.00	70.65
2	14.00	8.00	70.65
3	14.00	8.00	70.65
4	14.00	4.40	70.65
5	14.00	11.60	70.65
6	11.60	8.00	70.65
7	16.40	8.00	70.65
8	14.00	8.00	67.05
9	14.00	8.00	72.25
10	14.00	8.00	70.65
11	14.00	8.00	70.65

*These compositions and those in Tables 40 and 41 form a central composite experimental design. The fourth independent variable (X_4) is weight % 0.5-μm ammonium perchlorate.

**Bimodal blend of 60% - 0.5-μm and 40% - 90-μm ammonium perchlorate.

NOTE: Remainder of propellant is HTPB binder.

TABLE 80. MEAN X-RAY INTENSITY RATIOS FOR UNCURED HIGH RATE HTPB PROPELLANT ANALYSES (EXPERIMENT-3)

Batch	Aluminum R_1	Ballistic Modifier R_2	Ammonium Perchlorate R_3
1	0.187	1.425	0.784
2	0.179	1.417	0.779
3	0.193	1.412	0.795
4	0.211	0.804	0.830
5	0.191	2.272	0.767
6	0.162	1.448	0.799
7	0.202	1.491	0.763
8	0.278	1.502	0.733
9	0.170	1.446	0.804
10	0.544	1.858	0.638
11	0.144	1.242	0.815

The theoretical counting error for an individual emission line peak intensity measurement is fixed by the total number of counts collected. A tabulation of theoretical counting errors for various fixed counts is given in Table 82. Thus, the analyst can control the counting error. The resolution of the counting error from the other sources of error in these experiments is not straightforward, as shown in Appendix A, because of the manner in which the reference standard and propellant samples were analyzed. The measurement scheme that will be used and the counting error that can be tolerated will depend on the relative magnitudes of the counting error and other sources of error as well as the amount of time that can be allotted to the measurement.

Although a detailed discussion of the various sources of error for PBAA propellant analysis is given in Appendix A, it is worthwhile to compare just the sampling errors for low- and high-rate propellant analyses as shown in Table 83. The sampling errors in Table 83 are the estimated relative standard deviations for individual sample analyses. The sampling error includes the counting error, propellant inhomogeneity,

TABLE 81. MULTIPLE REGRESSION DATA FOR UNCURED HIGH RATE HTPB PROPELLANT ANALYSES (EXPERIMENT-3, VARIABLE PARTICLE SIZES AND CONCENTRATIONS, DATA IN TABLES 50, 51, 53, 54, 79 AND 80)

$$\hat{R}_i = b_{i0} + b_{i1}X_1 + \ldots + b_{i4}X_4 + b_{i12}X_1X_2 + \ldots + b_{i34}X_3X_4 + b_{i11}X_1^2 + \ldots + b_{i44}X_4^2$$

Ingredient	Coefficient Level	Coefficient	S_b	t	S_e	R^2
Aluminum	b_{i0}	21.40660			0.026101	0.96939
	b_{11}	0.30746	0.42888	0.7169		
	b_{12}	-0.77164	0.28927	-2.6675		
	b_{13}	-0.49287	0.42991	-1.1465		
	b_{14}	-0.07753	0.02866	-2.7050		
	b_{112}	0.00905	0.00427	2.1198		
	b_{113}	-0.00411	0.00524	-0.7834		
	b_{114}	-0.00017	0.00044	-0.3754		
	b_{123}	0.00907	0.00342	2.6545		
	b_{124}	0.00003	0.00026	0.1184		
	b_{134}	0.00077	0.00035	2.1917		
	b_{111}	-0.00270	0.00390	-0.6932		
	b_{122}	0.00030	0.00173	0.1703		
	b_{133}	0.00297.	0.00266	1.1189		

TABLE 81. (Continued)

Ingredient	Coefficient Level	Coefficient	S_b	t	S_e	R^2
Aluminum (Concluded)	b_{144}	0.00016	0.00002	6.5336		
Ballistic Modifier	b_{20}	39.44070			0.058736	0.98823
	b_{21}	-0.20230	0.96511	-0.2096		
	b_{22}	-0.88524	0.65096	-1.3599		
	b_{23}	-0.87858	0.96743	-0.9082		
	b_{24}	-0.08434	0.06449	-1.3076		
	b_{212}	0.00991	0.00961	1.0317		
	b_{213}	0.00027	0.01179	0.0228		
	b_{214}	-0.00008	0.00099	-0.0818		
	b_{223}	0.01276	0.00768	1.6596		
	b_{224}	-0.00121	0.00059	-2.0565		
	b_{234}	0.00102	0.00079	1.2976		
	b_{211}	0.00351	0.00877	0.3996		
	b_{222}	0.00684	0.00390	1.7536		
	b_{233}	0.00505	0.00598	0.8450		
	b_{244}	0.00011	0.00006	1.9920		

TABLE 81. (Concluded)

Ingredient	Coefficient Level	Coefficient	S_b	t	S_e	R^2
Ammonium Perchlorate	b_{30}	-21.16984			0.014483	0.95892
	b_{31}	-0.19123	0.23798	-0.8036		
	b_{32}	0.36703	0.16052	2.2866		
	b_{33}	0.55307	0.23855	2.3185		
	b_{34}	0.07382	0.01590	4.6417		
	b_{312}	-0.00411	0.00236	-1.7369		
	b_{313}	0.00377	0.00290	1.2984		
	b_{314}	-0.00001	0.00024	-0.0524		
	b_{323}	-0.00451	0.00189	-2.3831		
	b_{324}	-0.00020	0.00014	-1.3935		
	b_{334}	-0.00088	0.00019	-4.5656		
	b_{311}	-0.00152	0.00216	-0.7069		
	b_{322}	0.00068	0.00096	0.7090		
	b_{333}	-0.00364	0.00147	-2.4720		
	b_{344}	-0.00006	0.00001	-4.2808		

TABLE 82. X-RAY COUNTING STATISTICS-RELATIVE STANDARD DEVIATION, $100/\sqrt{n}$

No. of Counts (n)	σ	95% Confidence Limit	99% Confidence Limit	3 σ
100	10.0	19.6	25.8	30.0
200	7.07	13.9	18.2	21.2
500	4.47	8.76	11.5	13.4
1000	3.16	6.19	8.15	9.48
2000	2.24	4.39	5.78	6.72
5000	1.41	2.76	3.64	4.23
10,000	1.00	1.96	2.58	3.00
20,000	0.707	1.39	1.82	2.12
50,000	0.447	0.876	1.15	1.34
100,000	0.316	0.619	0.815	0.948
200,000	0.224	0.439	0.578	0.672
500,000	0.141	0.276	0.364	0.423
1,000,000	0.100	0.196	0.258	0.300
2,000,000	0.0707	0.139	0.182	0.212
5,000,000	0.0447	0.0876	0.115	0.134
10,000,000	0.0316	0.0619	0.0815	0.0948

effects, and error caused by short-term instrumental variations. The error associated with measurement of the reference standard is not included. The counting error in the table is the theoretical value from Table 82.

Except for the determination of PBAA polymer in cured propellant, the sampling errors for all ingredients in the low-rate propellant are less than 1%. This shows that the propellant was very homogeneously mixed and that the sample preparation procedure used provided for very repeatable sample analyses. The repeatability of ammonium perchlorate and aluminum determinations was not as good for two ultrahigh burning

TABLE 83. ESTIMATED SAMPLING ERRORS FOR PBAA AND HTPB PROPELLANT ANALYSES BY X-RAY SPECTROMETRY (RELATIVE STANDARD DEVIATIONS)

Propellant Type	Ferric Oxide			Ammonium Perchlorate			PBAA Polymer			Aluminum			Ballistic Modifier	
	Degrees of Freedom	Sampling Error	Counting Error	Degrees of Freedom	Sampling Error	Counting Error	Degrees of Freedom	Sampling Error	Counting Error	Degrees of Freedom	Sampling Error	Counting Error	Degrees of Freedom	Sampling Error
Uncured PBAA (See Table 15)	24	0.76	0.45	24	0.79	0.14	24	0.75	0.12	24	5.56	0.32		
Cured PBAA (See Table 50)	20	0.84	0.45	20	0.91	0.10	20	1.42	0.71	20	6.75	0.32		
Ultrahigh-Rate Uncured HTPB-1				52	1.74					52	4.47		52	1.34
Ultrahigh-Rate Uncured HTPB-2										52	5.30	0.45		
High-Rate Uncured HTPB				32	0.28	0.14				58	4.83	0.45		

rate propellants tested. This is attributed to the ultrafine ammonium perchlorate agglomeration problem that was discussed in Section II.B. However, the ammonium perchlorate sampling error for high-rate HTPB propellant is very small. In fact, it is significantly better than that for the low-rate propellant. This excellent repeatability for ammonium perchlorate determinations is typical for high- and ultrahigh-rate propellants made with current improved processes. The sampling errors for aluminum determinations in high- and ultrahigh-rate propellants, on the other hand, are typically in the range of 4% to 5%. Because this is for a single aluminum determination, the precision for analysis of a particular propellant batch can be substantially improved by making several sample replications and averaging the results. The lower precision for high-rate propellant aluminum determinations is due to the high sensitivity of AlK_α radiation to the inhomogeneous ammonium perchlorate agglomerates.

The true accuracy of the X-ray fluorescence method was not directly evaluated by analyzing primary propellant standards. Nevertheless, based on extensive experience with the calibration procedure used, which provides an accurate representation of the true intensity-concentration relationships, and the residual errors obtained (Tables 25, 38, 57, and 64), it is expected that low-rate propellant ingredients can be determined with a relative accuracy of 1% or better. The accuracy of high-rate propellant determinations will be somewhat less, particularly for aluminum, because of the ultrafine ammonium perchlorate agglomeration problem.

Application of the recommended X-ray fluorescence analysis method to a specific propellant, as for example in production, will result in the estimation of ingredient percentages using an expression such as Equation (9). The estimated percentages will differ from the actual (nominal) percentages because of the experimental error of the method. Consequently, the analyst must determine whether there is a high probability that the estimated ingredient percentages could have been generated from a propellant formulation having the nominal or expected composition. This determination can be made by placing joint confidence interval estimates on the actual ingredient percentages (concentrations). The methodology for doing this is developed and illustrated for uncured PBAA propellant analyses in Appendix B.

VIII. CONCLUSIONS

The X-ray fluorescence spectrometric method described in this report has been demonstrated to be an excellent procedure for monitoring and determining the compositions of solid composite propellants. The recommended method is nondestructive, rapid, and capable of a high degree of precision and accuracy. Typically, the composition of a composite propellant batch can be determined within 15 to 30 min, thus enabling substandard batches either to be discarded or corrected prior to casting into motors. The method applies equally well to cured and uncured propellant samples.

The X-ray fluorescence method is unique in its ability to determine ingredient percentages and in-situ particle sizes as well as combinations of these parameters. The estimated relative standard deviation for the determination of ingredients in low-rate propellants and ammonium perchlorate in high-rate propellants is 1% or less. The estimated relative standard deviation for determining aluminum in high-rate propellants is larger (4% to 5%) because of problems caused by ultrafine ammonium perchlorate agglomeration. The ability of the method to detect and quantify the ultrafine ammonium perchlorate agglomeration is a very valuable feature for high burning rate propellant applications. Because of the influence of ultrafine ammonium perchlorate agglomeration on propellant properties, this capability for agglomeration analysis alone justifies the application of the method to high-rate propellant manufacture. With four to six sample replications, the accuracy for determining all ingredient percentages is of the order of 1% to 2% relative or better.

The X-ray fluorescence method does have some practical limitations with respect to propellant analysis. It is an elemental emission method capable of detecting, from a practical standpoint, elements of atomic No. 12 (magnesium) and higher. Therefore, organic propellant ingredients such as hydroxyl-terminated polymers, plasticizers, and some ballistic modifiers cannot be detected. Consequently, a complete analysis requires that these ingredients be determined by an alternative procedure. It should be emphasized, however, that a substandard propellant composition can be detected by the X-ray method if the percentage of a detectable element changes, even if the change is caused by an error in the percentage of a nondetectable ingredient.

IX. RECOMMENDED IMPLEMENTATION

The X-ray fluorescence method described here has potential application to all types of solid composite propellants used in Army missile systems. The method is ideal for application to propellant production because of its speed, precision, and nondestructive nature. VIPER propellant, which is in engineering development, is an excellent candidate at this time, because of the anticipated large production rate and the high propellant cost. The method has been recommended to the VIPER Project Office. Their personnel have been apprised of its salient features. The method should also be considered for application to the propellant manufacturing processes for the PATRIOT and PERSHING missile systems.

This MTT project should logically progress to a Manufacturing Methods and Technology (MM&T) project to demonstrate specific application of the developed test method to a propellant manufacturing process. The MM&T project would perhaps best be conducted by the appropriate missile system propulsion subcontractor. Such a project should include the purchase, installation, and demonstration of automated, computer controlled instrumentation that would be more suitable for a production

application than the manual instrumentation used in this MTT project. The necessary automated instrumentation is commercially available at a cost of approximately $100,000.

Finally, the X-ray fluorescence test procedure will be prepared in the proper format and submitted for possible inclusion in MIL-STD-286B as a tentative method. MIL-STD-286B currently contains no test methods for finished composite propellants.

Appendix A. RESOLUTION OF ERROR VARIANCES

Section IV clearly outlined that the experimental technique involved taking two pairs of observations at each concentration (batch) of the mixture for both uncured and cured PBAA propellant samples, one pair from the first sample and another pair from the second sample. An important point is that within a sample, the measurement in seconds on the reference standard is taken only once. Hence the numerator of both ratios will be the same. However, the reference standard is measured again for the observations of the second sample. The intensity data in seconds were given in Table 17. The four ratios for the uncured samples from which the average ratios in Table 19 were calculated are shown in Table 18. The first number in each block in Table 17 is the reading in seconds for the reference standard and the next two the readings for the unknown in question, all for the first sample from that batch. Directly below the first sample measurement are three similar measurements for the second sample from the same batch. Tables 29 and 30 give the seconds and intensity ratios, respectively, for the cured samples. The number of counts varied from ingredient to ingredient. These are shown in Table 16.

It is of interest to the experimenter to know the relative orders of magnitude of the different sources of variance in the experiment. It is expected that the different batches would cause the greatest variation because the concentrations are changing across batches. The other sources are the sample to sample variation and within-sample variation. Theoretically, the latter consists of two components: (1) variance due to the counting error, and (2) propellant inhomogeneity and other errors — electronic, etc. These error variances shall be called as σ_c^2 and σ_ε^2, respectively.

1. Counting Error

The number of radiation counts used in an experiment will be called n. It is generally assumed that the probability model describing the number of counts produced by the counting device in time t is the Poisson distribution [25] with probability function

$$p(x) = \frac{e^{-\lambda t}(\lambda t)^x}{x!} \qquad (x = 0,1,2,\ldots) \qquad (A\text{-}1)$$

where λ is the counting rate in counts per unit time. Parrish [26] in reviewing the general problem of counting error says "Two measurements of a constant intensity in which counting is performed during equal times t, will not in general yield the same number n of counts, owing to a random distribution." He mentions approximating this with a Gaussian distribution with mean $\bar{N}$ and standard deviation $\sigma = \sqrt{\bar{N}}$, where $\bar{N}$ is an average of the number of counts in time t obtained from a large number of experiments. This corresponds to the normal approximation to the Poisson distribution for the number of counts in a given time t for the fixed time procedure. The procedure used here is the fixed

count procedure. The measurement used here is the ratio of the time t_s that it takes any n_s counts to be taken on the standard to t_u, the time that it takes for n_u counts to be made on the component of unknown concentration. Thus, if the counting variance is to be separated from the other variations in the experiment, the variance of this ratio is required.

Either the numerator or denominator of that ratio, i.e., the time t for n counts is considered. If the number of counts in time t follows the Poisson law as given by Equation (A-1), and if x denotes the random variable representing the time to the nth count, then

$$P_r(X < 0) = 0 \qquad \text{(A-2)}$$

and

$$P_r(0 \leq X \leq t) = \sum_{k=n}^{\infty} \frac{(\lambda t)^k e^{-\lambda t}}{k!} \quad . \qquad \text{(A-3)}$$

The first follows because this time cannot be negative. The second equation merely says that the probability of getting n or more counts in time t is the probability of requiring t or less time for n counts. Thus, Equations (A-2) and (A-3) describe the distribution function for this random variable X. Equations (A-2) and (A-3) can then be differentiated with respect to t in order to obtain the probability density function.

$$\frac{\partial}{\partial t} \sum_{k=n}^{\infty} \frac{(\lambda t)^k}{k!} e^{-\lambda t} = e^{-\lambda t} \sum_{k=n}^{\infty} \frac{(\lambda t)^{k-1} \cdot \lambda}{(k-1)!} - e^{-\lambda t} \sum_{k=n}^{\infty} \frac{(\lambda t)^k \cdot \lambda}{k!}$$

$$p(t) = \frac{\lambda^n t^{n-1} e^{-\lambda t}}{\Gamma(n)} \quad . \qquad \text{(A-4)}$$

This describes the well-known Gamma density function with parameters n-1 and $1/\lambda$. Thus the waiting time for n counts is a Gamma distribution. The distribution of t_1/t_2 is required where t_1 and t_2 are both Gamma variables.

At the outset, it will be assumed that the measurements involve different counting rates λ_1 and λ_2 and different numbers of counts n_1 and n_2. Thus,

$$p(t_1) = \frac{\lambda_1^{n_1} (t_1)^{n_1-1} e^{-\lambda_1 t_1}}{\Gamma(n_1)} \qquad (t_1 > 0;\ n_1, \lambda_1 > 0)$$

$$p(t_2) = \frac{\lambda_2^{n_2} (t_2)^{n_2-1} e^{-\lambda_2 t_2}}{\Gamma(n_2)} \qquad (t_2 > 0;\ n_2, \lambda_2 > 0)$$

If the independence of t_1 and t_2 is assumed,

$$p(t_1,t_2) = \frac{\lambda_1^{n_1} \lambda_2^{n_2}}{\Gamma(n_1)\Gamma(n_2)} t_1^{n_1-1} t_2^{n_2-1} e^{-(\lambda_1 t_1 + \lambda_2 t_2)} .$$

Letting $u = t_1/t_2$, the required ratio and $z = t_2$, the following is obtained:

$$P(u,z) = p(t_1,t_2) \left[\frac{\partial(t_1,t_2)}{\partial(z,u)} \right] . \qquad (A-5)$$

After evaluating the Jacobian and simplifying, Equation (A-5) becomes

$$p(u,z) = C\, u^{n_1-1} z^{n_1+n_2-1} e^{-(\lambda z\, u + \lambda_2 z)} \qquad (A-6)$$

where

$$C = \frac{\lambda_1^{n_1} \lambda_2^{n_2}}{\Gamma(n_1)\Gamma(n_2)} .$$

The density function for u is required, so if z is integrated out, the following is obtained

$$p(u) = C\, u^{n_1-1} \int_0^{\infty} z^{n_1+n_2-1} e^{-(\lambda_1 zu + \lambda_2 z)} dz$$

$$= \frac{\lambda_1^{n_1} \lambda_2^{n_2} u^{n_1-1} \Gamma(n_1 + n_2)}{\Gamma(n_1)\Gamma(n_2)(\lambda_1 u + \lambda_2)^{n_1+n_2}} . \qquad (A-7)$$

The moments of this distribution can then be found in the usual way. The mean is as follows:

$$E(u) = E\left(\frac{t_1}{t_2}\right) = \frac{\lambda_2}{\lambda_1}\frac{n_1}{n_2 - 1} \quad .$$

If n_1 and n_2 are both large, this quantity reduces to λ_2/λ_1, the ratio of the counting rates. To obtain the variance of this ratio, first the crude second moment must be found:

$$E(u^2) = K\int_0^\infty \frac{u^{n_1+1}}{(\lambda_1 u + \lambda_2)^{n_1+n_2}}\,du$$

where

$$K = C\cdot\Gamma(n_1 + n_2).$$

$$E(u^2) = K\int_0^\infty \frac{u^{n_1+1}}{\left(1 + \frac{\lambda_1 u}{\lambda_2}\right)^{n_1+n_2}(\lambda_2)^{n_1+n_2}}\,du \quad .$$

If $\lambda_1 u/\lambda_2 = X$, then the preceding integral becomes

$$E(u^2) = \frac{K}{(\lambda_2)^{n_1+n_2}}\left(\frac{\lambda_2}{\lambda_1}\right)^{n_1+2}\int_0^\infty \frac{X^{n_1+1}}{(1 + X)^{n_1+n_2}}\,dx \quad . \qquad \text{(A-8)}$$

After integrating and simplifying, Equation (A-8) becomes

$$E(u^2) = \frac{\lambda_2^2}{\lambda_1^2}\frac{(n_1 + 1)n_1}{(n_2 - 1)(n_2 - 2)} \quad .$$

For the variance of u the following is obtained:

$$\sigma^2_u = E(u^2) - [E(u)]^2$$

$$= \frac{\lambda_2^2}{\lambda_1^2}\left[\frac{(n_1 + 1)n_1}{(n_2 - 1)(n_2 - 2)} - \frac{n_1^2}{(n_2 - 1)^2}\right]$$

$$= \frac{\lambda_2^2}{\lambda_1^2}\left[\frac{(n_2 - 1)(n_1 + 1)(n_1) - n_1^2(n_2 - 2)}{(n_2 - 1)^2(n_2 - 2)}\right]$$

$$= \frac{\lambda_2^2}{\lambda_1^2}\left[\frac{n_1(n_1 - 1) + n_1 n_2}{(n_2 - 1)^2(n_2 - 2)}\right] \quad . \qquad \text{(A-9)}$$

If $n_1 = n_2 = n$, i.e., if the same number of counts is used for the standard as for the unknown, and if it is further assumed that n is large, Equation (A-9) will reduce to

$$\sigma^2_u \simeq \frac{\lambda_2^2}{\lambda_1^2}\left(\frac{2}{n}\right) \quad . \qquad \text{(A-10)}$$

Equations (A-9) and (A-10) give the variance of the ratio t_1/t_2 under the conditions specified. It is interesting to note from Equation (A-9) that if the experimenter is willing to allow $n_1 \neq n_2$, he can reduce the variance by making $n_2 \gg n_1$. Thus it appears that in terms of counting precision it is best to use a larger number of counts on the component of unknown concentration, rather that splitting up a large number of counts equally among the standard and unknown. For example, if $n_1 = n_2 = 10{,}000$ is used, $\sigma^2_u \simeq \lambda_2^2/\lambda_1^2$ 0.0002; whereas if $n_1 = 1000$ and $n_2 = 20{,}000$ is used, $\sigma^2_u \simeq \lambda_2^2/\lambda_1^2$ 0.0000025.

2. Linear Model

It was necessary to arrive at a method of using the data in Tables 17, 18, 29, and 30, along with the theoretical information obtained in this appendix on the counting variance to make an overall evaluation of the error variances. If it is assumed that the ratio data (for the

cured and uncured propellant samples) for the Kth ingredient follows the model

$$x_{ijl}^{(k)} = u^{(k)} + B_i^{(k)} + S_{j(i)}^{(k)} + C_{ijl}^{(k)} + \epsilon_{ijl}^{(k)}$$

where

$B_i^{(k)}$ = batch effect, with variance $\sigma_\beta^{2(k)}$

$S_{j(i)}^{(k)}$ = effect of the sample within batches with variance $\sigma_s^{2(k)}$

$C_{ijl}^{(k)}$ = counting error with variance $\sigma_c^{2(k)}$

$\epsilon_{ijl}^{(k)}$ = within sample error **not** including counting error, e.g., inhomogeneity and sample instrumental error, with variance $\sigma_\epsilon^{2(k)}$.

It is particularly important to determine what portion of the within-sample variation is due to counting variance and what portion is due to the remaining errors because the experimenter can control the counting variance. The ratio data in Tables 18 and 30 were analyzed as a hierarchial [27] (subsampling) classification not in order to make any particular tests but to estimate the variance components. Tables A-1 and A-2 show the mean squares for the uncured and the cured propellant data, respectively.

Certain linear combinations of the mean squares are unbiased estimates of the variance components. It is reasonably easy to show that the following expressions represent the expected mean squares. The k superscript will be dropped at this stage.

$$E(MS_E) = \sigma_\epsilon^2 + \sigma_c^2 \qquad (MS_E \text{ is error mean square})$$

$$E(MS_{B(A)}) = \sigma_\epsilon^2 + \sigma_c^2 + 2\sigma_s^2 \qquad (MS_{B(A)} \text{ is mean square samples within batches})$$

$$E(MS_A) = \sigma_\epsilon^2 + \sigma_c^2 + 2\sigma_s^2 + 4\sigma_\beta^2 \qquad (MS_A \text{ is mean squares batches}) \quad .$$

TABLE A-1. VARIANCE ANALYSIS* FOR UNCURED PBAA PROPELLANT

Source	DF	SS	MS
Ferric Oxide			
Batch	11	0.40205711	0.03655064
Samples	12	0.00196559	0.00016371
Error	24	0.00141607	0.00005900
Ammonium Perchlorate			
Batch	11	0.05074630	0.00461330
Samples	12	0.00112890	0.00009407
Error	24	0.00108068	0.00004502
PBAA Polymer			
Batch	11	0.17377193	0.01579744
Samples	12	0.00099994	0.00008332
Error	24	0.00095275	0.00003969
Aluminum			
Batch	11	0.12441220	0.01131020
Samples	12	0.00159362	0.00013280
Error	24	0.00196859	0.00008202

*This is a nested analysis in which "samples" are actually "samples within batches" and error represents the variation "between observations within samples," and batches.

DF = Degrees-of-freedom
SS = Sum of squares
MS = Mean square

Therefore, the estimates are given by the following:

$$MS_E \text{ estimates } \sigma_\varepsilon^2 + \sigma_c^2$$

$$\frac{MS_{B(A)} - MS_E}{2} \text{ estimates } \sigma_s^2$$

$$\frac{MS_A - MS_{B(A)}}{4} \text{ estimates } \sigma_\beta^2 \quad . \qquad \text{(A-11)}$$

TABLE A-2. VARIANCE ANALYSIS* FOR CURED PBAA PROPELLANT SAMPLES

Source	DF	SS	MS
Ferric Oxide			
Batch	9	0.32633644	0.03629200
Samples	10	0.00187111	0.00018011
Error	20	0.00147753	0.00007388
Ammonium Perchlorate			
Batch	9	0.01225774	0.00136197
Samples	10	0.00050185	0.00005018
Error	20	0.00068033	0.00003401
PBAA Polymer			
Batch	9	0.13362281	0.01484697
Samples	10	0.00194809	0.00019480
Error	20	0.00196067	0.00009803
Aluminum			
Batch	9	0.12455100	0.01383900
Samples	10	0.00189946	0.00018994
Error	20	0.00138341	0.00006917

*This is a nested analysis in which "samples" are actually "samples within batches" and error represents the variation "between observations within samples", and batches.

DF = Degrees of freedom
SS = Sum of squares
MS = Mean square

The results in Tables A-1 and A-2 can then be used to arrive at estimates of these variance components for each of the ingredients for both the uncured and cured propellant. However, an elaboration must be made concerning σ_c^2, the actual theoretical counting variance. Using Equation (A-10), σ_c^2 can be computed because in all cases $n_1 = n_2 = n$ with n being greater than 20,000. MS_E represents the within-sample variation in the data, i.e., the variation between two replicates within a sample. However, it was emphasized earlier that within a sample the same measurement on the reference standard was used in the numerator

of both ratios. Therefore, while the theoretical counting variance derived in Paragraph 1 is the true one, it is not the one which is being estimated by MS_E because the latter does not take into account counting error associated with the standard. Thus, to be able to isolate an estimate of $\sigma_\epsilon^{2(k)}$, an alteration in the counting variance must be made to account for the experimental procedure used here.

The variable $v = 1/t_2$ is considered where t_2 follows a Gamma distribution. The distribution, mean, and variance of this random variable will be found. For expedience the n_2 and λ_2 notation will not be used as before. Instead, the usual notation for a Gamma density, namely, parameters α and β will be used. Therefore, $\alpha = n_2 - 1$ and $1/\lambda_2 = \beta$. It follows that

$$p(t_2) = \frac{t_2^{\alpha} e^{-t_2/\beta}}{\Gamma(\alpha+1)\beta^{\alpha+1}}$$

$$g(v) = \frac{\frac{1}{v}^{\alpha} e^{-1/v\beta}}{\Gamma(\alpha+1)\beta^{\alpha+1}} \cdot \left| \frac{\partial t_2}{\partial v} \right| \quad . \qquad \text{(A-12)}$$

The value of the Jacobian is $1/v^2$. Thus $g(v)$ can be simplified to

$$g(v) = \frac{\left(\frac{1}{v}\right)^{\alpha+2} e^{-1/\beta v}}{\Gamma(\alpha+1)\beta^{\alpha+1}} \quad .$$

The first two moments of this distribution will now be found:

$$E(v) = \int_0^{\infty} \frac{v^{-\alpha-1} e^{-1/v}}{\Gamma(\alpha+1)\beta^{\alpha+1}} dv$$

$$= \frac{1}{\Gamma(\alpha+1)\beta^{\alpha+1}} \int_0^{\infty} \frac{(\beta v)^{-\alpha-1} e^{-1/\beta v}}{\beta^{-1-1}} dv \quad .$$

If $z = 1/\beta v$, then the preceding expression becomes

$$E(v) = \frac{1}{\Gamma(\alpha+1)\beta} \int_0^{\infty} z^{\alpha-1} e^{-z} dz = \frac{\Gamma(\alpha)}{\Gamma(\alpha+1)\beta} = \frac{1}{\beta\alpha}$$

$$E(v^2) = \frac{1}{\Gamma(\alpha+1)\beta^{\alpha+1}} \int_0^\infty v^{-\alpha} e^{-1/\beta v}\, dv$$

$$= \frac{1}{\Gamma(\alpha+1)\beta^{\alpha+1}} \int_0^\infty \frac{(\beta v)^{-\alpha} e^{-1/\beta v}}{\beta^{-\alpha}}\, dv \quad . \tag{A-13}$$

As before, $z = 1/\beta v$. Equation (A-13) then becomes

$$E(v^2) = \frac{1}{\Gamma(\alpha+1)\beta} \int_0^\infty z^{\alpha} e^{-z} \left(-\frac{1}{\beta z^2}\right) dz$$

$$= \frac{\Gamma(\alpha-1)}{\Gamma(\alpha+1)\beta^2} = \frac{1}{\beta^2 \alpha(\alpha-1)}$$

$$\sigma^2 v = E(v^2) - [E(v)]^2 = \frac{1}{\beta^2 \alpha^2 (\alpha-1)} \quad . \tag{A-14}$$

Substituting $n_2 = \alpha + 1$ and $\lambda_2 = 1/\beta$ into Equation (A-14) the following is obtained

$$\sigma^2 v = \frac{\lambda_2^2}{(n_2 - 1)^2 (n_2 - 2)} \tag{A-15}$$

$$\approx \frac{\lambda_2^2}{n^3} \tag{A-16}$$

for the case where $n_2 = n$ and n is large. Equation (A-16) gives an expression for the variance of $1/t_2$. Actually $\mathrm{Var}(t_1/t_2)$ is needed where t_1 is considered to be a constant; $\mathrm{Var}(t_1/t_2) = t_1^2(\lambda_2^2/n^3)$. On the average for $n_1 = n_2 = n$, it is expected that $t_1 = n/\lambda_1$. Thus, an approximation to the required variance is:

$$\mathrm{Var}\ \frac{t_1}{t_2} = \left(\frac{\lambda_2^2}{\lambda_1^2}\right)\left(\frac{1}{n}\right) = \sigma_v'^2 \quad . \tag{A-17}$$

It must be emphasized here that this is not the counting variance. The latter was given earlier in Paragraph 1. This is, however, the variance which is estimated by MS_E in these experiments.

3. Estimation of Variance Components

The expressions in Equation (A-11) were used to compute the batch and sample variance components. Equation (A-10) was used to compute the true counting variance σ_c^2 and Equation (A-17) was used to compute σ'^2_v; σ^2_ϵ was computed by $MS_E - \sigma'^2_v$.

The occurrence of λ_2 and λ_1 in the formulae for the variance presents a bit of a problem. Strictly speaking, these λ's are not a qualitative function of the ingredient but a quantitative one. That is, the λ's depend on the concentration of each ingredient. The λ's were estimated for a particular ingredient by taking the counting rate for that ingredient averaged over all the data. The λ_1's were found in the same way. Table A-3 gives the estimated variance components for each ingredient for the cured and uncured propellants. Also included is σ_c^2, the true counting variance.

As expected, $\hat{\sigma}^2_\beta$ is always large. The estimate of within-sample variance (excluding counting) $\hat{\sigma}^2_\epsilon$ is approximately the same for each component for both uncured and cured propellant with the exception of PBAA polymer in the uncured propellant where this variance seems to be exceptionally small. Otherwise the order of magnitude of $\hat{\sigma}^2_\epsilon$ seems to be in the vicinity of 3.7×10^{-5}. In comparing this variance with the theoretical counting variance (which is the proper comparison to make, i.e., $\hat{\sigma}^2_\epsilon$ should be compared with σ_c^2), it is noted that for n in the range of 20,000 to 50,000 σ^2_ϵ and σ_c^2 seem to be about the same order of magnitude. That is, for n in this range the within-sample variance is approximately 50% due to counting and 50% due to other errors. An increase from 50,000 to 500,000 decreases σ_c^2 by a factor of 10. As previously mentioned, it is expected that the counting variance is best reduced, not by increasing the total number of counts but by taking more counts on the unknown and fewer on the standard. It must be emphasized though that the overall variance within samples is small and it is doubtful that reassigning n_1 and n_2 would reduce the overall variance within samples, i.e., $\hat{\sigma}^2_\epsilon + \sigma_c^2$ by more than a factor of two. Of course it is assumed that all of this reduction is accounted for by the decrease of σ_c^2.

TABLE A-3. VARIANCE COMPONENTS AND ESTIMATES OF VARIANCE COMPONENTS

Parameter	Ferric Oxide	Ammonium Perchlorate	PBAA Polymer	Aluminum
	Uncured PBAA Propellant			
$\frac{\lambda_2}{\lambda_1}$ est.	1.003425	0.843652	0.832587	1.049921
n	50,000	500,000	20,000	100,000
$\hat{\sigma}^2_\beta$	0.009097	0.001130	0.003928	0.002794
$\hat{\sigma}^2_s$	5.235×10^{-5}	2.452×10^{-5}	2.182×10^{-5}	2.539×10^{-5}
$\hat{\sigma}^2_c$	4.027×10^{-5}	2.847×10^{-6}	6.932×10^{-5}	2.205×10^{-5}
$\hat{\sigma}^2_\varepsilon$	3.880×10^{-5}	4.360×10^{-5}	0.5037×10^{-5}	7.100×10^{-5}
σ'^2_v	2.014×10^{-5}	0.1423×10^{-5}	3.466×10^{-5}	1.102×10^{-5}
	Cured PBAA Propellant			
$\frac{\lambda_2}{\lambda_1}$ est.	1.01193	0.962473	0.742861	1.129778
n	50,000	1,000,000	20,000	100,000
$\hat{\sigma}^2_\beta$	0.008168	0.0003279	0.003663	0.003412
$\hat{\sigma}^2_s$	5.662×10^{-5}	0.8084×10^{-5}	4.839×10^{-5}	6.039×10^{-5}
$\hat{\sigma}^2_c$	4.096×10^{-5}	1.853×10^{-6}	5.518×10^{-5}	2.552×10^{-5}
$\hat{\sigma}^2_\varepsilon$	5.339×10^{-5}	3.309×10^{-5}	7.044×10^{-5}	5.641×10^{-5}
σ'^2_v	2.049×10^{-5}	0.0926×10^{-5}	2.759×10^{-5}	1.276×10^{-5}

Appendix B. CONFIDENCE INTERVAL ESTIMATE OF CONCENTRATION: EVALUATION OF PROPELLANT PRODUCTION

The purpose of this appendix is to develop and illustrate a method for determining how well the point estimates described in Section IV estimate the concentrations. The obvious way of attempting this type of determination is via the route of joint confidence interval estimates on the actual concentrations. There are certain nominal concentrations that the production process will attempt to attain. It remains then to determine if there is strong reason (i.e., high probability) to believe that the intensity ratios from the sample or the estimates of the concentrations from Equations (15) could have been generated from mixtures with the nominal concentrations. This procedure represents a "go" or "no go" type of situation, i.e., based on the confidence intervals, it is concluded that the true concentrations either are or are not what they are supposed to be. The underlying theory on which these confidence intervals are based is found in the following paragraphs. The theory and development is general. The application was made here only to uncured PBAA propellant samples where ingredient particle sizes were held constant.

Box and Hunter [28] discuss the problem of finding joint confidence interval estimates on the solution of a set of simultaneous equations when the coefficients are subject to error. Their work was actually part of a more specific problem of finding a confidence region for a stationary point in response surface analysis. However, the theory can be applied to the problem discussed here because the estimates of the concentrations are found by solving a set of simultaneous regression equations.

It is supposed that there are m simultaneous equations of the type:

$$\sum_{j=0}^{m} b_{ij} X_j = 0 \qquad (i = 1,2,\ldots,m) \qquad \text{(B-1)}$$

where the b_{ij} are subject to error. The quantities

$$\sum_{j=0}^{m} b_{ij} \xi_j = \delta_i \qquad (i = 1,2,\ldots,m) \qquad \text{(B-2)}$$

are considered where the ξ are the values of the X's that would satisfy Equation (B-1) if the actual regression coefficients were used in place of the b_{ij}. For this work, the ξ's represent the actual concentrations; thus Equation (B-2) is

$$R_i - \hat{R}_i = \delta_i \quad ,$$

where

$$\hat{R}_i = h_{i0} + \sum_{j=1}^{4} b_{ij}\xi_j \quad .$$

Then it is desirable to attach joint confidence intervals on ξ_1, ξ_2, ξ_3, and ξ_4.

If a vector of the δ's is considered, say $\underline{\delta}$, as having a multivariate normal distribution with mean vector $\underline{o}$ and variance-covariance matrix $E(\underline{\delta}\ \underline{\delta}') = V$, then $\underline{\delta}'\ V^{-1}\ \underline{\delta}$ follows a χ^2 distribution with m degrees-of-freedom (m = 4 in this case). The remarks made here rely on the assumption that the ε_{ij} in Equation (7) follow a normal distribution with zero mean and some variance σ^2. For estimates of the elements of V, the following is obtained:

$$\hat{\text{Var}}\ (R_i - \hat{R}_i) = s_{ii}\left[1 + \frac{1}{n} + \sum_h \sum_l C_{hl}\xi_h\xi_l\right] = s_{ii}\cdot H \qquad \text{(B-3)}$$

$$\hat{\text{Cov}}\ (R_i - \hat{R}_i,\ R_k - \hat{R}_k) = s_{ik}\left[1 + \frac{1}{n} + \sum_h \sum_l C_{hl}\xi_h\xi_l\right]$$

$$= s_{ik}\cdot H \quad , \qquad \text{(B-4)}$$

where s_{ii} is the sample estimate of the error variance and s_{ik} is the sample estimate of the covariance between the ε_{ij} and the ε_{kj} (j = 1,2,...,n) in Equation (7). C_{hl} is the (hl) element of the inverse of the matrix of corrected sums of squares and cross products of the y's for the calibration sample. Replacing V by its estimate, and dividing by the appropriate degrees-of-freedom, the following ratio is obtained:

$$\frac{n-8}{4} \sum_i \sum_k \frac{\delta_i \delta_k w^{ik}}{H}$$

which is distributed as F with 4 and n-8 degrees-of-freedom. Here w^{ik} is the (ik) element of the inverse of the matrix W, the matrix of residual sum of squares and cross products of the R's from the original data. The following is obtained:

$$\delta_i = \sum_j b_{ij}\hat{X}_j - \sum_j b_{ij}\xi_j = R_i - \hat{R}_i \quad . \qquad \text{(B-5)}$$

If δ_i is replaced in the preceding F statistic by the expression given in Equation (B-5), the following is obtained:

$$F_{4,n-8} = \frac{n-8}{4} \frac{\sum_i \sum_j \sum_k \sum_l (\hat{X}_j - \xi_j)(\hat{X}_l - \xi_l)\, b_{ij} b_{kl} w^{ik}}{H}$$

$$= \frac{n-8}{4} \frac{\sum_j \sum_l (\hat{X}_j - \xi_j)\,(\hat{X}_l - \xi_l)\, q_{jl}}{H} \qquad \text{(B-6)}$$

where q_{jl} is the (jl) element of the matrix:

$$Q = B'\, W^{-1}\, B \quad .$$

B is the matrix of regression coefficients for the set of 4 regression lines. Equation (B-6) represents joint confidence intervals on the actual concentrations. That is, given values of the estimates $\hat{X}_1$, $\hat{X}_2$, $\hat{X}_3$, and $\hat{X}_4$, particular values of ξ_1, ξ_2, ξ_3, and ξ_4 can be substituted into Equation (B-6) and if the resulting expression is less than $F_{\alpha,4,n-8}$ (upper tail point) then the ξ's fall inside the 100 (1-α) % confidence region. The W^{-1} and Q matrices for the uncured PBAA propellant data are:

$$W^{-1} = \begin{bmatrix} 7214.8162 & 2554.8459 & -3201.5790 & 3439.8046 \\ & 4014.0983 & -1714.2325 & 2122.4663 \\ & & 2679.7650 & -1867.4456 \\ & & & 2825.4942 \end{bmatrix}$$

$$Q = \begin{bmatrix} 24274.424 & -15.343 & -274.4115 & 219.582 \\ & 2.4899 & 2.8058 & 0.77389 \\ & & 10.8662 & -36781 \\ & & & 5.3264 \end{bmatrix} \quad .$$

The obvious ξ's to consider are the nominal concentrations. If the $\hat{X}$'s are close to the ξ's, then this F value in Equation (B-6) will be close to zero, the nominal values would be covered by, say a 95% confidence region and hence it would be concluded that the mixture concentrations do not deviate from the target values. In case the

estimates deviate significantly from the target, i.e., if the F value is significant, the target ξ's fall outside the 95% confidence region and it is concluded that the mixture composition is not what it should be. It can be said that there is 0.05 probability that the set of estimates calculated could have been generated, for which the 95% joint confidence interval would not cover the true concentrations. Thus, there is good protection against wrong conclusions that the process is not producing the desired concentrations.

Very often the difficulty with this kind of procedure is that the width or area covered by the confidence region is very large. That is, it is often impractical because it could always be concluded that the production process is attaining ingredient concentrations that do not differ significantly from those desired. This means that the sensitivity of the confidence interval method is low, or in terms of hypothesis testing language, the power (in classifying the concentrations as not differing from the nominal ones when, in fact, there are differences) is very low. This problem did not appear in this work. The confidence regions were narrow and the results have much practical use.

The nominal concentrations of uncured PBAA propellant ingredients for this example correspond to the midpoint of the design (Table 15) and are: $\xi_1 = 0.5$, $\xi_2 = 68.0$, $\xi_3 = 13.5$, and $\xi_4 = 16.0$. All of these are in weight percent. This leaves 2.0% for the remaining binder components. If a sample is taken from a batch of propellant of unknown ingredient concentrations and analyzed for each ingredient and if Equations (15) result in the estimated concentrations $\hat{X}_1 = 0.5$, $\hat{X}_2 = 68.0$, $\hat{X}_3 = 14.5$, and $\hat{X}_4 = 17.0$, then substituting into Equation (B-6) yields an F value of 7.45. The numerator and denominator degrees-of-freedom are both 4 because n = 12 for the original experiment. The upper 95% point is 6.39. This means that the nominal concentrations are not covered by the 95% confidence region; thus it is concluded that this analyzed mixture has true concentrations that deviate significantly from the nominal ones. The estimates did not deviate a great deal from the ξ's; yet the procedure was able to detect the difference. As another example, if $\hat{X}_1 = 0.49$, $\hat{X}_2 = 68.0$, $\hat{X}_3 = 13.5$, and $\hat{X}_4 = 15.5$, an F value of 5.021 will result. This value is less than the 95% point; thus it is concluded that the concentrations do not deviate a significant amount from the nominal ones.

It should be noted here that Equation (B-6) should contain not the actual ξ's and $\hat{X}$'s, but the corrected ξ's and $\hat{X}$'s, i.e., each corrected for the average concentration of that component in the original calibration mixtures shown in Table 15. These averages are:

$$\bar{\xi}_1 = 0.494$$

$\bar{\xi}_2 = 68.26$

$\bar{\xi}_3 = 13.37$

$\bar{\xi}_4 = 16.02$.

Therefore, for the previous example, the following should be inserted into Equation (B-6):

$\hat{X}_1 = 0.49 - 0.494$, $\hat{X}_2 = 68.0 - 68.26$, etc.

$\xi_1 = 0.5 - 0.494$, $\xi_2 = 68 - 68.26$, etc.

As mentioned earlier, the C's in Equation (B-6) are the elements of the inverse matrix of sum of squares and products using the original calibration mixes. This matrix is

$$C = \begin{bmatrix} 34.72988 & 1.00642 & 1.13464 & 0.83355 \\ & 4.29894 & 4.89776 & 4.38275 \\ & & 4.20892 & 4.29237 \\ & & & 4.59324 \end{bmatrix}$$

Several charts were prepared which illustrate the use of this method for evaluating a propellant mix of unknown ingredient concentrations. Figures B-1 through B-7 are given in which, for the ξ's held at the nominal values, contours of constant probability P were plotted for variable values of the $\hat{X}$'s, the estimates. The contours represent constant $(1 - \alpha)$ probability corresponding to a confidence level whose confidence region contains the nominal ξ's exactly at the boundary. For example, for a set of estimates $\hat{X}_1$, $\hat{X}_2$, $\hat{X}_3$, and $\hat{X}_4$, a value of P of, say, 0.1 means that the nominal ξ's are at the boundary of a 90% confidence region. A good rule of thumb might be to consider a probability of 0.95 as being significant, i.e., if $p > 0.05$, then the deviation between the estimates and the nominal concentrations is considered to be significant.

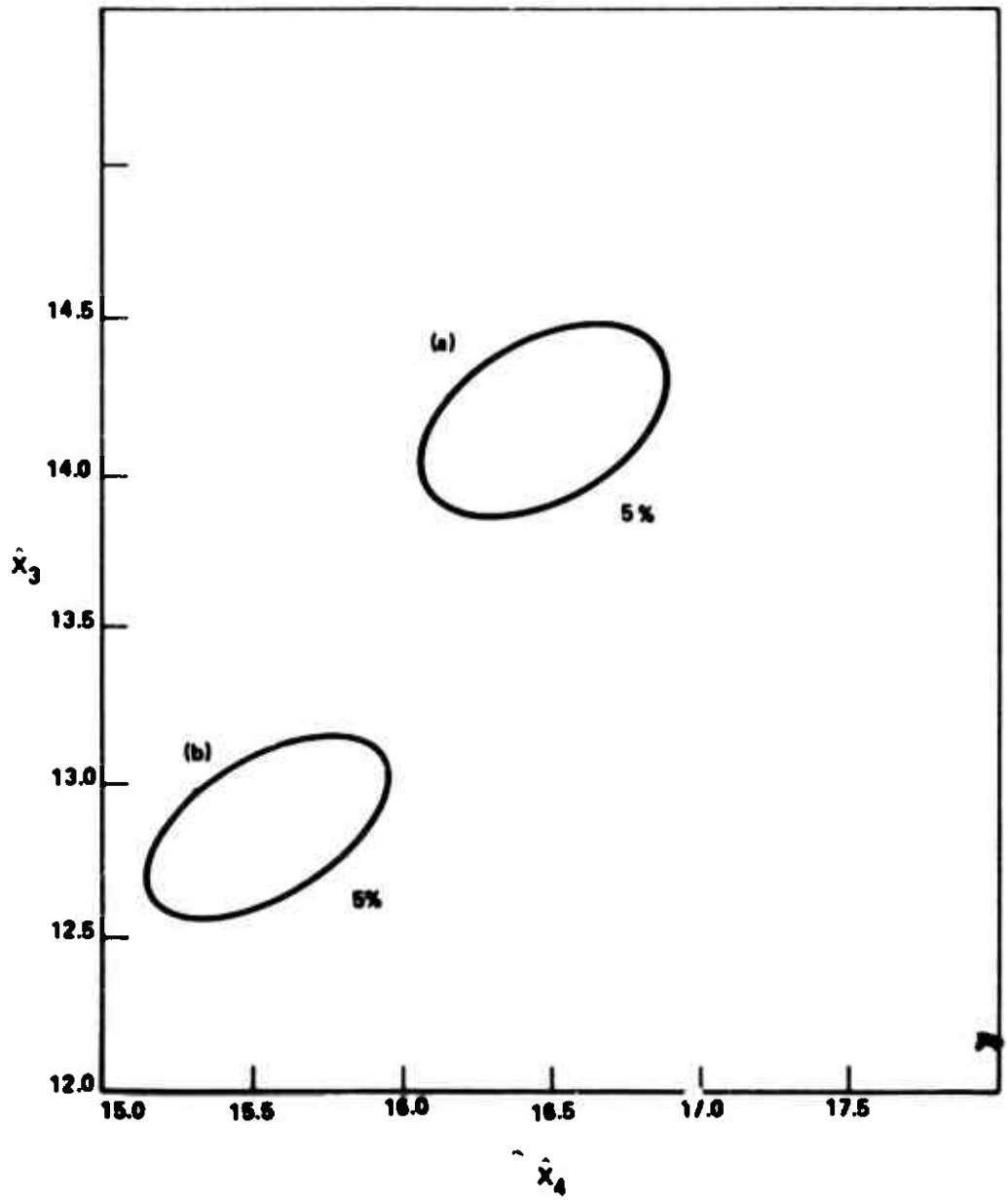

Figure B-1. Probability contours for $\hat{X}_3$ and $\hat{X}_4$ when (a) $\hat{X}_2$ = 66.0%, $\hat{X}_1$ = 0.50% and (b) $\hat{X}_2$ = 70.0%, $\hat{X}_1$ = 0.50%.

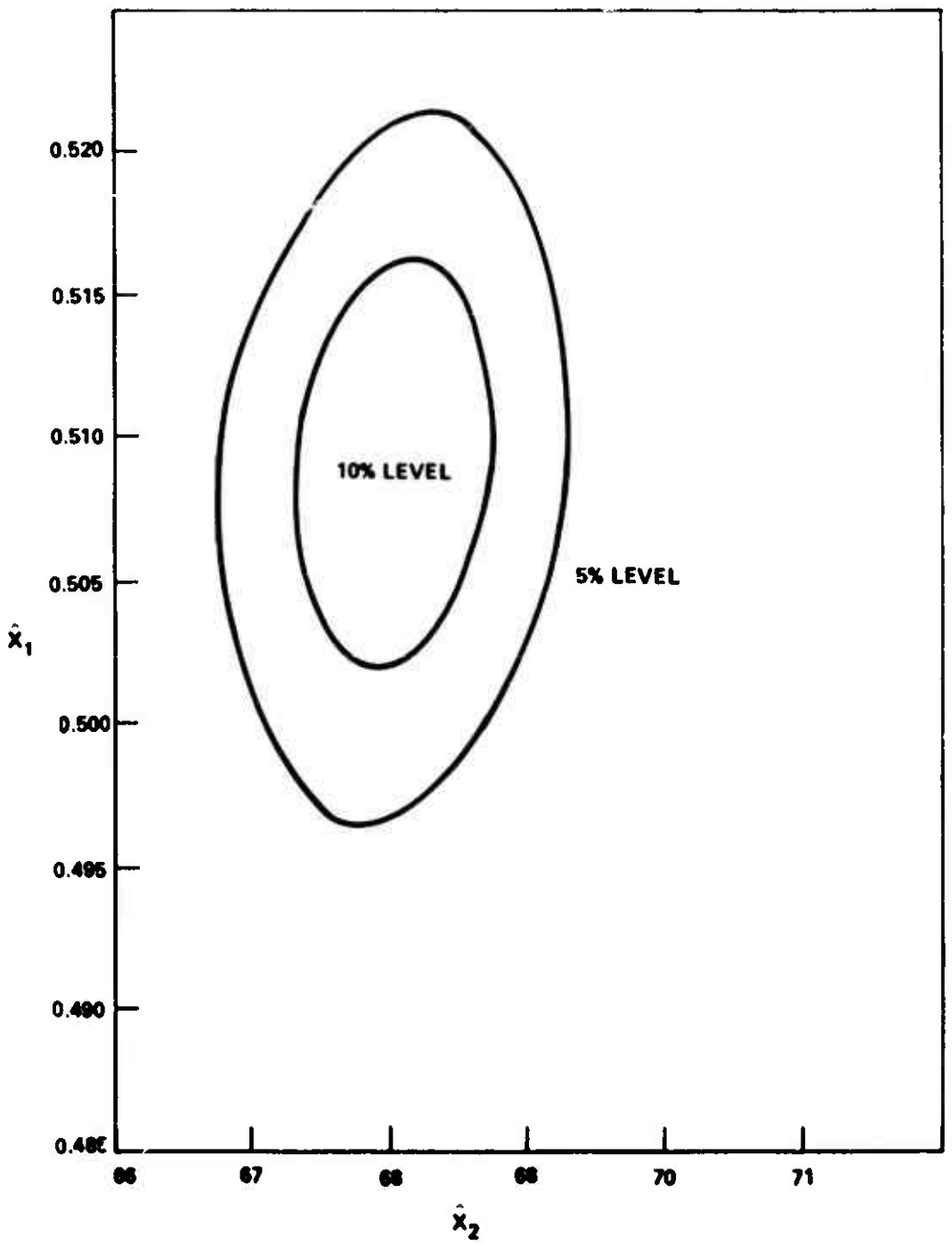

Figure B-2. Probability contours for $\hat{X}_1$ and $\hat{X}_2$ when $\hat{X}_3$ = 13.5%, $\hat{X}_4$ = 15.0%.

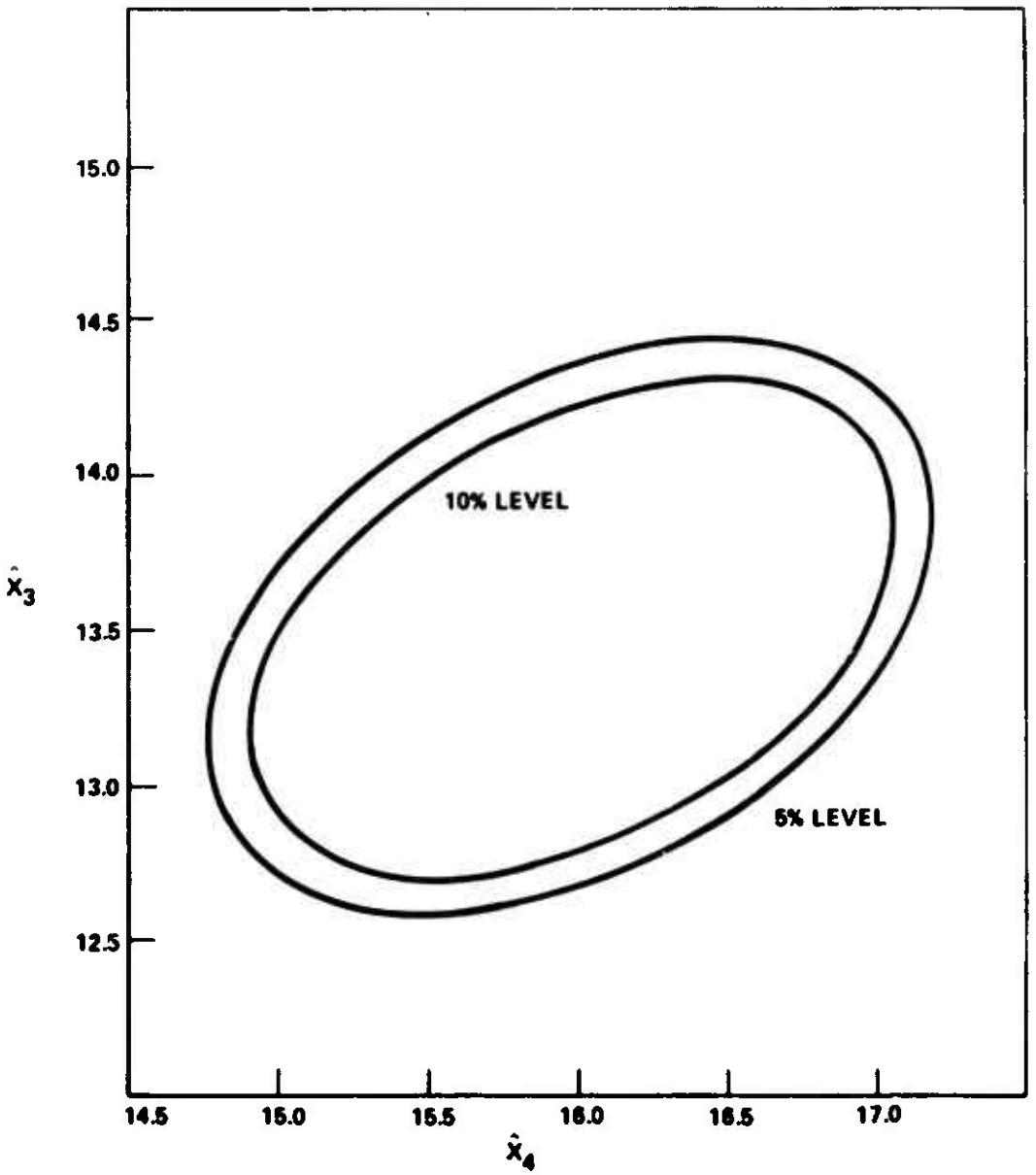

Figure B-3. Probability contours for $\hat{X}_3$ and $\hat{X}_4$ when $\hat{X}_1$ = 0.500%, $\hat{X}_2$ = 68.0%.

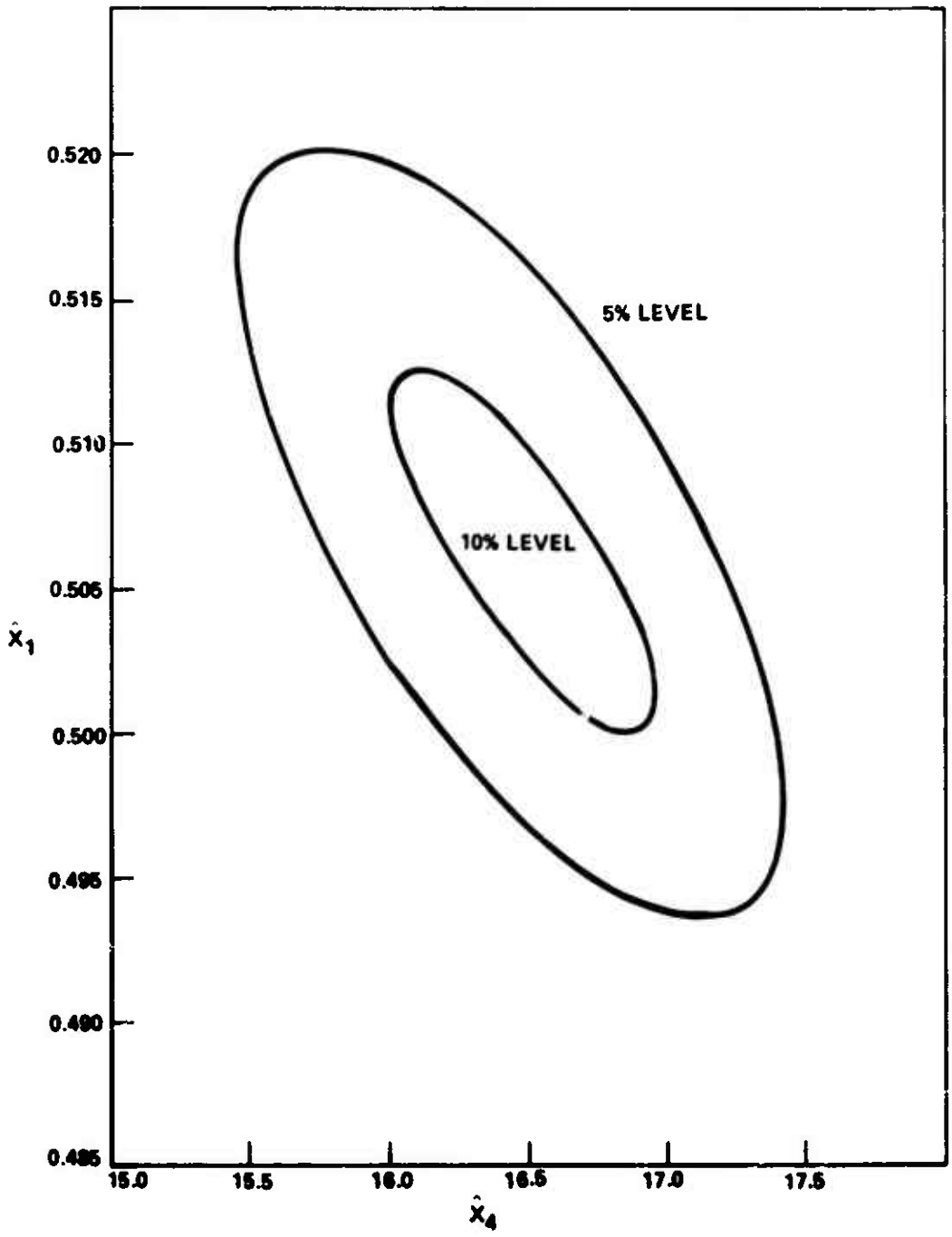

Figure B-4. Probability contours for $\hat{X}_1$ and $\hat{X}_4$ when $\hat{X}_2$ = 67.0%, $\hat{X}_3$ = 14.5%.

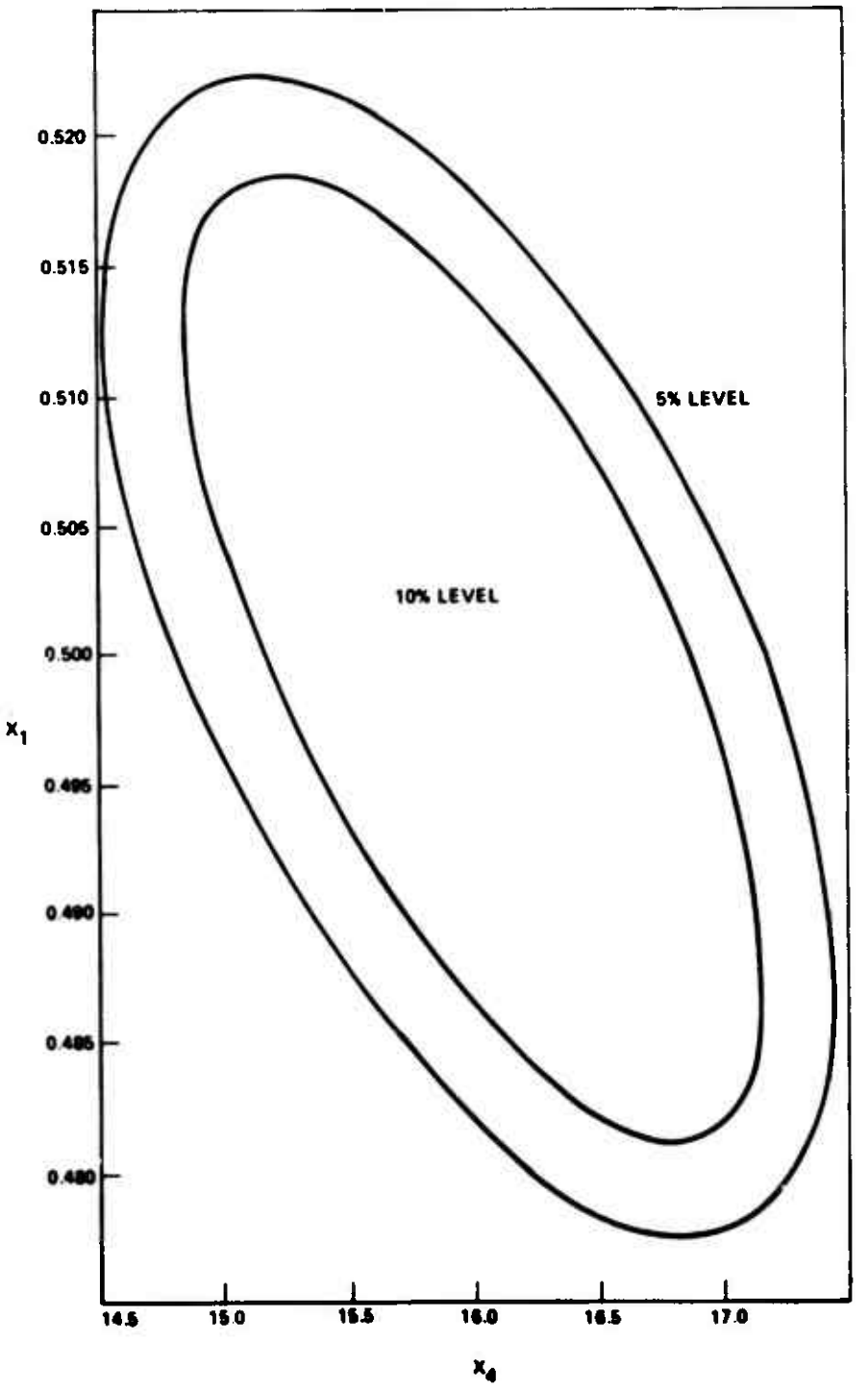

Figure B-5. Probability contours for $\hat{X}_1$ and $\hat{X}_4$ when $\hat{X}_2$ = 68.0%, $\hat{X}_3$ = 13.5%.

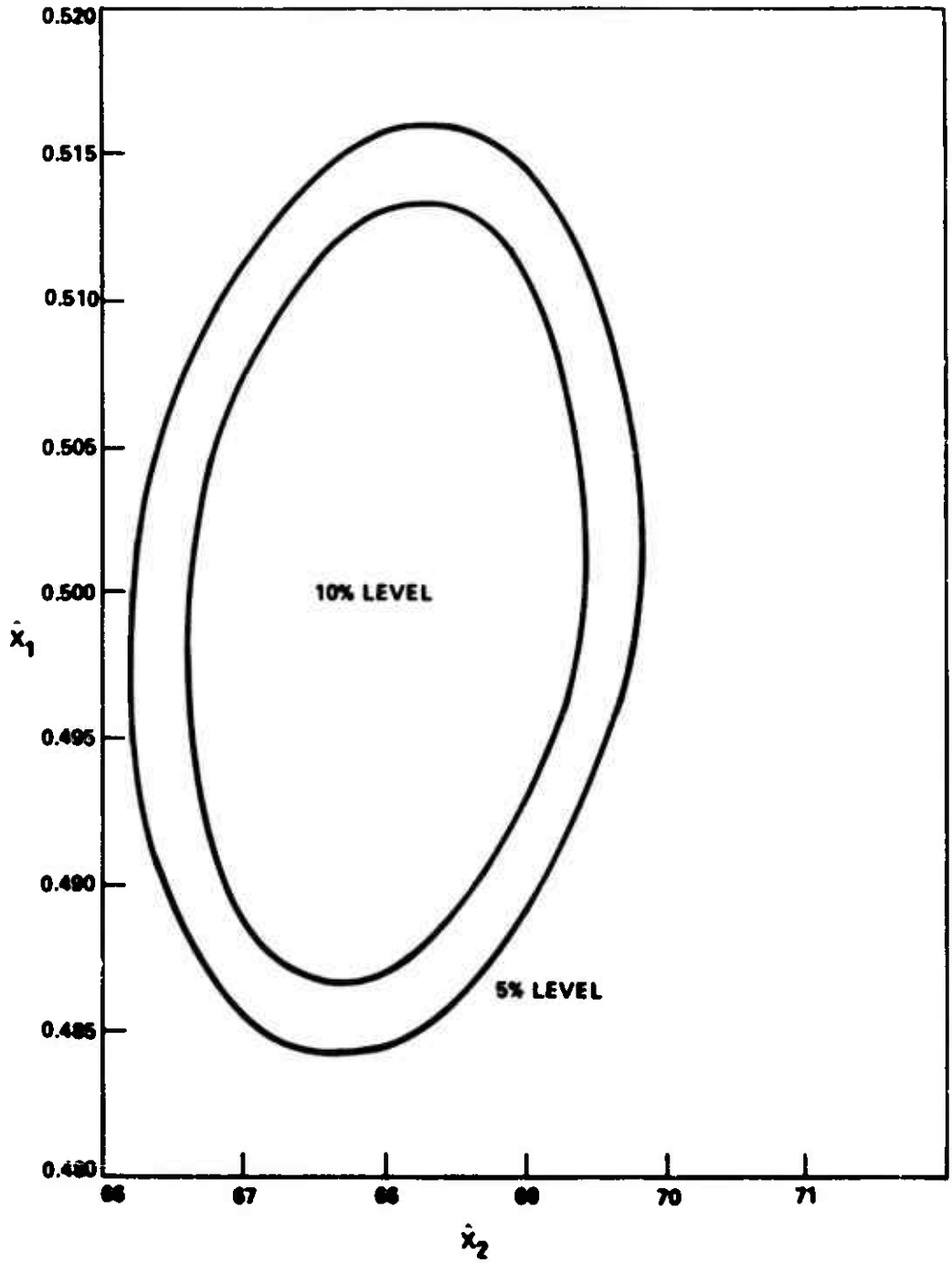

Figure B-6. Probability contours for $\hat{X}_1$ and $\hat{X}_2$ when $\hat{X}_3$ = 13.5%, $\hat{X}_4$ = 16.0%.

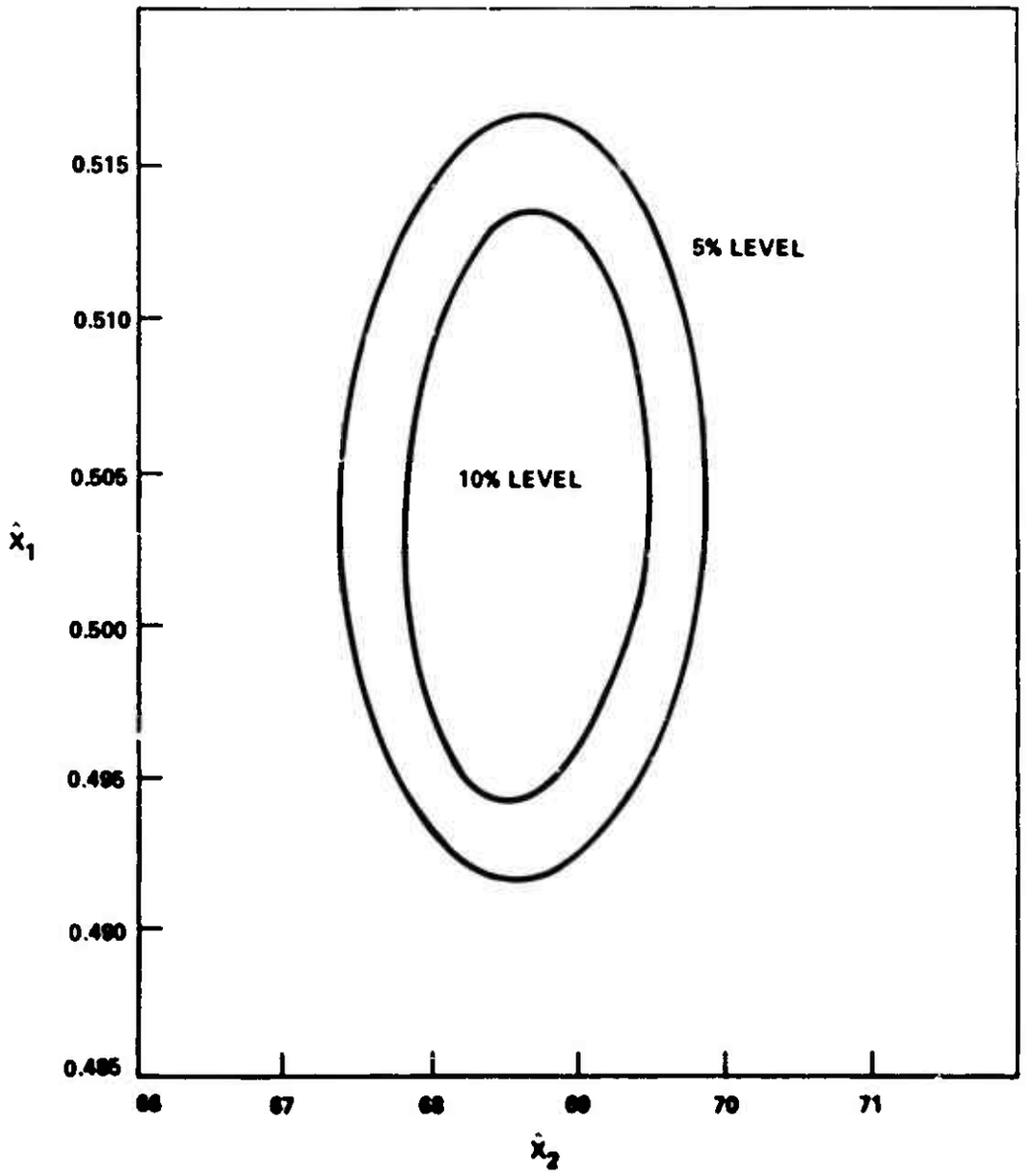

Figure B-7. Probability contours for $\hat{X}_1$ and $\hat{X}_2$ when $\hat{X}_3$ = 13.0%, $\hat{X}_4$ = 16.0%.

REFERENCES

1. Alley, B. J. and Higgins, J. H., X-ray Fluorescence Method for Analyzing Polybutadiene-Acrylic Acid (PBAA) Propellants, US Army Missile Command, Redstone Arsenal, Alabama, 1 March 1963, Report No. RK-TR-63-4 (Unclassified).

2. Puslipher, H. G., Sorenson, F. J., and Ashcraft, H. B., The Use of X-ray Fluorescence for In-process Control of Solid Propellant, Thiokol Chemical Corporation, Brigham City, Utah, November 1963, CPIA publication No. 30 (Unclassified).

3. Jenkins, R., An Introduction to X-ray Spectrometry, London: Heyden and Son Ltd., 1974.

4. Alley, B. J. and Higgins, J. H., "Empirical Corrections for Variable Absorption of Soft X-rays by Mylar," Norelco Reporter, Volume 10, No. 2, April-June 1963, pp. 77-80.

5. Mitchell, B. J., Encyclopedia of Spectroscopy, New York: Reinhold, 1960, p. 736.

6. Alley, B. J. and Myers, R. H., "Corrections for Matrix Effects in X-ray Fluoreacence Analysis Using Multiple Regression Methods," Anal. Chem., Volume 37, No. 13, December 1965, pp. 1685-1690.

7. Williams, E. J., Regression Analyais, New York: Wiley, 1959.

8. Berkson, J., "Are There Two Regressions," J. of the Am. Statistical Association, Volume 45, 1950, pp. 164-181.

9. Myers, R. H., Womeldorph, D., and Allay, B. J., "A Method for Adjusting for Particle Size and Matrix Effects in the X-ray Fluoreacence Analysis Procedure," Anal. Chem., Volume 39, July 1967, pp. 1031-1033.

10. Hicks, C. R., Fundamental Concepts in the Design of Experiments, New York: Holt, Rinehart and Winston, 1964, p. 75.

11. Davies, O. L., ed., Design and Analysis of Induatrial Experiments, Second Edition, New York: Hafner Publishing Co., 1956, p. 532.

12. Scheffs, H., "Experiments with Mixtures," J. Royal Statistical Society, Series B, Volume 20, 1958, pp. 344-360.

13. Womeldorph, D. E., Estimation in the Use of the X-ray Fluorsacence Method and Uss of Referencs Components in Mixturs Experimental Designs, Doctorate Thesis, Virginia Polytechnic Inatitute, Blacksburg, Virginia, May 1966.

14. Alley, B. J. and Myers, R. H., "Calibration Method for the X-ray Fluorescence Analysis of Multicomponent Mixtures," Norelco Reporter, Volume 15, Nos. 3-4, July-December 1968, p. 87.

15. McLean, R. A. and Anderson, V. L., "Extreme Vertices Design of Mixture Experiments," Technometrics, Volume 8, No. 3, 1966, pp. 447-454.

16. Thompson, W. O. and Myers, R. H., "Response Surface Designs for Experiments with Mixtures," Technometrics, Volume 10, No. 4, 1968, pp. 739-756.

17. Draper, N. R. and Smith, H., Applied Regression Analysis, New York: Wiley, 1966.

18. Hicks, C. R., Fundamental Concepts in the Design of Experiments, New York: Holt, Rinehart and Winston, 1964, p. 25.

19. Alley, B. J. and Beason, L. R., "Recent Developments in High-Burning-Rate Solid Rocket Propellants (U)," J. of Defense Research, Summer 1969, pp. 121-137 (Confidential).

20. Alley, B. J., Dykes, H. W. H., and Ayers, O. E., "High Rate Composite Propellants for Advanced Terminal Interceptors (U)," US Army Missile Command, Redstone Arsenal, Alabama, November 1973, CPIA Publication 242, Volume 1, pp. 735-756 (Confidential).

21. Claisse, F. and Samson, C., "Heterogeneity Effects in X-ray Analysis," Advances in X-Ray Analysis, Volume 5, 1962, pp. 335-354.

22. Gunn, E. L., "The Effect of Particles and Surface Irregularities on the X-ray Fluorescent Intensity of Selected Substances," Advances in X-ray Analysis, Volume 4, 1961, pp. 382-400.

23. Jenkins, R., An Introduction to X-ray Spectrometry, London: Heyden and Son, Ltd., 1974, pp. 115-117.

24. Alley, B. J., Dykes, H. W. H., and Howard, W. W., Particle Size Analysis of Fine Ammonium Perchlorate and Correlation with Propellant Burning Rates (U), US Army Missile Command, Redstone Arsenal, Alabama, April 1968, Report No. RK-TR-68-4, pp. 43-57 (Confidential).

25. Wu and Rainwater, J. of Nucleonics, October 1967, p. 61.

26. Parrish, W., "X-ray Intensity Measurements with Counter Tubes," Philips Technical Review, Volume 17, No. 7-8, 1956 pp. 206-221.

27. Wine, R. L., Statistics for Scientists and Engineers, New York: Prentice-Hall Inc., 1964.

28. Box, B. E. P. and Hunter, J. S., "A Confidence Region for the Solution of a Set of Simultaneous Equations with an Application to Experimental Design," Biometrika, Volume 41, pp. 190-199.

DISTRIBUTION

	No. of Copies
CPIA Distribution List	96
Metals and Ceramics Information Center Battelle Columbus Laboratories 505 King Avenue Columbus, Ohio 43201	2
Office of Chief of Research and Development Department of the Army ATTN: CRDPES Washington, D.C. 20310	1
Commander Army Research Office P. O. Box 12211 Research Triangle Park, North Carolina 27709	1
Commander US Army Material Development and Readiness Command ATTN: DRCQA	1
DRCQA-E	2
-P	2
DRCLDC, Mr. R. Zentner	1
DRCRL	1
DRCDE-EA	1
DRCDE-E	1
DRCRP-OIP	1
5001 Eisenhower Avenue Alexandria, Virginia 22333	
Commander US Army Electronics Command ATTN: DRSEL-CB	2
-PP-PO	1
-WM	1
-RD-GI	1
-PA-C	1
Fort Monmouth, New Jersey 07703	
Commander Picatinny Arsenal ATTN: SARPA-RT-S	1
-VA6, Mr. H. DeFazio	1
-VC2, Mr. T. M. Roach, Jr.	1
-VG, Mr. A. Clear	1
-ND-1, Mr. D. Stein	1
-FR-M-D, A. M. Anzalone, Bldg. 176	1
Dover, New Jersey 07801	
Commander US Army Mobility Equipment Research and Development Command ATTN: DRSME-Q	1
-QP	1
-QR	1
-QE	1
-M	1
-P	1
-R	1
	1
4300 Goodfellow Boulevard St. Louis, Missouri 63120	
Commander US Army Armament Command ATTN: DRSAR-SC, Dr. C. M. Hudson	1
DRSAR-PPW-PB, Mr. Francis X. Walter	1
Technical Library	2
Rock Island, Illinois 61201	

	No. of Copies
Commander US Army Natick Research and Development Command ATTN: DRXNM-QE	1
DRXNM-GE	1
Kansas Street Natick, Massachusetts 01760	
Commander US Army Tank-Automotive Research and Development Command ATTN: DRDTA-RXMT, Mr. J. Dudzinski	1
-RXMT, Mr. F. Lemmer	1
-RXMT, Mr. W. Wulf	1
-RGD, Mr. O. Renius	1
-QEE, Mr. P. Dufka	2
28251 Van Dyke Avenue Warren, Michigan 48090	
Commander US Army Test and Evaluation Command ATTN: DRSTE-TA-A	2
Aberdeen Proving Ground, Maryland 21005	
Commander US Army Test and Evaluation Command ATTN: STEAP-MT, Mr. J. M. McKinley	1
-TL	1
Aberdeen Proving Ground, Maryland 21005	
Commander Edgewood Arsenal ATTN: SAREA-TSP	1
-QAE	1
-QAI	1
-QAP	1
-QAIP	1
DRDAR-QAC-E, Dr. W. J. Maurits	1
Edgewood, Maryland 21010	
Commander US Army Foreign Science and Technology Center ATTN: DRXST-SD2	1
220 7th Street, N.E. Charlottesville, Virginia 22901	
Commander Frankford Arsenal ATTN: SARFA-P3300	1
-C2500	1
-Q1000	1
-Q2100	2
-N3100-202-1, Mr. E. Roffman	1
-Q6120-64-1, Mr. W. Shebest	1
-Q6130-64-1	1
-A2000	1
-F6000	2
-L300, Mr. J. Corrie	1
Philadelphia, Pennsylvania 19137	
Commander Harry Diamond Laboratories ATTN: DRXDO-EDE	2
2800 Powder Mill Road Adelphi, Maryland 20783	

	No. of Copies
Commander Rock Island Arsenal ATTN: SARRI-L, Dr. Royce Beckett	1
-LEQ	1
-LRM	2
-ENM, Mr. W. D. McHenry	1
Rock Island, Illinois 61201	
Director US Army Production Equipment Agency ATTN: DRXPE-MT	1
Rock Island Arsenal Rock Island, Illinois 61201	
Commander US Army Aeronautical Depot Maintenance Center ATTN: SSMAC-Q	1
Corpus Christi, Texas 78419	
Commander US Army Ammunition Procurement and Supply Agency ATTN: SMUAI-E	2
Joliet, Illinois 60436	
Commander US Army Mobility Equipment Research and Development Command ATTN: Technical Documents Center, Bldg 315	1
DRXFB	1
DRXFB-P	1
-M	1
-X	1
-A	1
-B	1
-H	1
-J	1
-F	1
-QM	1
-Q	1
-QQ	1
-QE, Mr. Jacob K. Mauzy	1
-MW, Dr. J. W. Bond	1
-VC, Mr. S. Levine	
Fort Belvoir, Virginia 22060	
Commander Watervliet Arsenal ATTN: SARWV-QA, Mr. J. Miller	1
SARWV-QA, Quality Assurance Otc	1
Watervliet, New York 12189	
Commander Anniston Army Depot ATTN: DRXAN-QA	
Anniston, Alabama 36202	
Commander Atlanta Army Depot ATTN: DRXAT-CSQ	1
Forest Park, Georgia 30050	
Commander Letterkenny Army Depot ATTN: DRXLE-CQ	1
DRXLE-NSQ	1
Chambersburg, Pennsylvania 17201	
Commander Lexington-Bluegrass Army Depot ATTN: DRXLX-QA	1
Lexington, Kentucky 40507	

	No. of Copies
Commander New Cumberland Army Depot ATTN: DRSNC-256	1
New Cumberland, Pennsylvania 17070	
Commander Pueblo Army Depot ATTN: DRXPU-BF	1
Pueblo, Colorado 81001	
Commander Red River Army Depot ATTN: DRXRR-QAO	1
Texarkana, Texas 75502	
Commander Sacramento Army Depot ATTN: DRXSA-QA	1
Sacramento, California 95801	
Commander Savanna Army Depot ATTN: DRXSV-QAO	1
Savanna, Illinois	
Commander Seneca Army Depot ATTN: DRXSE-AXI	1
Romulus, New York 14541	
Commander Sharpe Army Depot ATTN: DRXSH-CQ	1
Lathrop, California 95330	
Commander Sierra Army Depot ATTN: DRXSI-QA	1
Herlong, California 96113	
Commander Tobyhanna Army Depot ATTN: DRXTO-Q	1
Tobyhanna, Pennsylvania 18466	
Commander Tooele Army Depot ATTN: DRXTE-QAD	1
Tooele, Utah 84074	
Commander Umatilla Army Depot ATTN: DRXUM-QA	1
Hermiston, Oregon 97838	
Chief Bureau of Naval Weapons Department of the Navy Washington, D.C. 20390	1
Chief Bureau of Ships Department of the Navy Washington, D.C. 20315	1
Commander Wright Air Development Division ATTN: ASRC	2
AFML/MBC/Mr. Stanley Schulman	1
Wright-Patterson Air Force Base, Ohio 45433	

	No. of Copies
Commander	
US Army Aviation Systems Command	
ATTN: SRSAV-R-R	1
-R-EGE	1
-A-L	1
-LE	1
-A-LV	1
-A-V	1
St. Louis, Missouri 63166	
Director	
Army Materials and Mechanics Research Center	
ATTN: DRXMR-PL	2
-AG	1
DRXMI-RA, Mr. F. Valente	2
Watertown, Massachusetts 02172	

	No. of Copies
Superior Technical Services, Inc.	
ATTN: T. Ward	1
4308 Governors Drive	
Huntsville, Alabama 35802	
DRSMI-FR, Mr. Strickland	1
-LP, Mr. Voigt	1
DRDMI-X, Dr. McDaniel	1
-T, Dr. Kobler	1
-TBLD	
-TSM	1
-TTR, Mr. H. T. Lawson	1
-Q	2
-M	1
-TKC	10
-EAT, Mr. R. Talley	1
-TBD	3
-TI (Record Set)	1
(Reference Copy)	1